

**AN EXPLORATION OF CHEMICAL CUES AS MEDIATORS OF
MARINE PREDATOR-PREY INTERACTIONS**

A Dissertation
Presented to
The Academic Faculty

by

Marisa R. Cepeda

In Partial Fulfillment
of the Requirements for the Degree
Doctor of Philosophy in the
School of Chemistry and Biochemistry

Georgia Institute of Technology
August 2023

COPYRIGHT © 2023 BY MARISA R. CEPEDA

**AN EXPLORATION OF CHEMICAL CUES AS MEDIATORS OF
MARINE PREDATOR-PREY INTERACTIONS**

Approved by:

Dr. Julia Kubanek, Advisor
School of Biological Sciences
School of Chemistry and Biochemistry
Georgia Institute of Technology

Dr. Pamela Peralta-Yahya
School of Chemistry and Biochemistry
School of Chemical and Biomolecular
Engineering
Georgia Institute of Technology

Dr. Facundo Fernandez
School of Chemistry and Biochemistry
Georgia Institute of Technology

Dr. Will Gutekunst
School of Chemistry and Biochemistry
Georgia Institute of Technology

Dr. Mark Hay
School of Biological Sciences
Georgia Institute of Technology

Date Approved: July 14, 2023

To my parents, grandparents, and partner

ACKNOWLEDGEMENTS

The years I spent in graduate school at Georgia Tech were some of the most challenging and rewarding of my life. I feel very fortunate to have had so many great mentors who fostered my love for science and inspired me to become a chemist. To say the least, the path to a PhD was not what I expected, but I am very grateful for those who supported me along the way.

First, I would like to thank Dr. Alexander Olis, my high school chemistry teacher and the first person I ever met with a PhD. There was never a dull moment with Dr. Olis and it was in his classroom that I realized I wanted to pursue a career in chemistry. I want to thank Dr. Beth Stroupe, for taking me into her lab as a first year undergraduate student, and my graduate student mentors who have since all defended their theses as well: Dr. Joe Pennington, Dr. Isabel Askenasy, Dr. Mike Kopylov, and Dr. Travis Hand. Some of my fondest memories at Florida State University were of my time in the Stroupe Group, learning how to do research. I would also like to especially thank Dr. Walter Tschinkel, for all the time he invested in me as a young scientist. Having him as a mentor during my undergraduate studies was transformative for me as our discussions really fostered my intellectual growth and shaped the way I think about research.

As a graduate student at Georgia Tech there were many individuals who mentored me and supported my professional development, but none more so than my advisor Dr. Julia Kubanek. I would like to thank her for her guidance, for always making time for me when I needed it, and for constantly believing in me. I am forever grateful that she always supported my career endeavors both inside and out of the lab. I would like to thank all of

the members of the Kubanek Lab for their friendship, support, and countless much-needed hallway conversations: Dr. Sam Mascuch, Dr. Nazia Mojib, Dr. Serge Lavoie, Dr. Remy Poulin, Dr. Anne Marie Sweeney-Jones, Dr. Bhuwan Chhetri, Dr. Emily Brown, Nolan Barrett, Gabi Chebli, Nikki Aiosa, Maggie Straight, Shreya Kothari, and Benton Jaco. I would also like to thank my undergraduate mentees Hailey Loehde-Woolard, Samantha Spano, William Buzzeo, and Ethan Bar-Nur for all of their contributions to my various research projects.

I am grateful for my thesis committee members Dr. Mark Hay, Dr. Facundo Fernandez, Dr. Will Gutekunst, and Dr. Pamela Peralta-Yahya for their invaluable feedback on my research over the years. I would like to thank Alex Van Grouw as well as Georgia Tech core facility scientists Dr. Les Gelbaum, Dr. Hanno Leisen, Dr. David Gaul, and Sam Moore for their guidance with analytical techniques. I am thankful for my collaborators on the crab urine project Dr. Marc Weissburg, Dr. Lee Smee, Dr. Ben Belgrad, and Sarah Roney. I would also like to add that I am especially thankful for Dr. Facundo Fernandez and Sam Moore whose guidance was pivotal in accelerating my research progress.

Lastly, I would like to thank my parents, my family, my friends, and my partner Arun for all of their love and support throughout my time in graduate school. Words cannot describe how grateful I am for mami, papi, and Arun who were always there for me through my toughest times, especially whenever I wanted to quit and needed someone to lift me up. They helped me find my strength in the times I needed it the most and made sure I never gave up on my dreams. Los amo.

TABLE OF CONTENTS

ACKNOWLEDGEMENTS	iv
LIST OF TABLES	viii
LIST OF FIGURES	x
LIST OF SYMBOLS AND ABBREVIATIONS	xviii
SUMMARY	xxi
CHAPTER 1. Common fear molecules induce defensive responses in marine prey across trophic levels	1
1.1 Abstract	1
1.2 Introduction	2
1.3 Methods	5
1.3.1 Predator Cue Bioassay (July – Sept. 2020)	6
1.3.2 Homarine and Trigonelline Dose Response Experiment (June – Aug. 2021)	10
1.3.3 Urine Dose Response Experiment (July – Oct. 2022)	12
1.3.4 Quantification of Homarine and Trigonelline	13
1.3.5 Statistical Analyses	15
1.4 Results	16
1.4.1 Oyster Shell Strengthening Induced by Predator Cues	16
1.4.2 Homarine and Trigonelline in Blue Crab Urine Do Not Fully Explain Induced Oyster Defenses	17
1.4.3 Oyster Response to Cue Concentration is Dose-Dependent	21
1.5 Discussion	24
CHAPTER 2. Predator cues induce defensive responses in diverse marine prey: a metabolomics decoding of blue crab urine biomarkers	33
2.1 Abstract	33
2.2 Introduction	34
2.3 Methods	37
2.3.1 Blue Crab Urine Preparation	37
2.3.2 Oyster Shell Strengthening Assay	38
2.3.3 Mud Crab Feeding Assay	38
2.3.4 Estimating Protein Content in Blue Crab Urine	39
2.3.5 Blue Crab Urine Chemical Profiling	40
2.3.6 Multivariate Statistical Analyses of Spectroscopic Data and Variable Selection	43
2.3.7 Annotation of Blue Crab Urine Biomarkers via LC-MS/MS Spectra	44
2.4 Results	44
2.4.1 Predator Diet Does Not Influence Oyster Perception of Predation Risk	44
2.4.2 Blue Crab Urine is Not a Source of Nutrients	48

2.4.3	Blue Crab Urine Biomarkers Indicative of Predation Risk: Specific and Common Fear Cues Utilized by Multi-trophic Prey	51
2.5	Discussion	55
CHAPTER 3.	Assessing algal biofuel pond system exometabolomes: insights for protection from pests	60
3.1	Abstract	60
3.2	Introduction	62
3.3	Methods, results, and discussion	64
3.3.1	Chemical Profiling of Bacterial Consortia Exometabolomes	64
3.3.2	A Comparison of SPE Methods for Extracting Algal Culture Conditioned Media	72
3.3.3	Anti-rotifer Natural Products from Aquatic Bacterial Isolates	79
3.3.4	Sanger and Illumina Next Generation Sequencing to Identify Aquatic Bacterial Isolates	84
3.3.5	Aquatic Bacterial Natural Product Induction in Response to Rotifer Cues	91
3.3.6	Testing Higher Concentrations of Bacterial Extracts for Rotifer Mortality	95
3.3.7	Natural Products from Aquatic Bacterial Isolates for Controlling Phagotrophic Algae	97
3.3.8	Generation of Bacterial Extracts to Screen for Anti-phagotrophic alga Activity	98
3.3.9	Anti-chytrid Natural Products from Aquatic Bacterial Isolates	107
3.4	Conclusions	108
CHAPTER 4.	Conclusions and future directions	110
APPENDIX A.	Supplementary figures and tables for chapter 1	113
REFERENCES		116

LIST OF TABLES

Table 2.1	Top ten positive ion MS features that correlated with increased oyster shell strength. A list of 78 features was compiled by cross-comparing four PLS-R models generated for the oyster shell strengthening assay. These models were built using a subset of variables that were selected by genetic algorithm variable selection and are more robust for predicting oyster shell strength. Features are ordered by variable importance parameter (VIP) scores from highest to lowest, where higher scores indicate greater importance to the model.	54
Table 2.2	Top ten positive ion MS features that correlated with reduced mud crab feeding. A list of 81 features was compiled by cross-comparing four PLS-R models generated for the mud crab feeding assay. These models were built using a subset of variables that were selected by genetic algorithm variable selection and are more robust for predicting reduced mud crab feeding. Features are ordered by variable importance parameter (VIP) scores from highest to lowest, where higher scores indicate greater importance to the model.	54
Table 2.3	Seven positive ion MS features that correlated with both increased oyster shell strength and reduced mud crab feeding. This list was compiled by cross-comparison of all of the oyster and mud crab bioassay PLS-R models generated from features chosen by genetic algorithm variable selection. Features are ordered by variable importance parameter (VIP) for the oyster bioassay. Scores are ordered from highest to lowest, where higher scores indicate greater importance to the model.	55
Table 3.1	Validation of strain purity for nine bacterial samples. Sequencing of 16S rDNA revealed that four of nine bacterial samples consisted of multiple strains or species. The criteria for strain purity used here are as follows: 1) the percent of total reads for a single species must be greater than 98.5% and 2) no other single classification category may have a percent of total reads greater than 0.2%. Classification of 16S rDNA sequences (greater than 0.2% of total reads) from illumina Next Generation sequence analysis is synthesized from both Sanger and illumina Next Generation sequence comparison with reference libraries NCBI Blast and "RefSeq RDP 16S v3 May 2018 DADA2 32 BP" used by illumina in the 16S Metagenomics application, respectively. The illumina sequencing was performed on the V2 region of the 16S rDNA coding region and does not	86

perfectly predict the classification of the bacteria with 100% certainty. This table was created by Nolan Barrett.

Table 3.2	The bacterial families represented in the 36 bacterial samples are all found in the marine environment and known to produce a wide array of potentially useful secondary metabolites. This table was created by Nolan Barrett.	90
Table A1	pH and salinity values recorded with Orion Star TM A121 Portable pH Meter during June – Sept. 2020 bioassay experiments. Values were recorded directly before water changes in each aquarium.	113
Table A2	The number of blue crab individuals making up urine treatment mixtures for blue crabs fed an oyster diet and mud crab diet. All blue crabs were between 11-19 cm size and were fed the appropriate diet for one week before urine extraction began.	114
Table A3	Concentrations of homarine and trigonelline for the dose response experiment and number of replicates for each dose. Replicates were excluded from analysis if they experienced high mortality of oyster spat (less than 6 spat alive). Concentrations of homarine and trigonelline for the homarine + trigonelline dose response curve are the same as those used for the dose response curves of the individual cues. Single asterisks (*) indicate the natural concentration upper limits for homarine and trigonelline in blue crab urine (oyster diet). Double asterisks (**) indicate that these doses were excluded from additional statistical analyses because they exceeded the natural concentration range.	114
Table A4	Concentrations and corresponding volumes of blue crab urine doses used in the 2022 urine dose response experiment. Urine was collected and pooled from 22 crabs that ranged 13 – 18 cm in size and each crab produced 1.31 ± 0.18 mL on average. Cue concentration estimates are based on the assumption that in 1 mL of blue crab urine, the concentrations of homarine and trigonelline are 13 ± 21 μ M and 3.6 ± 6.9 μ M, respectively, as quantified from urine in the 2020 predator cue bioassay. Asterisks (*) indicate that urine was diluted to the appropriate concentration (based on trigonelline values) and dosed using a 1 mL aliquot volume.	115

LIST OF FIGURES

- Figure 1.1 Oyster spat were exposed to predator water (n=7), blue crab urine (n=9 per diet type), pure chemical compounds homarine or trigonelline (n=9), a combination of homarine + trigonelline (n=8), or seawater (n=9). Their shells were crushed and the measured force was normalized to shell width (i.e., standardized crushing force). A one-way ANOVA followed by an uncorrected Fisher's LSD test compared the means of all treatments to the seawater control. Predator water, blue crab urine of both diets, homarine (15.1 μM) and homarine + trigonelline induced significantly stronger oyster shells than seawater. Trigonelline (24.6 μM) did not significantly induce stronger shells. This box-and-whisker plot shows the median of each treatment, the upper and lower quartiles, and the minimum and maximum bounds for each treatment. Treatments are denoted as significant with * at $P \leq 0.05$, ** at $P \leq 0.01$ and **** at $P \leq 0.0001$. 17
- Figure 1.2 Concentrations of homarine (A) and trigonelline (B) quantified for 24 blue crab urine mixtures (oyster or mud crab diet) via LCMS. Homarine concentrations were generally higher than corresponding trigonelline concentrations for the same urine mixture. Concentrations for both metabolites spanned three orders of magnitude. Homarine concentrations ranged from 0.4 – 65 μM . Trigonelline concentrations ranged from 0.1 – 22 μM . Black bars represent the mean for each treatment. Data were excluded for samples where concentrations were below the limit of quantitation. 19
- Figure 1.3 Linear regression of homarine versus trigonelline concentrations for 23 blue crab urine samples ($F(1, 21) = 246$, $P < 0.0001$, $R^2 = 0.92$). Although the ratio of these metabolites is not fixed, there is a significant positive correlation for homarine and trigonelline concentrations when urine samples are analyzed irrespective of diet (mud crab or oyster). Data were excluded for concentrations below the limit of quantitation. 20
- Figure 1.4 Linear regression analyses of homarine and trigonelline concentrations quantified in urine of blue crabs fed two different diets. The positive correlations between homarine and trigonelline concentrations for mud crab (n = 12, circles) and oyster diets (n = 11, squares) are significant (mud crab diet, $F(1, 10) = 68.3$, $P < 0.0001$, $R^2 = 0.87$; oyster diet, $F(1, 9) = 150$, $P < 0.0001$, $R^2 = 0.94$). Data were excluded for concentrations below the limit of quantitation. 20

- Figure 1.5 Linear regression analyses of chemical cue concentrations quantified for blue crab urine from the predator cue bioassay. Models suggest that homarine (A), trigonelline (B) and their combined concentrations (C) were not reliable indicators of induced oyster shell strengthening for oysters exposed to blue crab urine. Analyses were performed for combined diets: A) homarine concentration ($F(1, 16) = 2.44, P = 0.14$), B) trigonelline concentration ($F(1, 15) = 4.47, P = 0.052$), and C) trigonelline + homarine concentration ($F(1, 15) = 2.44, P = 0.14$). Oyster spat were exposed to one of 17 crab urine mixtures (oyster diet, $n=8$, mud crab diet, $n=9$), crushed, and crushing force was standardized by oyster shell width. Each point is an average of 20 oyster spat. Data were excluded for concentrations below the limit of quantification. 21
- Figure 1.6 Linear regression analyses of chemical cue concentrations quantified for blue crab urine from the predator cue bioassay. Models suggest that homarine (A), trigonelline (B) and their combined concentrations (C) were not reliable indicators of induced oyster shell strengthening for oysters exposed to blue crab urine. Analyses were performed for combined diets: A) homarine concentration ($F(1, 16) = 2.44, P = 0.14$), B) trigonelline concentration ($F(1, 15) = 4.47, P = 0.052$), and C) trigonelline + homarine concentration ($F(1, 15) = 2.44, P = 0.14$). Oyster spat were exposed to one of 17 crab urine mixtures (oyster diet, $n=8$, mud crab diet, $n=9$), crushed, and crushing force was standardized by oyster shell width. Each point is an average of 20 oyster spat. Data were excluded for concentrations below the limit of quantification. 23
- Figure 1.7 A dose response curve for oyster spat exposed to urine of blue crabs fed exclusively oysters. Eight different urine concentrations were tested spanning several orders of magnitude. Urine potency increased significantly with concentration (non-linear regression, $F(1, 43) = 44.0, P < 0.0001, R^2 = 0.5785$). Urine doses along the x-axis are the total volume of undiluted blue crab urine applied to the experimental aquaria. Each point is an average of 32 oyster spat and crushing force was standardized by oyster shell width. A one-way ANOVA revealed that the lowest potent urine volume is 1.50×10^{-7} ($P = 0.012$). 24
- Figure 1.8 Linear regression models suggested that homarine (A) and trigonelline (B) concentrations were not reliable indicators of induced oyster shell strengthening for oysters exposed to blue crab urine. Analyses were performed for individual diets: A) homarine concentration for individual diets (oyster diet, $n = 9, F(1, 7) = 3.48, P = 0.10$; mud crab diet, $n = 9, F(1, 7) = 0.0481, P = 0.83$), and B) 27

trigonelline concentration for individual diets (oyster diet, $n = 8$, $F(1, 6) = 5.48$, $P = 0.058$; mud crab diet, $n = 9$, $F(1, 7) = 0.969$, $P = 0.36$). Oysters were exposed to one of 18 crab urine mixtures for eight weeks, spat were crushed, and crushing force was standardized by oyster shell width. Each point is an average of 20 oysters. Data were excluded for concentrations below the limit of quantitation.

- Figure 2.1 Complementary ^1H NMR and LC-MS spectra were acquired for 24 blue crab urine samples: mud crab diet ($n=12$) and oyster diet ($n=12$). A) Representative ^1H NMR spectra for urine of each blue crab diet: oyster (blue spectrum) and mud crab (gold spectrum). B) Overlaid LC-MS chromatograms for all 24 urine samples. Mass spectra were acquired using positive ionization electrospray mode. 45
- Figure 2.2 Principal component analyses of ^1H NMR (A) and LC-MS (B) blue crab urine metabolomics datasets. ^1H NMR and mass spectra were acquired for 24 urine samples: mud crab diet ($n = 12$) and oyster diet ($n = 12$). Strong separation of treatments for both models indicates distinct chemical profiles for urine of blue crabs fed different diets. 46
- Figure 2.3 Trigonelline and homarine are two blue crab urine metabolites that contribute to distinct chemical profiles for blue crab urine of different diets. A) Structures of homarine and trigonelline with their ^1H NMR chemical shifts. Two representative ^1H NMR spectra (B) and the corresponding loadings plot (C) for the principal component analysis of the ^1H NMR blue crab urine metabolomics dataset. Black arrows point to peaks for trigonelline, and gray arrows point to peaks for homarine. Trigonelline and homarine peaks are negative in the loadings plot indicating that these features are enriched in the mud crab diet (yellow arrow). Feature enriched in the oyster diet are positive for PC 1 in the loadings plot (blue arrow). 47
- Figure 2.4 Partial least squares regression analyses for ^1H NMR (A) and MS (B) metabolomics datasets related to oyster shell strengthening. For both models, measured oyster shell standardized crushing force is regressed against spectroscopic chemical features to predict standardized crushing force values for each urine sample. Lines of best fit for the ^1H NMR and MS metabolomics models have R^2 values of 0.97 and 0.64 respectively, where higher R^2 values are indicative of a better predictive model. 49
- Figure 2.5 Partial least squares regression analyses for ^1H NMR (A) and MS (B) metabolomics datasets related to mud crab feeding suppression. For both models, measured urine potency is regressed 50

against spectroscopic chemical features to predict urine potency values for each urine sample. Plotted lines of best fit are for the ^1H NMR and MS metabolomics calibrated models ($R^2 = 0.98$ and 0.97 respectively). Higher urine potency indicates reduced mud crab feeding and higher R^2 values are indicative of a better predictive model.

- Figure 2.6 Variable importance parameter plot for the ^1H NMR metabolomics partial least squares regression analysis. Peaks above the dashed red line are chemical features corresponding to molecules whose concentrations positively correlate with oyster shell strength. Black arrows point to features corresponding to trigonelline. 51
- Figure 2.7 Partial least squares regression models for the oyster shell strengthening (A) and mud crab feeding (B) assays using the positive ion MS metabolomics dataset. Only two of the final eight models (i.e., four PLS-R models per bioassay) are shown. Urine potency, measured for oysters as increased shell strength and for mud crabs as decreased food consumption, were regressed against mass spectral features to predict the potency of each urine sample. Plotted lines of best fit are for the MS metabolomics cross-validated models ($R^2 = 0.89$ for the oyster shell strengthening assay and $R^2 = 0.95$ for the mud crab feeding assay). Higher urine potency indicates stronger oyster shells or reduced mud crab feeding; Higher R^2 values are indicative of a better predictive model. 53
- Figure 3.1 Principal component analysis (PCA) of ^1H NMR spectral data acquired for lipid-soluble algal culture conditioned media extracts, in the presence and absence of bacteria. Two technical replicates were tested per sample type: no bacteria (green diamond), non-protective bacteria (consortium “B”, pink diamond), protective bacteria (consortium “F”, blue triangle). Bacterial metabolites most likely distinguish the protective treatment from the non-protective and no bacteria treatments along the PC 1 axis. 66
- Figure 3.2 A principal component analysis of ^1H NMR spectral data acquired for water-soluble algal culture conditioned media extracts. Two technical replicates were tested per sample type: no bacteria (green diamond), non-protective (pink diamond), protective (blue triangle). Bacterial metabolites separated one of the two protective treatment technical replicates from the non-protective and no bacteria treatments along the PC 1 axis. Distinct metabolites in the second technical replicate were likely too dilute to distinguish it from the other treatments. 67

- Figure 3.3 Base peak chromatograms from LCMS analysis of algal culture extracts a) Positive mode base peak ion chromatograms for extracts of algal cultures grown with a protective bacterial consortia (blue) or no bacteria (red). b) Negative mode base peak ion chromatograms for extracts of algal cultures grown with a protective bacterial consortia (blue) or no bacteria (red). 68
- Figure 3.4 ^1H NMR spectra of algal culture-conditioned media extracts: no bacteria (dark green), no bacteria + rotifers (light green), least protective consortium (navy blue), least protective consortium + rotifers (royal blue), most protective consortium (dark purple), and most protective consortium + rotifers (light purple). Although many bacterial consortia were tested in this experiment, only the no bacteria, most protective consortia, and least protective consortia treatments are shown because they are representative of the entire data set. Red circles draw attention to signals associated with molecules arising from exposure to bacteria. 70
- Figure 3.5 a) Liquid chromatography (LC) chromatogram for an algal-bacterial (strongly protective) culture conditioned media extract. The mass spectrum for peak A (gold outline) shows m/z signals for distinct metabolites (red circles). b) LC chromatogram for an algal-bacterial (moderately protective) culture conditioned media extract. The mass spectrum for peak A (blue outline) shows m/z signals for distinct metabolites (red circles). 72
- Figure 3.6 Algal growth curves for the *M. salina* and *A. macleodii* co-culture experiment: Axenic (blue), algae + rotifers (orange), algae + bacteria (grey), and algae + bacteria + rotifers (gold). 73
- Figure 3.7 Top) Principal component analysis (PCA) of reversed phase C18 LCMS data acquired for algae + rotifers and algae + bacteria + rotifers conditioned media extracts. Three different solid phase extraction (SPE) methods are represented by red (C8), blue (PPL), or yellow (StrataX) shapes. Extracts from cultures grown with bacteria are represented as squares while those of extracts for cultures grown without bacteria are represented as circles. Bottom) Loadings plot where each point represents an individual molecular mass with a corresponding retention time. 75
- Figure 3.8 Top) Principal component analysis (PCA) of normal phase BEH HILIC LCMS data acquired for algae + rotifers and algae + bacteria + rotifers conditioned media extracts. Three different solid phase extraction (SPE) methods are represented by red (C8), blue (PPL), or yellow (StrataX) shapes. Extracts from cultures grown with bacteria are represented as squares while those of extracts for cultures grown without bacteria are represented as circles. Bottom) 78

Loadings plot where each point represents an individual molecular mass with a corresponding retention time.

- Figure 3.9 A) Principal component analysis (PCA) for HILIC positive ionization mode LCMS data. PC 1 on the x axis and PC 2 on the y axis represent 54.6% and 15.7% of the variance among samples respectively B) Loadings plot of chemical features that correspond with samples in the PCA plot. Each feature is a molecular mass with a corresponding retention time and how they group results in the separation of treatment groups. 79
- Figure 3.10 24-hour rotifer toxicity assay initial screening results. One graph is shown for each 24-well plate assay. Asterisks denote when extracts of bacterial isolates ($n = 3$) were significantly more toxic than the corresponding negative control ($n = 3$; $p < 0.05$). The toxicity of the isolate 10 extract was comparable to that of the rotenone positive control ($\sim 0.75 \mu\text{M}$). Of all the extracts generated, isolate 10 was the most toxic, followed by isolate #3. 82
- Figure 3.11 24-hour rotifer toxicity assay follow-up experiment. Bacterial extracts for isolates #3, #4, #6, #10, #18, and #26 were generated in biological triplicate and screened for rotifer toxicity in a 24-well plate assay. Previously observed rotifer toxicity was not reproducible for any of the bacterial isolates. However, toxicity observed for both the rotenone positive control and marine media extract negative control was as expected. 84
- Figure 3.12 Induction Experiment. 36 bacterial isolates were grown in the presence of rotifer conditioned media, algal conditioned media, or artificial seawater. Induced bacteria were lysed with ceramic beads in a tissue homogenizer and extracted by liquid-liquid partitioning of the whole culture. Ethyl acetate bacterial extracts were screened in a 24-well rotifer toxicity assay. 93
- Figure 3.13 24-hour rotifer toxicity assay utilizing induced bacterial extracts screening results. One graph is shown for each 24-well plate assay. Asterisks denote both the positive control rotenone ($\sim 0.75 \mu\text{M}$) being significantly more toxic than the marine media extract negative control and when treatments from the same isolate were significantly different from one of the other treatments ($n = 3$; $p \leq 0.05$). Of all the extracts screened, the only significant difference within a set of isolate treatments was the rotifer and algal filtrate exposed bacterial extract in isolate #2 inducing greater rotifer mortality than the artificial seawater control counterpart ($n = 3$; $p = 0.024$); however, it was not statistically significant from the 94

negative control (n = 3; p > 0.05). (* = p ≤ 0.05; ** p ≤ 0.01; *** = p ≤ 0.001; **** p ≤ 0.0001).

- Figure 3.14 24-hour rotifer toxicity assay utilizing induced bacterial extracts at increased concentrations screening results. One graph is shown for each 24-well plate assay. Asterisks denote both the positive control rotenone (~0.75 μM) being significantly more toxic than the marine media extract negative control and when treatments from the same isolate were significantly different from one or the other treatments (n = 3; p < 0.05). Extracts were screened at a low (1.5-fold the original bacterial culture concentration) or high (3-fold the original bacterial culture concentration) concentration. Of all the extracts screened, the only significant differences were found in isolate #26, where the high concentrations of all 3 treatments were statistically different than the negative marine media control (n = 3, p values notes on graph). (* = p ≤ 0.05; ** p ≤ 0.01; *** = p ≤ 0.001; **** p ≤ 0.0001). 96
- Figure 3.15 Phagotrophic alga *Poteroiochromonas malhamensis* bioassay. Algae were enumerated using a FlowCam and exposed to chemical extracts in 10 mL culture tubes. Cells will be counted with a FlowCam before and after exposure to determine bioactivity. 97
- Figure 3.16 72-hour *P. malhamensis* growth inhibition assay initial screening results from the bacterial cellular extract induced verses non-induced experiment. Bacterial isolates (#2, #4, #6, #10, #32) were cultured in the presence (induced) and absence (non-induced) of *P. malhamensis* lysate to produce bacterial cell extracts corresponding to each isolate. *P. malhamensis* was grown exposed to these bacterial extracts, and growth rate was determined via flow cytometry. Induced and non-induced samples from the same isolate were compared to each other, and all non-induced samples were compared to the non-induced control while all induced samples were compared to the induced control. The two controls were compared to each other. There was no statistical significance between any of these comparisons (n = 3; p > 0.05). The greatest difference was between non-induced #6 and the noninduced control and non-induced #2 and the non-induced control (p = 0.12 and p = 0.13, respectively). However, all the induced vs non-induced comparisons were more similar (p > 0.70). Data acquisition and analysis were performed by Gabriella Chebli. 102
- Figure 3.17 72-hour *P. malhamensis* growth inhibition assay initial screening results from the bacterial supernatant extract induced verses non-induced experiment. Bacterial isolates (#2, #4, #10, #32) were cultured in the presence (induced) and absence (non-induced) of *P. malhamensis* lysate to produce bacterial supernatant extracts 104

corresponding to each isolate. *P. malhamensis* was grown exposed to these bacterial extracts, and growth rate was determined via flow cytometry. Induced and non-induced samples from the same isolate were compared to each other, and all non-induced samples were compared to the non-induced control while all induced samples were compared to the induced control. The two controls were compared to each other. The only statistically significant comparison was between the induced isolate #2 treatment and its respective control (n = 3; p = 0.038). There was no statistical significance between the other comparisons (n = 3; p = 0.12 to 0.89). Data acquisition and analysis were performed by Gabriella Chebli.

- Figure 3.18 72-hour *P. malhamensis* growth inhibition assay screening results where *P. malhamensis* was exposed to bacterial supernatant from 36 different bacterial isolates. *P. malhamensis* was grown exposed to these bacterial supernatant extracts, and growth rate was determined via flow cytometry. One graph is shown for each assay “set,” consisting of three bacterial isolates and one marine media control. Asterisks denote when extracts of bacterial isolates (n = 3) had a significantly greater impact on growth than the corresponding control (n = 3; p < 0.05 for * and p < 0.01 for **). Isolates #63 and #26 decreased the growth rate of *P. malhamensis* compared to the marine media control (p = 0.042, 0.0022, respectively), whereas isolates #59, #61, and #62 increased *P. malhamensis* growth rate (p = 0.022, 0.0019, 0.0031, respectively). Data acquisition and analysis were performed by Gabriella Chebli. 106
- Figure A1 A simple linear regression of the average spat size and crushing force per replicate in the predator water (A) and seawater (B) treatments from 2020 predator cue bioassay experiment. The relationship between size and crushing force follows a significantly positive linear relationship for both the positive and negative controls (PW, P = 0.01 and SW, P = 0.02), indicating that stronger individuals often have a larger shell. Because of this evidence for a linear relationship, we use standardized crushing force (crushing force/size) to report changes in shell strength from our series of experiments. 113

LIST OF SYMBOLS AND ABBREVIATIONS

^1H NMR	proton nuclear magnetic resonance
$^{\circ}\text{C}$	degrees Celsius
ANOVA	analysis of variance
Cal	calibration
CID	collision-induced dissociation
cm	centimeter
CV	cross validation
DDA	data dependent acquisition
eV	electron volt
HCD	higher-energy collisional dissociation
HILIC	hydrophilic interaction chromatography
HPLC	high-performance liquid chromatography
Hz	hertz
kV	kilovolt
L	liter
LC	liquid chromatography
LSD	least significant difference
LV	latent variable
m	meter
M	molar
m/z	mass to charge ratio
mg	milligram

MHz	megahertz
min	minute
mL	milliliter
mM	millimolar
mm	millimeter
MS	mass spectrometry
MS/MS	tandem mass spectrometry
N	newton
NG	next generation
nM	nanomolar
nm	nanometer
NRPs	Nonribosomal peptides
PC	principal component
PCA	principal component analysis
PLS-DA	partial least squared discriminant analysis
PLS-R	partial least squared regression
PmTG	peptonized milk, tryptone, and glucose media
ppm	parts per million
ppt	parts per thousand
PQN	probabilistic quotient normalization
RMSECV	root mean squared error of cross validation
rpm	rotations per minute
SNL	Sandia National Laboratories
sp.	species
SPE	solid phase extraction

UPLC ultra-performance liquid chromatography
μL microliter
μM micromolar
μm micrometer
VIP variable importance parameter
w/v weight per volume
YPD yeast extract, peptone, and dextrose media

SUMMARY

Chemical cues are the language of life (Meinwald et al., 2018), from the initial steps essential for reproduction (Gomez-Diaz & Benton, 2013) through death (Kats & Dill, 1998). The study of how these molecules mediate biological interactions, now known as chemical ecology, dates back to the late 19th century, with earlier research primarily focusing on terrestrial plants and insects (Hartmann, 2008). However, in more recent decades, pioneering work has been done with respect to chemically mediated interactions in aquatic environments (Ferrari et al., 2010; Hay, 2009), and within complex microbial communities (Schmidt et al., 2019), which are main themes of this thesis. Both macro and microorganisms that live underwater rely on chemical cues to inform important life events, especially in regard to locating food and avoiding predation (Hay, 2009). Some of these molecular messages are especially complex in that they are blends, released (i.e., excreted or secreted) into the water column by predators, prey, or even co-existing microorganisms. The effects of chemical mixtures are often much greater than those of individual molecules, but identifying all of the cues involved in specific biological phenomena is difficult (Poulin & Pohnert, 2019). This is especially true in cases where there is substantial naturally occurring chemical variation, the relevant bioassay is very laborious making multiple iterations impractical, the bioassay consumes a lot of material leaving little for structure elucidation methods, or the chemical cues are relatively unstable, such that they would survive an initial extraction, but not many rounds of chromatography.

Statistically driven metabolomics has proven to be an advantageous alternative to the traditional bioassay-guided fractionation method for deciphering important chemical

cues because it allows for circumvention of these obstacles, thus facilitating the elucidation of molecules that mediate marine predator-prey interactions for a deeper understanding of community dynamics (Bayona et al., 2022). Although metabolomics is a relatively young discipline, efforts have been made to begin standardizing methods within the field (Broadhurst et al., 2018; Fiehn et al., 2007; Spicer et al., 2017). Careful consideration of experimental design, sample preparation, and data acquisition is critical to reduce systematic error and avoid batch effects (Alseekh et al., 2021). In preparation for multivariate statistical analyses, spectroscopic data sets (e.g., ^1H NMR and mass spectra) are typically preprocessed via multiple mathematical transformations (Castillo et al., 2011; Dieterle et al., 2006; van den Berg et al., 2006) using various software (Chang et al., 2021; Misra, 2021). Statistical models are then built to pinpoint the most important spectral features that correlate with measured biological observations (Gromski et al., 2015; Xi et al., 2014). Machine learning and variable selection can be used to refine spectral feature lists and improve statistical models in cases where the majority of features are not predictive of the measured biological data (Andersen & Bro, 2010; Broadhurst et al., 1997; Liebal et al., 2020; Sorochan Armstrong et al., 2022). Additionally, many tools have been developed to accelerate the identification of corresponding metabolites using tandem mass spectra (Böcker, 2017; Cao et al., 2021; Dührkop et al., 2019; Kuhl et al., 2012; F. Wang et al., 2021).

Chapter 1 of this thesis explores whether two particular marine metabolites released in blue crab urine, homarine and trigonelline, are common fear cues, utilized by multiple prey to assess danger from this generalist predator. While both molecules were previously found to reduce mud crab feeding, the current investigation revealed that juvenile oysters

also respond to these cues by making stronger shells, a clear defensive response to perceived predation risk. Dose response experiments spanning environmentally relevant concentration ranges revealed that oyster response to these two metabolites is nuanced; oyster shell strengthening significantly increased with trigonelline concentration, while homarine was the most potent at the lowest concentration tested. When exposed to blue crab urine, oysters made stronger shells in a dose-dependent manner; however, homarine and trigonelline urine concentrations did not correlate with induced oyster shell strengthening, indicating that they are not the only, or even the primary cues oysters utilize to assess predation risk. Nonetheless, these results support the idea that common fear molecules exist, and that they may serve as the base for more complex cue mixtures used by specific prey for detecting predators.

In Chapter 2, the chemical composition of blue crab urine was explored using statistically driven metabolomics to determine which cues in this blend are the most important for oyster assessment of predation risk, and whether any of these molecules are also potentially used by mud crabs. Twenty-four blue crab urine mixtures were profiled using ^1H NMR spectroscopy and mass spectrometry, highlighting that urine of different diets (mud crab vs. oyster) is distinct as expected. Partial least squares regression (PLS-R) models revealed that oyster response to blue crab urine was unrelated to diet, unlike mud crabs which associated greater predation risk with urine of predators fed conspecifics. Low urine metabolite concentrations and poor cross-validation of PLS-R models made it impractical to pursue metabolite identification using ^1H NMR spectra, however these data supported that trigonelline was a minor component of the blue crab urine blend related to oyster shell strengthening. Since mass spectral features can be treated as independent

variables for modeling purposes, genetic algorithm variable selection was used to greatly improve the cross-validation of these analyses. Improved PLS-R models pinpointed seven metabolites that correlate with anti-predatory responses of both oysters and mud crabs, as well as additional cues specific to risk assessment by individual prey. These results reveal that there are similarities in fear cue blends used by different prey (i.e., common fear molecules exist), and that there are also blend components uniquely leveraged by specific prey. These distinct fear-inducing cues may be more reliable indicators of predation risk for oysters, therefore emphasizing the importance of their identification.

Chapter 3 investigates unique aquatic bacterial consortia for their potential to protect microalgal crops from pests. Since bacteria are known to produce their own chemical defenses, it was hypothesized that microalgal crops benefit from associations with specific bacterial species that produced protective secondary metabolites (i.e., natural pesticides). Chemical profiling was leveraged to explore the exometabolomes of these protective bacterial communities, but spectroscopic analysis showed very few differences distinguishing protective from non-protective consortia. Additionally, identification of these molecules was not pursued due to low concentrations, and cultures could not be scaled up for further analysis due to irreproducible growth of bacterial consortia. As a result, bacterial extracts were generated from 36 isolates with protective potential and a screening experiment revealed that six were toxic to rotifers. However, rotifer toxicity could not be reproduced, likely because the bacteria were in fact not clonal isolates, as revealed by sequencing results. Alternatively, induction of natural pesticide production by bacteria could require specific environmental conditions such as temperature, nutrients, the presence of competitors, or chemical cues released by predators. A subset of bacteria were

later grown with conditioned media in an attempt to induce the production of protective compounds, but none of these extracts were toxic to rotifers. Bacterial extracts were also generated from the same isolates for testing against a predatory alga, but algal growth appeared to be stimulated rather than suppressed, perhaps by extracted media components. Additionally, attempts were made to cultivate and develop a pesticide screening assay for chytrids, but the selected species grew too slowly, making them non-ideal model organisms for future studies. As a whole, these investigations shed light on the many challenges presented by complex bacterial communities, and their great potential to be leveraged as a source of natural pesticides.

In summation, this thesis explores two distinct biological systems, where communication between predators and prey are mediated by complex blends of waterborne metabolites. The multi-functionality of previously identified chemical cues was explored to determine that taxonomically distinct marine prey use the same molecules to assess predation risk. Metabolomics was leveraged to further investigate the chemical composition of urine from a shared generalist predator, accelerating the identification of additional common fear cues and potentially more reliable, specific blend components utilized by individual prey. Furthermore, chemical profiling of microalgal exometabolomes combined with an examination of associated unique bacteria stressed the difficulties associated with dereplicating chemical cues from non-model predator-prey systems and the need for development of new methods to address them. Overall, this work provides insights and emphasizes major challenges with respect to identification of important waterborne chemical mediators of predator-prey interactions.

CHAPTER 1. COMMON FEAR MOLECULES INDUCE DEFENSIVE RESPONSES IN MARINE PREY ACROSS TROPHIC LEVELS

The work presented in this chapter is the result of a collaborative project between chemists and ecologists (Roney et al., 2023). As a chemist, and one of the co-first authors of this study, I made substantial contributions to project design, method development, data acquisition, data analysis, interpretation of results, and writing. Data that I acquired and analyzed are in Figs. 1.1, 1.2, 1.3, 1.4, 1.5, 1.6, and 1.8. My analyses of quantitative ^1H NMR and mass spectral data (Fig. 1.2) ensured that all experiments used ecologically relevant concentrations of chemical cues. I conducted correlational analyses of quantified metabolites to determine their relationship to each other (Figs. 1.3 and 1.4), performed statistical analyses to assess the effect of predator cues on oyster shell strengthening (Fig. 1.1), and used regression analyses to probe the relationship between this induced defense and cue concentrations (Figs. 1.5, 1.6, and 1.8).

1.1 Abstract

Predator-prey interactions are a key feature of ecosystems and often chemically mediated, whereby individuals detect molecules in their environment that inform whether they should attack or defend. These molecules are largely unidentified, and their discovery is important for determining their ecological role in complex trophic systems. Homarine and trigonelline are two previously identified blue crab (*Callinectes sapidus*) urinary metabolites that cause mud crabs (*Panopeus herbstii*) to seek refuge, but it was unknown

whether these molecules influence other species within this oyster reef system. In the current study, homarine, trigonelline, and blue crab urine were tested on juvenile oysters (*Crassostrea virginica*) to ascertain if the same molecules known to alter mud crab behavior also affect juvenile oyster morphology, thus mediating interactions between a generalist predator, a mesopredator, and a basal prey species. Oyster juveniles strengthened their shells in response to blue crab urine and when exposed to homarine and trigonelline in combination, especially at higher concentrations. This study builds upon previous work to pinpoint specific molecules from a generalist predator's urine that induce defensive responses in two marine prey from different taxa and trophic levels, supporting the hypothesis that common fear molecules exist in ecological systems.

1.2 Introduction

Predator-prey interactions are a strong driver of community dynamics, as predator presence stimulates prey adaptations that can result in large ecosystem-wide effects (Hay, 1996, 2009; Lima, 1998). Mechanisms employed by prey to reduce predation risk include upregulating chemical defenses (Baldwin, 1998; Cronin & Hay, 1996), behavioral modifications or habitat shifts to avoid detection (Schmitz, 2008; Weissburg et al., 2016; Werner & Gilliam, 2003), morphological alterations (Brönmark & Miner, 1992), changes in life history (Peckarsky, 1980; Peckarsky et al., 2001), or some combination of these (Hammill et al., 2010). While evolutionary pressures like predation select for advantageous traits (Lima, 1998), considerable investment may be required to implement these strategies, which often come with trade-offs such as lower energy reserves and slower growth (Herms & Mattson, 1992; Lima, 1998; Nakaoka, 2000). Nevertheless, when these defenses are inducible, prey may strike a better balance between defending against predation and the

inevitable costs, especially when predators can be sensed reliably and predation risk is variable in space or time (Harvell, 1990).

Prey may use several sensory modes to recognize a predator (Weissburg et al., 2014), and substantial evidence supports the hypothesis that many prey rely on detecting a predator's scent (Kats & Dill, 1998), particularly when other cues are inaccessible. Organisms in early developmental stages and numerous invertebrates have rudimentary or undeveloped auditory and visual systems, so chemical cues are often their primary source of information about their surroundings (Hay, 2009). In aquatic habitats, chemical cues are essential for detecting predators because visual and auditory cues are frequently variable and therefore unreliable due to turbidity, low light, or other physical limitations (Dusenbery, 2001; Weissburg et al., 2014). For example, Western toad tadpoles exhibit anti-predator behavior when exposed to chemical, but not visual, cues of several different predators (Kiesecker et al., 1996), indicating that the discovery of these molecules is important for fully understanding the selection pressures that drive prey adaptations and distributions. In addition to reducing predation success, prey responses to chemical cues can lead to a wide range of non-consumptive effects including alterations to predator handling times, increases in basal resources, or changes in competitive ability (Brönmark & Miner, 1992; Relyea, 2001). Even though it is widely accepted that chemical cues play a significant role in shaping ecosystems, the specific metabolites that modulate predator-prey interactions in aquatic systems remain mostly unidentified (Lass & Spaak, 2003), especially for inducible prey defenses (Brönmark & Miner, 1992; Hammill et al., 2010; Smee & Weissburg, 2006).

Along the eastern and gulf coasts of the United States, the eastern oyster

Crassostrea virginica is a foundation species and major food source for diverse predators (O'Connor et al., 2008) highlighting the need for oysters to have robust defenses. Although exposure to seawater containing predator exudates causes oysters to develop heavier, stronger shells (Newell et al., 2007; Ponce et al., 2020; E. M. Robinson et al., 2014; Scherer et al., 2016; Scherer & Smee, 2017) their responses to chemical cues indicative of predation risk may vary substantially depending upon numerous factors such as predator type (Belgrad, Knudson, et al., 2023; E. M. Robinson et al., 2014), predator diet (Scherer et al., 2016, 2017), and temporal variation in risk response (Eason et al., 2021; Scherer et al., 2018). Yet, the bioactive molecules mediating these interactions remain unknown, and the variation in responses to predation risk remains ambiguous.

Mud crabs, *Panopeus herbstii*, prey upon oysters, filling a meso-trophic level (i.e., the intermediate prey) between this basal resource and their shared predator, the generalist blue crab *Callinectes sapidus*, which consumes a variety of species including mud crabs and oysters (Laughlin, 1982; Tagatz, 1968). These smaller crabs detect the presence of danger by interpreting specific metabolites, homarine and trigonelline, in blue crab urine as signs of high predation risk, with cue exposure inducing them to promptly hide instead of forage for food (Poulin et al., 2018; Weissburg et al., 2016). Oysters also respond defensively to this shared predator by strengthening their shells when exposed to exudates from blue crabs (Scherer et al., 2016, 2017), however, the molecules mediating this interaction are unknown. Given that this predator feeds on many types of prey, selection pressure may incentivize predator waste products as reliable cues, and as homarine and trigonelline are known components of blue crab waste excreted via urine, oysters may also associate these chemical cues with danger.

Since oysters and mud crabs coexist in estuarine reefs and are both preyed upon by blue crabs, we investigated whether juvenile oysters respond to the same metabolites as mud crabs and if this response is concentration-dependent. Although mud crabs and oysters are taxonomically distinct and occupy different trophic levels, selection pressure from predation risk by blue crabs may have prompted prey to evolve responses to the same predator cues, specifically in the waste products of this generalist predator. Thus, we hypothesize that common fear molecules exist in environments with heavy predation pressure from generalist consumers. Given that homarine and trigonelline are seemingly ubiquitous in the marine environment (Boysen et al., 2021; Dawson et al., 2020; Heal et al., 2021; Núñez-Pons & Avila, 2015), and known blue crab urine metabolites that reduce mud crab foraging, thus lowering their risk of predation (Poulin et al., 2018; Weissburg et al., 2016), this study probed whether both molecules also induce oysters to defend themselves by making stronger shells. Testing known ecologically relevant molecules is an essential step for a deeper comprehension of marine ecosystem dynamics, especially because chemical cues are known to regulate biological phenomena (Ferrari et al., 2010; Harborne, 2001; Hay, 2014; Pohnert et al., 2007). Therefore, it is imperative that these bioactive cues be identified to better predict how chemistry influences multi-trophic level interactions, and in turn prey evolution.

1.3 Methods

We performed a series of experiments to test how the effects of known metabolites in the urine of a generalist predator affected morphological defenses in one of their prey. We examined the effects of blue crab urine and two molecules, homarine and trigonelline, on oyster shell morphology as these molecules are known to be present in blue crab urine

and influence antipredator behavior in another species. We then performed dose response experiments to ascertain the relevant concentrations that elicited responses and confirm if concentration was also important for oysters in governing the strength of their response to predation risk. All biological experiments were performed at the Dauphin Island Sea Lab in Dauphin Island, AL, USA over three years (July – Sept. 2020, June – Aug. 2021, and Aug. – Oct. 2022). The predator cue bioassay was performed July – Sept. 2020, the homarine and trigonelline dose response experiment was performed June – Aug. 2021, and the blue crab urine dose response was performed August – Oct. 2022.

1.3.1 Predator Cue Bioassay (July – Sept. 2020)

For the predator cue bioassay, oyster spat were exposed to one of the following cues in individual aquaria: blue crab urine (mud crab or oyster diet), trigonelline (24.6 μM), homarine (15.1 μM), or trigonelline (24.6 μM) + homarine (15.1 μM). Additionally, we used natural seawater taken directly from the Gulf of Mexico (settled for 3 days to remove sediment) as a negative control and predator water, water from a tank with actively foraging blue crabs, as a positive control.

Diploid oyster larvae were purchased from the Auburn University Shellfish Laboratory and settled onto 4.5 cm \times 4.5 cm marble tiles to become oyster spat. For one week after settlement, spat on tiles were caged and kept in 1250 L mesocosms with natural flowing seawater from the Gulf of Mexico at a flow rate of 20 L/min. This time was necessary for spat to grow and become firmly attached to the tiles for subsequent experiments.

After one week, we moved the spat tiles into closed aquaria (without flowing seawater) to test oyster shell changes in response to our treatments. Only tiles with at least 15 spat were used. Tiles were tied together with high-density polyethylene fishing line with the side containing oyster spat facing outwards. Three tile pairs were placed in each aquarium, ensuring that every tile pair was upright to maintain good water flow around the spat. An intact, sun-bleached adult oyster shell was also placed into each aquarium for spat tile pairs to lean on so that they maintained an upright position to avoid smothering. Aquaria were filled with 2 L of natural seawater (with the exception of the predator water control, which received 1.5 L seawater + 0.5 L predator water). Seawater was supplemented with either Instant Ocean salt or deionized water to reach 20 ppt (± 2 ppt). Each aquarium was aerated with filtered air, covered with a lid to reduce evaporation, and stored outside under a covered pavilion in a water bath containing ambient flow-through seawater to regulate temperature. Aquarium aeration via airstone provided circulation within the system and because of the small volume (2 L) of each aquaria, circulation pumps were unnecessary. Spat were fed Reed Mariculture Instant Algae Shellfish Diet 1800 (a proprietary, non-living mixture of *Isochrysis*, *Pavlova*, *Tetraselmis*, *Thalassiosira weissflogii* and *Thalassiosira pseudonana*). At the start of the experiment, spat were fed 0.5 mL twice daily, but we increased this amount to 1 mL twice daily as spat grew larger. Complete water changes and aquarium cleanings were performed twice weekly to deter accumulation of ammonia, nitrates, food waste, and changes in pH, and 1 mL of predator chemical cues (i.e., blue crab urine, solutions of trigonelline, homarine, or a combination) were added to the aquaria immediately after water changes. The pH and salinity of each aquarium was recorded before water changes, and these physical factors did not cause

concern at any point in the experiment (Appendix A, Table A1). Predator water was created by housing 6 blue crabs (carapace width 12-17 cm) in a 238 L volume mesocosm of recirculating filtered natural seawater (50% water changes performed every 1-2 weeks) and feeding each crab an adult oyster (length 6-7 cm). Three to five hours after feeding crabs, 500 mL of this water was added to each positive control aquarium.

Homarine (15.1 μM) and trigonelline (24.6 μM) solutions used to induce oyster spat were prepared at natural concentrations found in urine of blue crabs fed an Eastern oyster diet (Poulin et al., 2018), and a later analysis revealed that our chosen experimental concentration of trigonelline occurs at the upper limit of natural concentration ranges in blue crab urine from our population (Fig. 1.2). Homarine (Santa Cruz Biotechnology Company) and trigonelline (Toronto Research Chemicals) were dissolved in deionized water to create individual stock solutions of each chemical, which were aliquoted and frozen at $-80\text{ }^{\circ}\text{C}$ to avoid repeated freezing and thawing of the chemical mixture. On days designated for cue addition, the stock solution aliquots were diluted to the experimental concentration (15.1 μM homarine and 24.6 μM trigonelline) and the trigonelline + homarine combination treatment was diluted and combined to achieve the same final concentration of each individual chemical solution (15.1 μM homarine + 24.6 μM trigonelline) to most realistically mimic urine. 1 mL of solution was then immediately added to each corresponding replicate aquarium. After chemical cue addition, final concentrations in aquaria were 7.55 nM homarine and 12.3 nM trigonelline. These concentrations fall within the range in which these molecules have been detected in the natural environment (Boysen et al., 2021; Dawson et al., 2020; Heal et al., 2021; Muslin, 2017; Rasyid, 2021) and should be comparable to the exposure oyster spat would

experience in a wild habitat.

Predator urine was collected from blue crabs fed two different diets, oysters or mud crabs. Blue crabs were collected from crab pots near Dauphin Island, AL, USA and housed in 1250 L mesocosms flowing with natural seawater. Crab size ranged from 11-19 cm, measured from spine to spine on the widest part of the carapace. Crabs were starved for 2-3 days and then were each fed either one adult oyster (~6-7 cm length) or ~5 g of frozen mud crabs every 48 hours to standardize diets. Mud crabs used for feeding were collected from either Priest's Landing, Skidaway Island, GA (31°57'44.89"N, 81° 0'48.22"W) or the North Inlet Estuary, SC (33°21'52"N, 79°10'03"W). Crabs were maintained on these diets for one week prior to the urine extraction regimen to ensure all extracted metabolites were from the specified diets and that crabs were not undergoing any starvation stress that could affect the chemistry of their urine. Urine was collected from individuals twice a week. Crabs were cooled to quiescence, then a 23 gauge-needle was inserted approximately 2 mm into the nephropore and urine was extracted with gentle vacuum suction (<10 psi) into clean glass vials. Urine used for the experiment was clear or yellow in color and foamy; urine was discarded if it appeared cloudy or bluish-gray in color, as this indicated contamination with hemolymph. Urine was frozen at -80 °C immediately after collection. Urine from blue crabs fed an oyster diet was collected from 161 crabs, each crab provided 4.08 ± 3.11 mL per collection, and urine was extracted from them 2.2 ± 1.0 times. Urine from blue crabs fed a mud crab diet was collected from 102 crabs; each crab provided 5.04 ± 4.07 mL per collection and was used for extraction 2.0 ± 1.0 times. We later combined the urine of different individuals into 9 mixtures using the fewest individuals possible,

where each mixture was considered a biological replicate (Appendix A, Table A2). These mixtures were then partitioned into 1 mL aliquots and stored at -80°C until use.

In this bioassay, all treatments and controls had 9 replicates. The experiment was performed July 2020 through Aug. 2020, for a total of 48 days before being disrupted due to heavy storms in Dauphin Island, AL. At the completion of the experiment, spat from each aquarium were randomly selected for assessment of shell strength. Approximately 20 oysters were crushed from each aquarium (distributed across tile pairs), except for one predator water replicate (15 oysters) and one trigonelline replicate (19 oysters) due to high mortality. Individual spat width was measured for each crushed oyster to 0.01 mm using a Vernier digital caliper. The force required to crush oysters was measured to the nearest 0.1 N using a Kistler 5995 charge amplifier and Kistler 9207 force sensor following standard protocol (E. M. Robinson et al., 2014). Crushing force was divided by spat width to produce a size-standardized metric of shell strength (i.e., standardized crushing force, N/mm) because larger individuals typically have a stronger shell as a byproduct of their size (Fig. A1). Standardized crushing force measurements for oysters within the same aquarium were averaged. Some measurements were removed from analysis if the oysters were found dead or if the crushing device malfunctioned, resulting in fewer spat contributing to an aquarium average. Some aquaria suffered high mortality and were unusable for analysis. When the experiment concluded, 9 replicate aquaria per treatment were used except for the predator water positive control (n=7) and trigonelline + homarine (n=8) treatments.

1.3.2 Homarine and Trigonelline Dose Response Experiment (June – Aug. 2021)

An experiment was designed for the following year (June – Aug. 2021) to test whether oysters respond to homarine, trigonelline, and both cues combined in a dose-dependent manner. Experimental set up and aquaria maintenance followed almost identical protocols to those used in 2020. Stock solutions for homarine (7.4 mM) (Santa Cruz Biotechnology Company), trigonelline (6.6 mM) (Toronto Research Chemicals), and homarine + trigonelline were prepared in liquid chromatography mass spectrometry (LCMS) grade water, aliquoted to avoid freezing and thawing the solutions more than once, and stored at -80°C . Serial dilutions for each cue were prepared in deionized water the same day they were added to their respective aquaria (Appendix A, Table A3). Concentrations were determined by calculating half-log steps encompassing the natural concentrations of homarine and trigonelline found in the urine of blue crabs fed an oyster diet (Fig. 1.2). On the day of cue addition, serial dilutions were performed with deionized water and using a micropipette (for volumes under 5 mL) and 10 mL graduated cylinder (for volumes greater than 5 mL). Mixtures were vortexed for 10 seconds and manually agitated for 10 seconds before continuing with the serial dilution. Dilutions for treatments of individual compounds and the homarine + trigonelline treatments were prepared at the same half-log concentrations (Appendix A, Table A3). The same stock solutions were used to prepare both the individual compound and homarine + trigonelline treatments. All serial dilutions were done in tandem. Once chemical mixtures were made, they were stored in glass bottles, and 1 mL of each solution was pipetted into the appropriate experimental aquaria with a clean pipette tip. Chemical solutions were added after water changes, which were performed twice weekly. This experiment also included a seawater control group, which received the same care (without cue addition) as all other experimental aquaria.

The preparation and maintenance of the homarine and trigonelline dose response experiment was identical to the previous predator cue bioassay except aquaria received four tile pairs per aquarium instead of three. The experiment was conducted for 56 days (8 weeks), and at the completion of the experiment tile pairs were removed from their aquaria, measured, and crushed according to the same methodology from the predator cue bioassay. There were four replicate aquaria per concentration, and within these replicate aquaria, we took an average of 17 crushed oysters. Replicates with high mortality (less than 6 spat alive) were excluded from statistical analyses. In total, 14 aquaria from the homarine dose array, 16 aquaria from the trigonelline dose array, and 17 aquaria from the trigonelline + homarine dose array were included in statistical analysis (Appendix A, Table A3).

1.3.3 Urine Dose Response Experiment (July – Oct. 2022)

A blue crab urine dose response experiment was designed to determine whether differences in oyster shell strengthening could be fully explained when considering the complete blend of blue crab urine cues. The experiment was conducted for 56 days (8 weeks) from Aug. 2022 – Oct. 2022. Blue crabs were collected from crab pots near Dauphin Island, AL and stored in the same facility and conditions as described for the predator cue bioassay (2020). Urine collection methods remained the same as for previous experiments (2020 predator cue bioassay) except urine was pooled from all crabs for this experiment. All crabs for this experiment were fed an oyster diet (i.e., one adult oyster (~6-7 cm in length) twice weekly). Crab were kept in aquaria for a one-week acclimation period before beginning a urine extraction regimen. Urine was collected twice weekly from 22 crabs that ranged 13 – 18 cm in size and each crab produced 1.31 ± 0.18 mL. Urine dose concentrations were determined based on the average concentrations of homarine and

trigonelline quantified in blue crab urine in the 2020 predator cue bioassay (homarine, $13 \pm 21 \mu\text{M}$; trigonelline, $3.6 \pm 6.9 \mu\text{M}$). It was assumed that 1 mL of pooled blue crab urine contained these concentrations, and doses were adjusted by half-log steps until approximated concentrations of homarine and trigonelline spanned four orders of magnitude (Appendix A, Table A4). Though initial experimental design was based on an assumed concentration of homarine and trigonelline, all urine doses were reported as urine volume divided by the total volume of seawater within an experimental aquaria. For the six lowest doses, 1 mL aliquots of blue crab urine were prepared via serial dilution. The two highest doses received 5.00 mL and 1.25 mL aliquots of pure urine respectively. All aliquots were frozen at $-80 \text{ }^\circ\text{C}$ to be used on the day of cue addition.

1.3.4 Quantification of Homarine and Trigonelline

All chemical analyses were performed at the Georgia Institute of Technology, Atlanta, GA, USA. Concentrations for stock solutions of trigonelline and homarine prepared for the predator cue bioassay (summer 2020) and quantitative standards were determined using nuclear magnetic resonance (NMR) spectroscopy (Bharti & Roy, 2012). For preparation of standards, trigonelline and homarine were dissolved in LC-MS grade water. Both stock solution and standard samples were prepared for quantitative NMR spectroscopic analysis by combining 138 μL sample, 46 μL phosphate buffer in D_2O and 16 μL D_2O . A caffeine standard (0.00949 mg) was dissolved in 138 μL LC-MS grade water, 46 μL phosphate buffer in D_2O and 16 μL D_2O . A benzene- d_6 NMR insert capillary tube was used as the reference standard. Spectroscopic data were acquired using a Bruker Avance IIIHD 800 MHz NMR spectrometer and processed in MestReNova 11.0.4. All calculations were done in Microsoft Excel (Office 365).

Standard solutions previously quantified using NMR spectroscopy were used for mass spectroscopic quantification of trigonelline and homarine in multiple samples: 24 blue crab urine mixtures (12 oyster diet and 12 mud crab diet) from the predator cue bioassay (summer 2020) and stock solutions of trigonelline and homarine prepared for the dose response experiment (summer 2021). For preparation of urine samples, 20 μL of urine was added to 180 μL of methanol, solutions were vortexed for mixing, centrifuged at $19980 \times g$ to pellet precipitate, and the supernatant was transferred to clean new vials. Serial dilutions of samples and standards were prepared using 90% aqueous methanol so that concentrations for homarine and trigonelline fell within the nanomolar range. All standards were injected in triplicate, as were dilutions prepared for the dose response curve stock solutions. These stock solutions were diluted to two concentrations within the linear range of the curve, each dilution was injected three times, and final concentrations were determined by averaging data from all six injections. Concentrations of analytes in urine were determined from a single injection. Peak areas were integrated using Xcalibur Version 4.3.73.11 (Thermo Fisher Scientific) and linear regression analyses were performed in GraphPad Prism 9.3.0 for Windows to generate standard curves. Concentrations for urine samples and stock solutions interpolated using standard curves were converted to natural concentration in micromolar using Microsoft Excel for Windows.

Data for standards and urine samples were acquired using a Vanquish ultraperformance liquid chromatography setup coupled to a high-resolution accurate mass Orbitrap ID-X Tribrid mass spectrometer (Thermo Fisher Scientific). A Waters Corporation ACQUITY UPLC BEH Amide column (2.1×150 mm, $1.7 \mu\text{m}$ particle size) was used for chromatographic separation. Analytes were eluted using 4:1 water/acetonitrile

with 10 mM ammonium formate and 0.1% formic acid (mobile phase A) and acetonitrile with 0.1% formic acid (mobile phase B) using the following gradient program: 0 min 5% A; 0.5 min 5% A; 8 min 60% A; 9.4 min 60% A; 9.5 min 5% A; 12 min 5% A. The flow rate was set at 0.40 mL/min, the column temperature was set to 40 °C, and the injection volume was 1 µL.

1.3.5 Statistical Analyses

For the predator cue bioassay, a one-way ANOVA was performed on the data (n=9 for all treatments except predator water, n=7, and trigonelline + homarine, n=8), followed by an uncorrected Fisher's Least Significant Difference (LSD) test for pairwise comparisons of each treatment and the seawater negative control (Fig. 1.1). Simple linear regression analyses were done to assess the relationship between chemical cue concentration (i.e., trigonelline, homarine, or trigonelline + homarine) in blue crab urine used for the predator cue bioassay and standardized crushing force (Figs. 1.3 and 1.5). One urine sample was excluded from the trigonelline analyses because the measured concentration was below the limit of quantitation. Additionally, quantified concentrations of homarine and trigonelline in blue crab urine were regressed against each other using simple linear regression (Figs. 1.4 and A1). All predator cue bioassay regression analyses were done for the individual diets (i.e., oyster or mud crab) and both diets combined.

For the pure cue (Fig. 1.6) and urine dose response (Fig. 1.7) experiments, cue concentration was regressed against standardized crushing force using semilog line regression where X is log and Y is linear. Concentrations of homarine and trigonelline above those naturally found in blue crab urine were excluded from analyses of the pure

chemical dose response (Appendix A, Table A3). A nested one-way ANOVA was used to compare cue concentrations for dose response curves where the slope of the linear model was not significantly non-zero, and an uncorrected Fisher's LSD test was used for pairwise comparisons of cue concentrations to seawater (i.e., Fig. 1.6A).

Values plotted on the x-axes for the trigonelline + homarine analyses (Figs. 1.5C and 1.6C) were generated by adding the concentrations of these molecules together. Considering their sum as a single independent variable allowed for the assessment of trigonelline + homarine as a blend. All statistical analyses were performed using GraphPad Prism 9.3.0 for Windows.

1.4 Results

1.4.1 Oyster Shell Strengthening Induced by Predator Cues

Predator chemical cues induced oysters to strengthen their shells (Fig. 1.1; ANOVA, $F(6, 53) = 3.97$, $P = 0.002$). Homarine (15.1 μM) (Fisher's LSD, $P = 0.008$) and predator water (Fisher's LSD, $P = 0.005$) significantly induced oyster shell strengthening when compared to the seawater control; however, trigonelline (24.6 μM) did not (Fisher's LSD, $P = 0.27$). Despite trigonelline not having an effect on its own at 24.6 μM , oysters made significantly stronger shells when exposed to a mixture of trigonelline (24.6 μM) + homarine (15.1 μM) (Fisher's LSD, $P < 0.0001$). Furthermore, mud crab and oyster diet blue crab urine treatments were both significantly potent (mud crab diet, Fisher's LSD, $P = 0.034$; oyster diet, Fisher's LSD, $P = 0.033$).

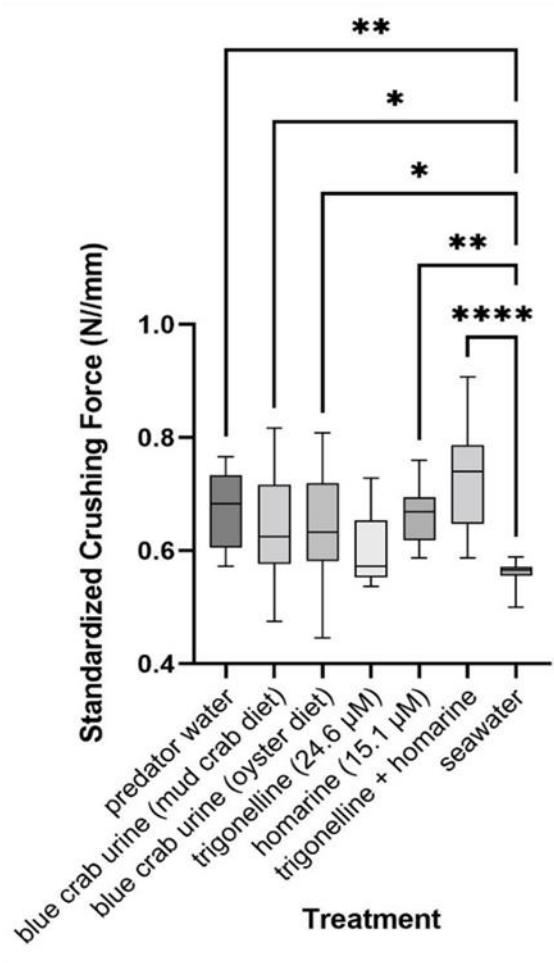


Figure 1.1 Oyster spat were exposed to predator water (n=7), blue crab urine (n=9 per diet type), pure chemical compounds homarine or trigonelline (n=9), a combination of homarine + trigonelline (n=8), or seawater (n=9). Their shells were crushed and the measured force was normalized to shell width (i.e., standardized crushing force). A one-way ANOVA followed by an uncorrected Fisher's LSD test compared the means of all treatments to the seawater control. Predator water, blue crab urine of both diets, homarine (15.1 μM) and homarine + trigonelline induced significantly stronger oyster shells than seawater. Trigonelline (24.6 μM) did not significantly induce stronger shells. This box-and-whisker plot shows the median of each treatment, the upper and lower quartiles, and the minimum and maximum bounds for each treatment. Treatments are denoted as significant with * at $P \leq 0.05$, ** at $P \leq 0.01$ and **** at $P \leq 0.0001$.

1.4.2 *Homarine and Trigonelline in Blue Crab Urine Do Not Fully Explain Induced Oyster Defenses*

For the quantification of chemical cues within natural blue crab urine mixtures,

concentrations of homarine and trigonelline were quite variable, spanning several orders of magnitude. Homarine concentrations ranged from 0.4 – 65 μM and trigonelline from 0.1 – 22 μM , respectively (Fig. 1.2). It was hypothesized and later confirmed that higher concentrations of homarine quantified in blue crab urine correlated positively with higher concentrations of trigonelline ($F(1, 21) = 246, P < 0.0001, R^2 = 0.92$; Fig. 1.3). This relationship was also significant when the two blue crab diets were analyzed separately (mud crab diet, $F(1, 10) = 68.3, P < 0.0001, R^2 = 0.87$; oyster diet, $F(1, 9) = 150, P < 0.0001, R^2 = 0.94$; Fig. 1.4). Additionally, concentrations of homarine ($F(1, 16) = 2.44, P = 0.14$), trigonelline ($F(1, 15) = 4.47, P = 0.052$), and homarine in combination with trigonelline ($F(1, 15) = 2.44, P = 0.14$) in blue crab urine trended negatively with standardized crushing force but not significantly (Fig. 1.5). This was also true when diets were analyzed separately (Fig. 1.3).

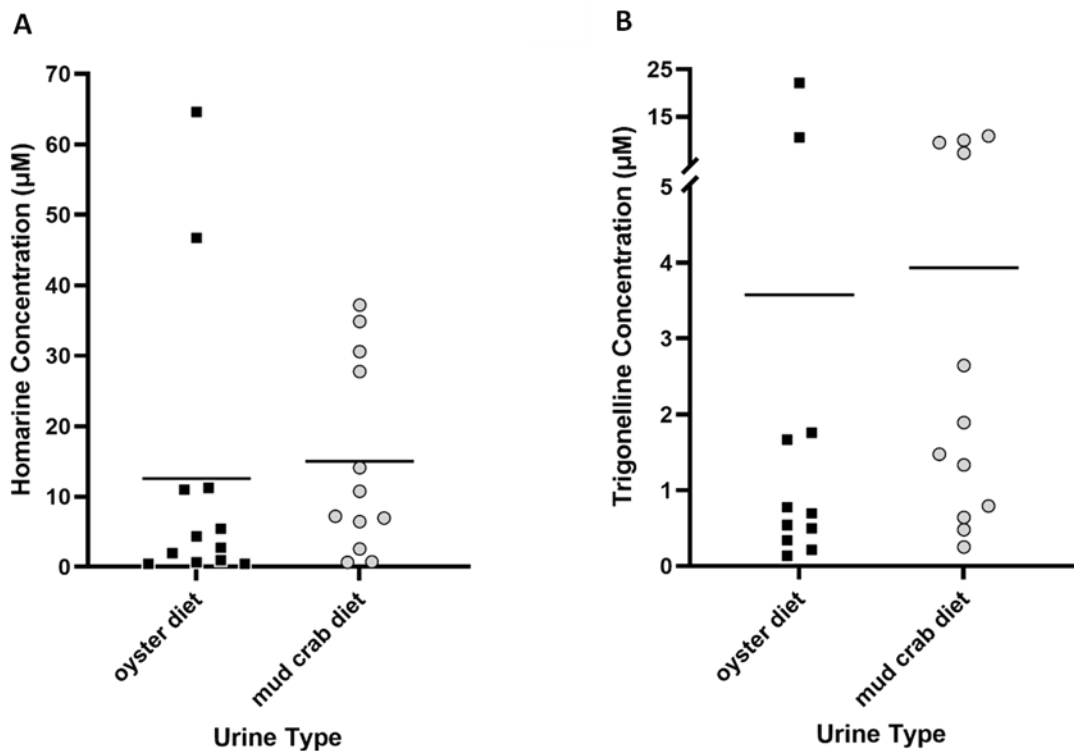


Figure 1.2 Concentrations of homarine (A) and trigonelline (B) quantified for 24 blue crab urine mixtures (oyster or mud crab diet) via LCMS. Homarine concentrations were generally higher than corresponding trigonelline concentrations for the same urine mixture. Concentrations for both metabolites spanned three orders of magnitude. Homarine concentrations ranged from 0.4 – 65 µM. Trigonelline concentrations ranged from 0.1 – 22 µM. Black bars represent the mean for each treatment. Data were excluded for samples where concentrations were below the limit of quantitation.

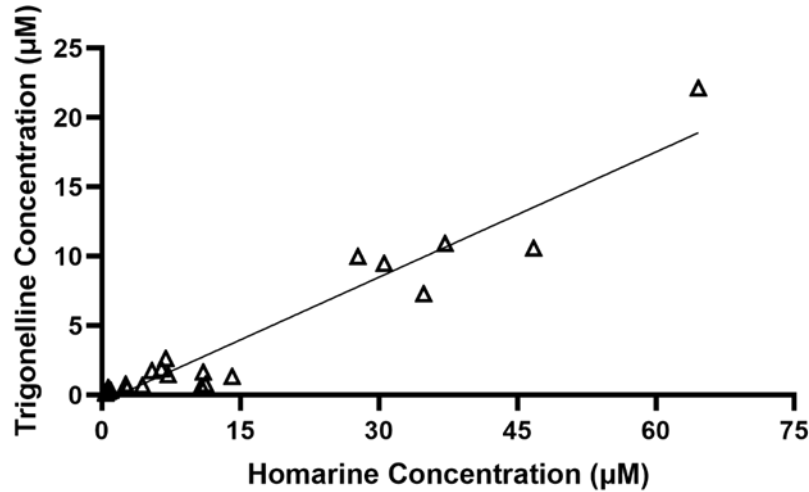


Figure 1.3 Linear regression of homarine versus trigonelline concentrations for 23 blue crab urine samples ($F(1, 21) = 246, P < 0.0001, R^2 = 0.92$). Although the ratio of these metabolites is not fixed, there is a significant positive correlation for homarine and trigonelline concentrations when urine samples are analyzed irrespective of diet (mud crab or oyster). Data were excluded for concentrations below the limit of quantitation.

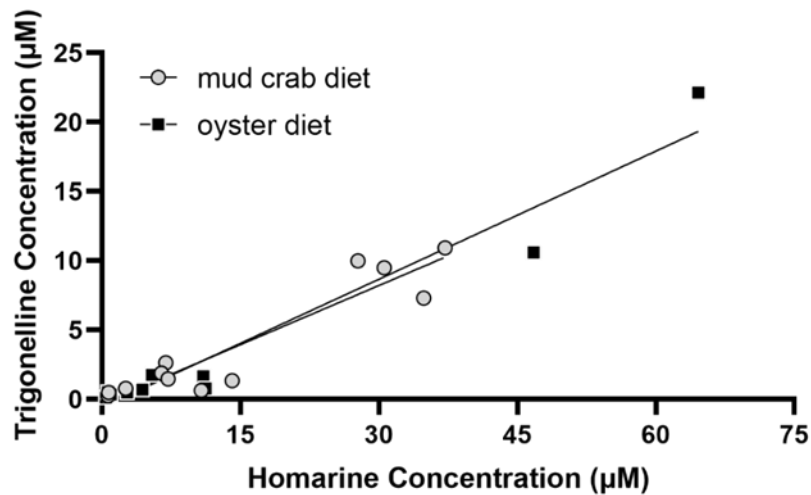


Figure 1.4 Linear regression analyses of homarine and trigonelline concentrations quantified in urine of blue crabs fed two different diets. The positive correlations between homarine and trigonelline concentrations for mud crab ($n = 12$, circles) and oyster diets ($n = 11$, squares) are significant (mud crab diet, $F(1, 10) = 68.3, P < 0.0001, R^2 = 0.87$; oyster diet, $F(1, 9) = 150, P < 0.0001, R^2 = 0.94$). Data were excluded for concentrations below the limit of quantitation.

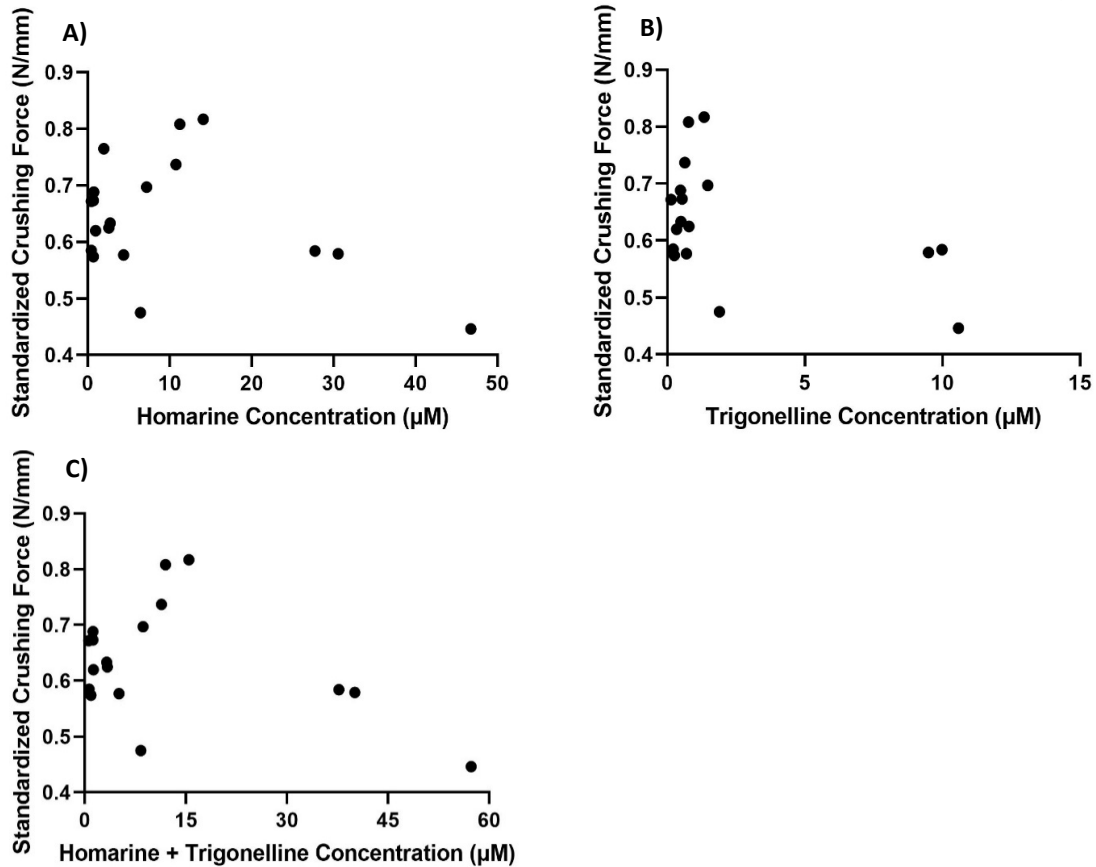


Figure 1.5 Linear regression analyses of chemical cue concentrations quantified for blue crab urine from the predator cue bioassay. Models suggest that homarine (A), trigonelline (B) and their combined concentrations (C) were not reliable indicators of induced oyster shell strengthening for oysters exposed to blue crab urine. Analyses were performed for combined diets: A) homarine concentration ($F(1, 16) = 2.44, P = 0.14$), B) trigonelline concentration ($F(1, 15) = 4.47, P = 0.052$), and C) trigonelline + homarine concentration ($F(1, 15) = 2.44, P = 0.14$). Oyster spat were exposed to one of 17 crab urine mixtures (oyster diet, $n=8$, mud crab diet, $n=9$), crushed, and crushing force was standardized by oyster shell width. Each point is an average of 20 oyster spat. Data were excluded for concentrations below the limit of quantification.

1.4.3 Oyster Response to Cue Concentration is Dose-Dependent

Results from the predator cue bioassay justified an evaluation of oyster response to a wider range of concentrations for pure chemical cues: trigonelline, homarine, and homarine + trigonelline (Fig. 1.1). Trigonelline potency increased with concentration up to

24 μM ($F(1, 18) = 10.2$, $P = 0.005$, $R^2 = 0.36$; Fig. 1.6B), which was close to the natural concentration maximum (22.1 μM) in blue crab urine from predator cue bioassays conducted in summer 2020 (Fig. 1.2). However, trigonelline did not induce stronger oyster shells at the slightly higher concentration, 24.6 μM , tested in the 2020 predator cue bioassay (Fig. 1.1), nor at higher concentrations tested within the dose response experiment (Appendix A, Table A3). In other words, juvenile oysters did not strengthen their shells when exposed to concentrations of trigonelline above natural concentrations in blue crab urine. In contrast, homarine potency did not significantly increase with concentration ($F(1, 16) = 4.01$, $P = 0.063$, $R^2 = 0.20$; Fig. 1.6A), however it did induce oysters to make the strongest shells at 0.85 μM , almost twice as strong as oysters exposed only to seawater. Notably, this was the lowest non-zero concentration of homarine tested (ANOVA, $F(5, 12) = 4.00$, $P = 0.023$; Fisher's LSD, $P = 0.001$, Fig. 1.6A), suggesting that even lower concentrations of homarine might induce a stronger response. The potency of homarine in combination with trigonelline also increased with concentration, providing more support for the hypothesis that these molecules have the strongest effect on oyster shell strength when presented together ($F(1, 19) = 13.6$, $P = 0.002$, $R^2 = 0.42$; Fig. 1.6C).

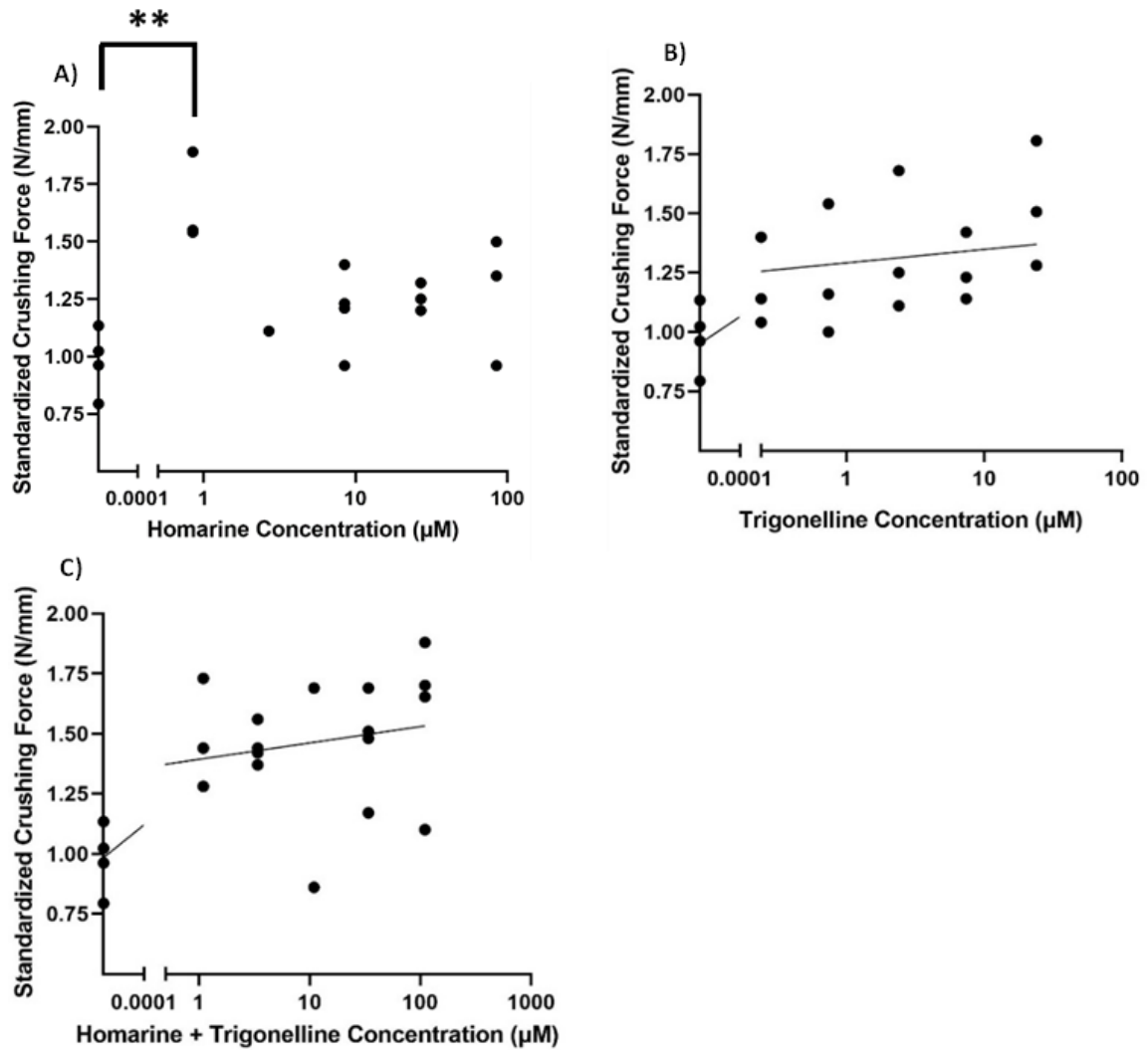


Figure 1.6 Dose response curves for oyster spat exposed to solutions of homarine (A), trigonelline (B), or a combination of homarine and trigonelline (C), with concentrations spanning five orders of magnitude. The slopes of B and C non-linear regression analyses are significantly non-zero ($P = 0.005$ and $P = 0.002$, respectively) indicating that standardized crushing force increases with higher concentrations of chemical cue. The non-linear regression analysis for A was not significantly non-zero ($P = 0.063$), however, the $0.84 \mu\text{M}$ homarine dose was significantly different from seawater (Fisher's LSD pairwise comparison, $P = 0.001$). Seawater controls are plotted on the y axes since the concentrations of chemical cue in these treatments is considered to be $0 \mu\text{M}$. Each point is an average of 6-17 oysters. Crushing force was standardized by oyster shell width.

Given that oyster response was not entirely explained by homarine and trigonelline concentrations (Fig. 1.5), an additional experiment was designed to test the dose

dependency of blue crab urine as a natural mixture. Blue crab urine potency significantly increased with concentration ($F(1, 43) = 44.0, P < 0.0001, R^2 = 0.5785$, Fig. 1.7), providing further evidence for the dose-dependent nature of oyster shell strengthening and the role of other urinary metabolites in this interaction. The 6.6 million-fold dilution of blue crab urine (i.e., 1.50×10^{-7} within experimental aquaria) was the lowest dose that significantly induced oyster defenses (one-way ANOVA w. multiple comparisons, $P = 0.012$, Fig. 1.7), and was notably much lower than the two-thousand-fold dilution that was previously observed to induce oyster shell strengthening (Fig. 1.1).

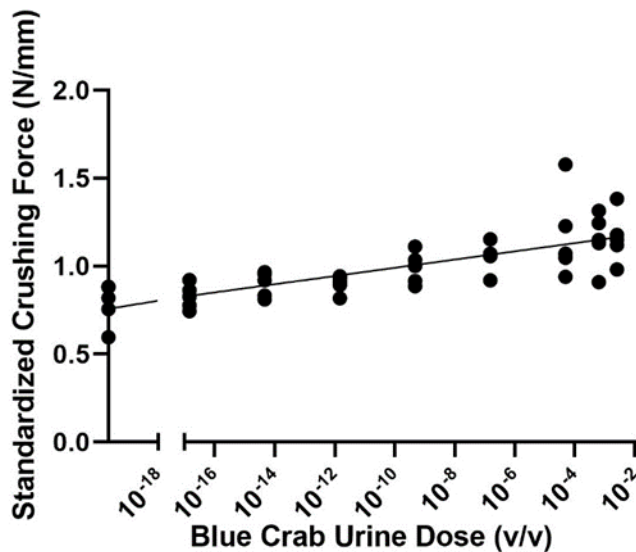


Figure 1.7 A dose response curve for oyster spat exposed to urine of blue crabs fed exclusively oysters. Eight different urine concentrations were tested spanning several orders of magnitude. Urine potency increased significantly with concentration (non-linear regression, $F(1, 43) = 44.0, P < 0.0001, R^2 = 0.5785$). Urine doses along the x-axis are the total volume of undiluted blue crab urine applied to the experimental aquaria. Each point is an average of 32 oyster spat and crushing force was standardized by oyster shell width. A one-way ANOVA revealed that the lowest potent urine volume is 1.50×10^{-7} ($P = 0.012$).

1.5 Discussion

Juvenile eastern oysters made stronger shells in response to blue crab urine as well as urine constituents homarine and trigonelline, the same cues that were previously found to reduce mud crab foraging behavior (Poulin et al., 2018). These results confirm that prey from different marine taxa and trophic levels respond to the same molecules released by a shared predator, providing insights about induced defense mechanisms in response to a generalist predator. While there have been a wide array of studies focusing on how chemical cues from predators influence prey in terrestrial and aquatic systems (Godard et al., 1998; Leonard et al., 1999; Maerz et al., 2001; Poulin et al., 2018; Scherer et al., 2016; Smee & Weissburg, 2006; Weissburg et al., 2016), previous efforts concentrate on how closely related prey respond to a common predator (Ferland-Raymond et al., 2010; Ferrero et al., 2011; Peckarsky, 1980). Considerably fewer studies explored the interaction between a shared predator with diverse prey (Osada et al., 2014), and experiments with marine organisms remain rare (Poulin et al., 2018). Our findings reveal that taxonomically diverse prey from multiple trophic levels within this model system detect and respond to the same predation risk cues, supporting the idea that common fear molecules may be capable of influencing other ecological systems through various non-consumptive effects. Furthermore, ragworms may reduce foraging in response to these same cues (Fletcher et al., 2023), potentially providing further evidence for the existence of common fear molecules. The effects of a generalist predator may reduce those of an intermediate predator on basal prey, where the defense of the intermediate prey lowers its own efficacy or contact rate (e.g., by reducing activity) when exploiting the basal prey. The presence of a generalist predator may also amplify the effect of an intermediate predator by increasing efficacy or contact rate with basal prey, such as when the response of the intermediate prey

is to move to refugia where basal prey are abundant. Furthermore, as is the case for multiple predator effects (Sih et al., 1998), pairwise interactions are not sufficient for explaining numerous prey responses to a multitude of cues from a single predator.

In the current study, oyster defenses were especially noteworthy when both homarine and trigonelline were present simultaneously (Fig. 1.1), indicating that chemical blends induce the greatest prey response. The potency of homarine and trigonelline in combination increased with dose within the natural concentration ranges of these molecules found in blue crab urine (Fig. 1.6), and as hypothesized, the potency of blue crab urine as a whole significantly increased with dose (Fig. 1.7). These data suggest that oysters use urine concentration as a proxy for danger, whereby high risk could correspond to several large crabs or higher numbers of smaller blue crabs present nearby. An oysters' ability to successfully interpret the risk of predator encounter and respond to chemical blends can increase the survival of individual spat in nature (Belgrad, Knudson, et al., 2023; Belgrad, Smee, et al., 2023), incentivizing the selection of accurate responses. Dose dependent responses to chemical cues are not unusual, whereby the magnitude of the response increases with cue concentration (Fraker, 2008; Tollrian, 1993), and it is not uncommon for this dose dependency to rely on a blend of multiple cues, including conspecific cues (Laforsch et al., 2006). Our findings suggest homarine and trigonelline are utilized by oysters for detecting blue crabs and it is likely that other bioactive molecules are also involved in this interaction. This is supported by the observation that there was no correlation between oyster shell strengthening and concentrations of homarine and trigonelline quantified from blue crab urine samples (Figs. 1.5 and 1.8), a relationship expected to be significant if these compounds alone were responsible for oysters

responding to predation risk. Although this does not negate the importance of homarine and trigonelline in mediating the interaction between oysters, blue crabs, and mud crabs, our findings suggest that these are only two of perhaps several molecules comprising a cue blend and that more work is needed to identify all relevant chemical cues in this interaction.

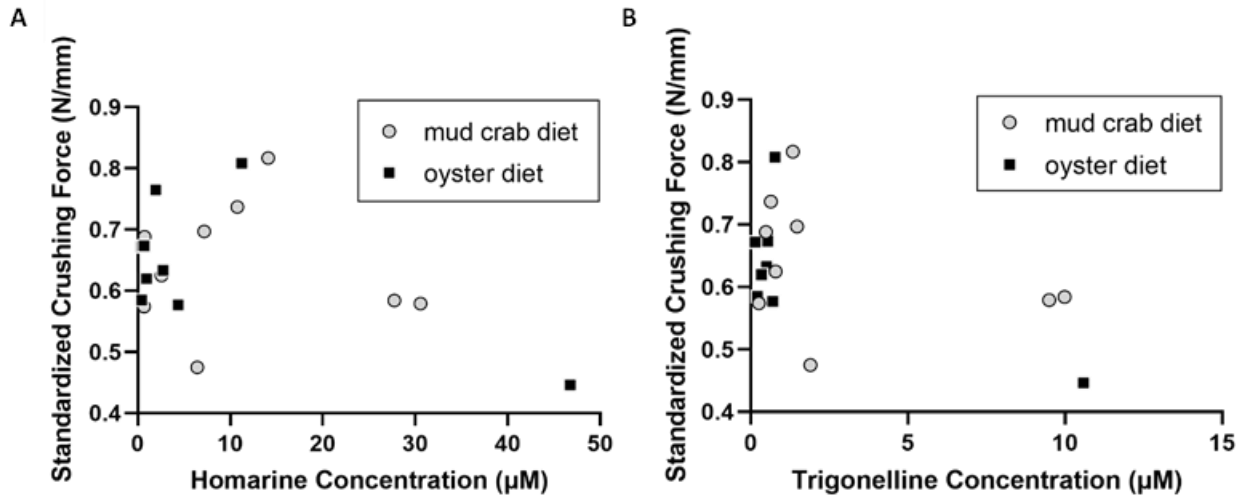


Figure 1.8 Linear regression models suggested that homarine (A) and trigonelline (B) concentrations were not reliable indicators of induced oyster shell strengthening for oysters exposed to blue crab urine. Analyses were performed for individual diets: A) homarine concentration for individual diets (oyster diet, $n = 9$, $F(1, 7) = 3.48$, $P = 0.10$; mud crab diet, $n = 9$, $F(1, 7) = 0.0481$, $P = 0.83$), and B) trigonelline concentration for individual diets (oyster diet, $n = 8$, $F(1, 6) = 5.48$, $P = 0.058$; mud crab diet, $n = 9$, $F(1, 7) = 0.969$, $P = 0.36$). Oysters were exposed to one of 18 crab urine mixtures for eight weeks, spat were crushed, and crushing force was standardized by oyster shell width. Each point is an average of 20 oysters. Data were excluded for concentrations below the limit of quantitation.

Generalist prey such as oysters may use a chemical blend as a proxy for danger, whereby the presence of multiple chemical cues at the right ratios indicates a greater risk, prompting a stronger response at higher concentrations (Tollrian, 1993). The use of chemical blends, and concentration-dependent responses, occurs across many systems in a variety of predator-prey interactions (Fraker, 2008; Hahn et al., 2019; Osada et al., 2014;

Poulin et al., 2018; Selander et al., 2015; Weiss et al., 2018). Blends, such as metabolic waste products, may be more reliable than individual cues because they reduce the possibility of falsely interpreting danger; therefore, selective pressure for this type of perception by prey is strong. The possibility of these cues originating from a relevant predator is higher if prey detect multiple molecules in the environment, especially if cues are primary metabolites shared by many predators, as certain combinations of chemical cues may act as an indicator of species type. Homarine and trigonelline may serve as these generalizable basal cues indicative of many marine predators, while the addition of unidentified chemical cues allows for marine prey to identify predator species; this explains the lack of trend between homarine and trigonelline concentration quantified in blue crab urine samples and standardized crushing force. This is also true for cue concentration, whereby prey may assess the concentration of a cue to determine relevant information for risk, including nearness, size, or species of a predator, time since last fed, or other clues to interpret risk of consumption (Fraker, 2008; Laforsch et al., 2006; Tollrian, 1993).

As an important basal resource to numerous consumers in coastal communities, eastern oysters experience considerable selection pressure to recognize the risk of predation, suggesting that the most reliable cues could be those common to many predators. Utilizing molecules involved in life-sustaining pathways shared by many taxa, as fear cues, is advantageous to oysters and mud crabs; these cues are produced and emitted by relevant predators that cannot prevent their release, making detection of these organisms by prey more certain. Furthermore, metabolites like homarine and trigonelline are enriched in the waste of some organisms in a diet-dependent manner (Poulin et al., 2018), and it is likely that many fear cues come from a predator's diet or result from other metabolic processes.

Sensing these urine molecules directly associates the predator with feeding on relevant prey because many marine invertebrates contain homarine and trigonelline within their tissues (Carr et al., 1996). This hypothesis is reinforced by evidence that homarine and trigonelline are more abundant in mud crab tissues compared to other blue crab prey, and that both cues were enriched in blue crab urine when blue crabs fed exclusively on mud crabs (Poulin et al., 2018). Since danger is associated with metabolic activity of the predator, primary metabolites are more definitive cues than those with a specialized function or which are non-diet derived. This notion may apply to many ecosystems, in which primary metabolites serve as common fear molecules for broadly consumed prey species, which in response have evolved to detect predation risk through metabolic waste products that are common to many predators. Therefore, primary metabolites in many taxa are likely to serve as common fear molecules within multiple ecosystems, although the distinction between primary and secondary is inexact as more and more metabolites are discovered to be multifunctional (Erb & Kliebenstein, 2020).

When a predator urinates, cues are released into the surrounding water as a concentrated plume, transported over space and time via diffusion or advection (Webster & Weissburg, 2009). Nearby prey may then be exposed to these cues at a range of concentrations depending on their spatial proximity to an excretion or secretion event, transport of the cue in the water column, or molecular diffusion from particulate organic carbon. While homarine and trigonelline have yet to be quantified in seawater from relevant oyster reef habitats (i.e., along the eastern coast of the United States through the Gulf of Mexico), several studies have detected these compounds in marine particles (Boysen et al., 2021; Heal et al., 2021), sea ice (Dawson et al., 2020), and environmental

seawater samples (Muslin, 2017; Rasyid, 2021; Sacks et al., 2022) at concentrations ranging from pM to μ M. These ambient concentrations are largely below the effective doses for trigonelline and homarine in the current study (Fig. 1.6C), although at the medium-to-high end, they overlap with concentrations at which these urinary metabolites can impact species interactions. Collectively these studies suggest that these molecules are prevalent in the marine environment, although the concentration range is wide, further supporting our conclusion that specific concentrations are required for inducing prey defenses and that these concentrations must be above an ambient threshold. Additionally, reported concentrations of homarine and trigonelline in seawater field samples (Muslin, 2017; Rasyid, 2021) support the hypothesis that they are present at lower levels in offshore waters than in coastal habitats where the presence of predators and associated fear cues are higher.

Identifying waterborne fear cues from seawater is challenging (Bayona et al., 2022; Berlinck et al., 2021), so it is unsurprising that such molecules have rarely been identified. Homarine and trigonelline are widespread metabolites (Carr et al., 1996), but their principal ecological role in marine environments remains elusive. Both molecules have been described as osmolytes (Dickson & Kirst, 1986; Gebser & Pohnert, 2013; Tikunov et al., 2010), and their prominence as primary metabolites is further supported by their ubiquity in the tissues of marine invertebrates (Ashihara, 2008; Ashihara et al., 2015; Carr et al., 1996; Dickson & Kirst, 1986; Mathias et al., 1960) and some vertebrates, such as elasmobranchs (Dove et al., 2012), as well as by their presence in the urine of diverse species (Gibson et al., 2020; Lapan, 1975; Poulin et al., 2018). These metabolites are also proposed to fulfill a variety of functions in other marine organisms and are perhaps more

specialized in purpose than expected. Homarine and trigonelline are necessary for proper polyp development and larval metamorphosis in hydroids (Berking, 1987), altering the morphology of these individuals, and both molecules were also identified as antifouling agents utilized by different species of soft corals (Kawamata et al., 1994; Targett et al., 1983). Additionally, some Antarctic soft corals use homarine as an antimicrobial defense (Slattery et al., 1997), while it serves as a predator feeding deterrent in Antarctic gastropods (McClintock et al., 1994). The pervasive roles of both cues in diverse ecological systems supports their utility as a general cue and implies that primary metabolites may be more important in ecological function than previously considered.

Discovery of new functions for known metabolites allows for study of ecological and evolutionary insights of predatory interactions, such as the plasticity of prey responses, subsequent evolution of sensory systems, and epigenetic consequences to morphological induced defenses. Currently, many studies rely on simply adding live predators to induce prey responses which places limits on researchers' ability to standardize experiments due to the individual nature of live organisms. However, the cue concentrations described here provide targets for researchers to begin providing known threat exposure treatments. As advancements are made towards discovery of additional molecules that mediate predator-prey interactions, accurate identification and verification of biological activity will be paramount for understanding and managing the impact of chemical cues on ecosystems. Future research should focus on identifying chemical cues from additional marine predators, analogous to studies of terrestrial systems to further understand the breadth of homarine and trigonelline as universal fear cues. Strong collaborations between ecologists and chemists continue to result in important breakthroughs for the field, notably where

efforts are directed towards the development of chemometric tools for metabolomics studies. Without these partnerships, identification of the molecules mediating these important interactions would be improbable.

CHAPTER 2. PREDATOR CUES INDUCE DEFENSIVE RESPONSES IN DIVERSE MARINE PREY: A METABOLOMICS DECODING OF BLUE CRAB URINE BIOMARKERS

2.1 Abstract

Prey strongly rely on chemical cues to detect predators, especially in coastal ecosystems where other signs of danger are concealed by turbid, dynamic waters. In the estuaries of the Gulf of Mexico and southeast Atlantic, oysters (*Crassostrea virginica*) respond morphologically to blue crab (*Callinectes sapidus*) chemical cues, while mud crabs (*Panopeus herbstii*), another blue crab prey, lower their risk of being detected by decreasing their own foraging activity. More specifically, particular natural concentrations of urinary metabolites homarine and trigonelline cause oysters to make stronger shells. The current study uses statistically driven metabolomics to leverage the individual variation in blue crab urine chemistry and pinpoints specific chemical features that correlate with induced defenses of two taxonomically distinct prey, therefore facilitating identification of new bioactive molecules comprising the waterborne cue. A strong positive correlation between crushing force required to break an oyster shell and specific blue crab urine mass spectral features indicated that a blend of distinct urine metabolites, unrelated to predator diet, induce oyster shell strengthening; This is in contrast to mud crabs which generally respond more strongly to urine of blue crabs fed mud crabs. Partial least squares regression (PLS-R) analyses of mass spectra coupled with bioassay data also confirmed that chemical features of yet-to-be identified urinary metabolites revealed by statistical models are of even greater importance for the fear-inducing blend than homarine and trigonelline, previously shown to play such a role. Seven new mass spectral features corresponding to seven separate unknown compounds were determined to serve as important cues

potentially used by both prey to detect a shared predator. These results indicate that some fear molecules are more widely used by prey, and hence more reliable indicators of risk than others.

2.2 Introduction

Communication between living organisms is mediated by a combination of chemical signals and cues that make up a complex language. Traditionally, studying these messenger molecules involved multiple rounds of different chromatographic separation techniques coupled with repeated measurements of biological activity, gradually leading to one or more pure compounds responsible for a biological effect (Prince & Pohnert, 2010; Weller, 2012). Development of unique bioassays was centered around physiological, morphological, or behavioral responses elicited by organisms when exposed to the chemical message at natural concentrations. This method, known as bioassay-guided fractionation, has proven useful in many instances, resulting in a plethora of natural product and chemical ecology discoveries, but it is not consistently successful in identifying all the components required for full biological activity (Kuhlisch & Pohnert, 2015). When attempting to isolate such molecules from their source, bioactivity is often greatly reduced or lost after several separation steps. Possible reasons for this include, but are not limited to, chemical instability, inefficient recovery following separation steps, or the need for multiple components to be present in specific ratios (Poulin & Pohnert, 2019).

Metabolomics is a modern approach for studying these molecular messages because it relies on chemical profiling coupled with statistics to identify metabolites of potential interest. Comparative and targeted metabolomic approaches allow for the identification of chemical features associated with dramatic or subtle differences between bioactive samples and non-active controls (Poulin & Pohnert, 2019; Prince & Pohnert, 2010). With the aid of online metabolomics databases, chemical features represented in

multivariate statistical models can be traced back to spectroscopic fingerprints of specific molecules, supporting compound identification. If bioactive molecules are new secondary metabolites, they are then typically isolated and characterized using a combination of spectroscopic techniques. In the past decade metabolomics has provided a platform for generating chemical profiles of many marine organisms such as corals (Sogin et al., 2014), sponges (Bauvais et al., 2017), microalgae (Chen et al., 2017), and bivalves (Aru et al., 2017; May et al., 2017). It has also been successfully applied to discover a diatom sex pheromone (Gillard et al., 2013) and the effects of allelopathic phytoplankton competition (Poulson-Ellestad et al., 2014), however, only a few studies have identified chemical cues that mediate perception of predators by their prey (Hahn et al., 2019; Poulin et al., 2018; Selander et al., 2015; Weiss et al., 2018).

Detection of and response to chemical cues increases fitness of many organisms, allowing predators to find prey and for prey to avoid predation, each party leveraging chemical information from the environment for their benefit. When predators locate a potential food source, they rely on taste and smell to determine whether it is palatable and safe to eat (Long & Hay, 2006). At the same time, prey assess predation risk by detecting molecules released by predators, conspecifics, and other neighboring species within a shared habitat (Ferrari et al., 2010). More specifically the ‘smell of death’ can be a mixture of exudates from injured prey and metabolic waste released by feeding predators: together these cues affect behavior (e.g., changes in eating habits) (Long & Hay, 2006), physiology (Bristow et al., 2019), morphology, and life history; hence they can significantly impact community structure and ecosystem function via non-consumptive effects of predation, not only the effects of direct removal of prey by predators.

Urine is an important cue source rich in small organic molecules capable of influencing animal behavior (Osada et al., 2015). The water-soluble and volatile properties of urinary metabolites facilitate transport from emitter to recipient. Given that many

animals urinate frequently, it is evidently advantageous for prey to use predator urine for assessing predation risk. Commonalities exist between urine of different species (Ferrero et al., 2011), but the majority of chemistry efforts have focused on characterizing human urine (Bouatra et al., 2013; Putnam, 1971), especially in relation to aspects such as diet (Playdon et al., 2016), age, and sex which are known to affect its composition (Hesse et al., 1986). Resulting individual variation and chemical complexity can potentially impact urine potency as a chemical cue, as demonstrated by studies relating urine of different predator diets to danger perceived by prey (Nolte et al., 1994; Poulin et al., 2018). Specific cue combinations at unique ratios and concentrations are typically critical for proper interpretation of chemical messages, as these key factors determine the uniqueness, and hence reliability of a particular scent (Deland et al., 1993; Grunseich et al., 2021).

There has been relative success identifying urine cues in terrestrial systems (Osada et al., 2015), whereas few cue molecules have been characterized from marine predators (Poulin et al., 2018). This is because waterborne molecules are challenging to isolate from seawater due to low natural concentrations in a high salt matrix (Berlinck et al., 2021). However, the ability to acquire urine directly from the predator presents a unique situational advantage whereby scientists mostly avoid the complications associated with analyzing molecules in dilute seawater. Additionally, metabolomics has proven to be an excellent tool for investigating the chemistry of urine (Bouatra et al., 2013), as it facilitates the simultaneous analysis of individual molecules from complex mixtures and reduces the risk of metabolite decomposition exacerbated by sequential chemical separation steps. Minimal sample preparation increases efficiency in comparison to the more traditional route of bioassay-guided fractionation, especially if the accompanying bioassays are slow, labor-intensive, and consume substantial quantities of chemical cue.

The present metabolomics study leverages genetic algorithms and multivariate statistics to identify blue crab urine biomarkers indicative of predation risk to oysters, as

well as fear cues that they may have in common with mud crabs. Previous work identified homarine and trigonelline as two urine constituents important for both prey species; however it was evident in those studies that these are not the only cues used to detect predatory blue crabs (Poulin et al., 2018; Roney et al., 2023). The current study provides insights about the commonalities and differences between fear cue blends originating from a common predator, emphasizing the complexity of these cues, especially in the context of predator-prey interactions.

2.3 Methods

Experiments were designed to use metabolomics for discovering chemical cues in blue crab urine that result in evaded predation by two prey, mud crabs and eastern oysters. For each respective bioassay, prey were repeatedly exposed to the same blue crab urine samples to identify chemical cues that induce oyster shell strengthening, reduced mud crab feeding, or both.

All seawater used in aquaria and mesocosm tanks was drawn from offshore from Mobile Bay, AL, USA and allowed to settle in a tank for three days to remove particulates. Seawater salinity was maintained at 20 ± 2 ppt throughout all experiments. Oyster and mud crab bioassays were performed at the Dauphin Island Sea Lab in Dauphin Island, AL, USA from July – Sept. 2020.

2.3.1 Blue Crab Urine Preparation

Blue crabs (*Callinectes sapidus*) were caught in commercial crab traps on the Mobile Bay side of Dauphin Island Sea Lab and housed in individual tanks with natural seawater. Crabs were starved for two to three days prior to being fed either oysters (*Crassostrea virginica*) or mud crabs (*Panopeus herbstii*) once every two days. All blue crabs were maintained on a constant diet for one week before beginning urine collection,

which was performed twice per week. Crabs were chilled on ice to quiescence prior to siphoning urine from the nephropore using a 23 gauge-needle and light vacuum suction (Roney et al., 2023).

Urine collected from individual crabs was combined into mixtures to provide enough urine for both the oyster shell strengthening and mud crab feeding assays. Urine samples from individual blue crabs was stored at -80°C before being combined, ensuring that the smallest number of crabs contributed to each mixture. This maximized the chemical diversity of each urine sample, as desired for metabolomics analysis. For the current study, each mixture was composed of urine from 3-12 individual blue crabs, constituting one biological replicate. The same 24 urine mixtures (n=12 mud crab diet and n=12 oyster diet) were used for both bioassays, enabling direct comparison of chemical features associated with each biological response.

2.3.2 Oyster Shell Strengthening Assay

The purpose of this bioassay was to determine the effect of blue crab urine on oyster shell strengthening. The Auburn University Shellfish Laboratory provided diploid oyster larvae which were settled onto marble tiles and allowed to grow for one week in 1250 L mesocosms prior to experimentation. These oyster spat were transferred to aquaria and exposed to blue crab urine (mud crab or oyster diet) or natural seawater (negative control) for a period of 48 days. Twenty oyster spat were crushed from each biological replicate to assess shell strength. Oyster shell width was measured with calipers and crushing force with a Kistler 5995 charge amplifier coupled to a 9207 force sensor. Crushing force was divided by shell width to calculate standardized crushing force, which was averaged for oysters within the same aquaria. Additional details for the oyster bioassay and the statistical analysis are provided in Roney, et al., 2023.

2.3.3 Mud Crab Feeding Assay

As it was already known that homarine and trigonelline are two blue crab urine metabolites that induce fear in mud crabs (Poulin et al., 2018), the goal of this assay was to determine whether mud crabs use any of the same chemical cues as oysters to assess blue crab predation risk. Methods were based on Poulin et al., 2018. Mud crabs were collected from the area surrounding Priest Landing on Skidaway Island, GA, USA and transported in coolers to Dauphin Island Sea Lab. They were acclimated in a 2 m diameter mesocosm with recirculating natural seawater approximately 1 m deep, and fed satiating amounts of shrimp every few days.

Prior to experimentation, mud crabs were starved for 24 hours. Aquaria were filled with 1.5 L water and the bottoms covered with sun-bleached oyster shells to serve as refuge for mud crabs. Four mature mud crab adults, 2-3 cm wide with at least one individual of each sex, were added to each aquarium and allowed to acclimate for at least an hour. All mud crabs had two chelipeds and were not missing more than two legs. Meanwhile, frozen shrimp were fully thawed and blotted to remove excess water before measuring their initial weight. Food (i.e., thawed shrimp) and 3.75 mL urine cue were added to corresponding aquaria simultaneously, resulting in mud crabs being exposed to blue crab urine at a concentration of 2.5 mL/L). Crabs were allowed to eat for 4 hours in the dark, after which excess water was removed before measuring final weights for the remaining shrimp in each aquarium. Given space constraints, the experiment was performed in four blocks consisting of all treatments in each block (i.e., one aquarium per cue mixture per day, totaling four replicates per mixture) and 12 urine mixtures were tested per diet (mud crab or oyster). Each block had two seawater negative control replicates, with the exception of block four which had six seawater replicates. Feeding assays were deliberately conducted at night when mud crabs are the most active (Griffen et al., 2012). Data were statistically analyzed by ordinary one-way ANOVA using GraphPad Prism 9.3.0.

2.3.4 Estimating Protein Content in Blue Crab Urine

Separate from urine's role as a predator risk cue, oyster spat could potentially utilize blue crab urine as a nutritional source, thus enabling production of stronger shells. To rule out this confounding hypothesis, total protein (as one important measure of nutritional value) was compared between blue crab urine and Reed Mariculture Instant Algae Shellfish Diet 1800 which was the source of food for oyster spat during the shell strengthening assay. The number of algal cells in 1 mL was estimated using a Fluid Imaging FlowCam since this was the volume of algae administered to each tank per day. Algal cells were lysed using the OMNI Bead Rupter Elite via two 45 second cycles at 7.1 m/s separated by a 30 second dwell time. Protein concentrations were measured using a Thermo Fisher Scientific Pierce Modified Lowry Protein Assay Kit following the microplate procedure. All standards and reagents were prepared in liquid chromatography mass spectrometry (LC-MS) grade water which was also used as the blank. Urine, algal samples, bovine serum albumin standards, and media controls were transferred to a 96-well plate and absorbance was measured at 750 nm using a BioTek Synergy H4 Hybrid plate reader. A quadratic standard curve was constructed using GraphPad Prism 9.3.0 to interpolate protein concentrations in urine samples, lysed algal cells, artificial seawater 22 ppt, and 20 ppt L1 media.

2.3.5 Blue Crab Urine Chemical Profiling

Separate from urine's role as a predator risk cue, o Aliquots of the same 24 blue crab urine samples used for both bioassays were brought from Dauphin Island Sea Lab to the Georgia Institute of Technology, GA, USA where they were stored at -80°C. ¹H NMR spectroscopy and mass spectrometry datasets were acquired for all urine samples at the Georgia Institute of Technology. These complimentary data were used to explore the metabolic composition of blue crab urine.

2.3.5.1 NMR Metabolomics

Samples were prepared for NMR spectral analysis by combining 138 μL blue crab urine, 46 μL phosphate buffer (0.1 M pH 7.4), and 16 μL 0.1% w/v 3-(trimethylsilyl)propionic-2,2,3,3-d₄ acid (TMSP). Phosphate buffer and TMSP solutions were made in D₂O (99.9% atom D₂O; Cambridge Isotope Labs). Solutions were mixed via micropipette and 175 μL were transferred to 3 mm NMR precision tubes (Wilmad-LabGlass). All spectra were acquired using a Bruker Avance IIIHD 800 MHz spectrometer equipped with a 3 mm cryoprobe. For water suppression, the Bruker zgpr pulse sequence was used with a relaxation delay of 10 s. Spectra were centered at 3758.89 Hz, spectral width was set to 13.9 ppm, receiver gain was set to 16, and 256 scans were acquired per sample.

Data were processed in Metabolab (Ludwig & Günther, 2011). Spectra were phased, the TMSP reference peak was set to 0 ppm, and spline baseline corrected choosing baseline points spanning the entire spectral width. The TMSP peak, residual artifacts from the suppressed water peak, and regions with a noisy baseline were excluded as they are not relevant for statistical analyses. Spectra were aligned, filtered for noise, and then binned using a width of 0.005 ppm. Probabilistic quotient normalization (PQN) was applied to reduce systematic variation. Processed spectra were exported as a .mat file and imported into PLS Toolbox 9.0 where they were general log transformed and mean centered prior to multivariate statistical analyses.

2.3.5.2 Untargeted Mass Spectrometry Metabolomics

Blue crab urine was thawed at room temperature and then kept on ice during sample preparation. Pooled urine samples for each diet (mud crab and oyster) were prepared by combining equal volumes of all samples for a single diet. For both pooled and biological replicate urine samples, 20 μL urine was added to 180 μL LC-MS methanol, vortexed for

proper mixing, centrifuged at $19980 \times g$ for 10 minutes to pellet any precipitate, and all supernatant was transferred to a clean vial.

Ultra-performance liquid chromatography mass spectrometry (UPLC-MS) was performed using a Vanquish HPLC coupled to an Orbitrap ID-X Tribrid mass spectrometer (Thermo Fisher Scientific). Chromatographic separation was conducted for 1 μL sample injections at a temperature of $40\text{ }^{\circ}\text{C}$ using an ACQUITY UPLC BEH Amide column ($2.1 \times 150\text{ mm}$, $1.7\text{ }\mu\text{m}$ particle size, Waters Corporation). Compounds were eluted from the column at 40 mL/min using 80:20 water/acetonitrile with 10 mM ammonium formate and 0.1% formic acid (mobile phase A), and acetonitrile with 0.1% formic acid (mobile phase B) for the following gradient program: 0 min 5% A; 0.5 min 5% A; 8 min 60% A; 9.4 min 60% A; 9.5 min 5% A; 12 min 5% A (Optima, LC-MS grade, Fisher Scientific).

The Orbitrap ID-X Tribrid mass spectrometer is a high resolution ($500,000\text{ FWHM}$ at 200 m/z), accurate mass ($<1\text{ ppm}$) instrument with dual detectors (i.e., an orbitrap and an ion trap). The following settings were used for the heated electrospray ionization (HESI) source: positive ion mode, a vaporizer temperature of $275\text{ }^{\circ}\text{C}$, a spray voltage of 3.5 kV , and sheath, auxiliary, and sweep gas flows of 40 , 8 , and 1 L/hr , respectively. For the untargeted metabolomics experiment, full scan data from $70\text{-}600\text{ m/z}$ were acquired with the orbitrap at a resolution of $60,000$ followed by data-dependent acquisition (DDA) of tandem mass spectra with the ion trap to ensure accurate mass spectra using both higher energy collisional dissociation (HCD, collision energies 15 , 30 , and 45 eV) and collision-induced dissociation (CID, collision energy 35 eV). For HCD, precursor ions were isolated in the ion trap using a 0.8 m/z window and activated at 50% . Data acquisition was performed using Xcalibur Version 4.3.73.11 (Thermo Fisher Scientific) followed by processing in Compound Discoverer 3.3.0.550 (Thermo Fisher Scientific). Normalized peak areas were exported from Compound Discoverer and further processed in PLS Toolbox 9.0. The data was processed with and without PQN prior to applying a general log

transformation and mean centering, generating two base models that would later be used for partial least squares regression analyses (PLS-R).

2.3.6 *Multivariate Statistical Analyses of Spectroscopic Data and Variable Selection*

Both pre-processed ^1H NMR and LC-MS metabolomics datasets were analyzed in PLS Toolbox 9.0 by principal component analysis (PCA) and partial least squares discriminant analysis (PLS-DA). Then these spectral datasets were paired with either oyster shell strengthening or mud crab feeding assay data to build PLS-R models. Unlike for ^1H NMR spectroscopy, mass spectral features are considered independent variables so genetic algorithm variable selection was used to refine the mass spectrometry feature list by removing unwanted features that did not correlate with bioactivity, greatly improving the cross validation for these models. Different combinations of genetic algorithm parameters were compared to determine which ones resulted in the lowest root mean squared error of cross validation (RMSECV). A 2×2 factorial design was implemented to create four models for each bioassay: data processed with or without PQN either with or without a percent of variables target range (5-15% with a penalty slope of 0.05). The following parameters were used for all genetic algorithm runs: a population size of 256, 20% initial terms, 100 max generations, 50% at convergence, 0.005 mutation rate, single crossover, 10 max LVs, venetian blinds cross validation (6 splits and thickness = 1), 2 CV iterations, and 5 replicate runs. Although each genetic algorithm run tested hundreds of different variable combinations, selected variable lists are those with the lowest RMSECV. Variable importance parameter (VIP) scores were compared for all features, and those ≥ 0.75 or that were selected by at least two models were compiled into a prioritized list, as these features are the most ideal biomarker candidates. Pearson correlation coefficients were calculated for all features in Microsoft Excel (Microsoft 365). Permutation tests were performed in PLS Toolbox to confirm that all models were robust.

2.3.7 *Annotation of Blue Crab Urine Biomarkers via LC-MS/MS Spectra*

A follow-up targeted MS/MS experiment was later performed to acquire additional spectra targeting promising MS features arising from PLS-R models which produced feature lists using genetic algorithm variable selection. This was necessary because MS/MS spectra for some of these features were not acquired in the untargeted experiment. A pooled urine sample was prepared from equal volumes of all 24 urine samples as described previously. General method parameters were the same as for the untargeted MS/MS experiment; however, prioritized mass spectral features were split into 10 groups based on similar retention times so that only a subset of ions were targeted per injection. Assigning specific retention time windows to each group allowed for a higher number of scans per cycle time.

Acquired MS/MS spectra for high ranking PLS-R model features were compared to experimental and theoretical data accessed from the Human Metabolome Database (HMDB) and MassBank of North America (MoNA). Compound Discoverer in conjunction with a molecular formula calculator was used to propose potential molecular formulae for MS features of interest.

interactions.

2.4 Results

2.4.1 *Predator Diet Does Not Influence Oyster Perception of Predation Risk*

Complementary ^1H NMR and LC-MS datasets indicated that blue crab urine is chemically rich and complex, with appreciable concentrations of several hundred metabolites (Fig. 2.1). LC-MS analysis led to prioritization of 712 features, the majority of which are expected to be unique metabolites, although some represent different ions of the

same molecule. For PCA associated with ^1H NMR and LC-MS spectra, profiles of blue crab urine, mud crab, or oyster diets were separated by PC 1, accounting for 19.5% and 20.5% of the variance, respectively (Fig. 2.2). PLS-DA also supported the statistically significant separation of urine chemical profiles based on blue crab diet, with even clearer separation between treatments than for PCA (data not shown). Therefore, unsurprisingly, and in line with previous results (Poulin et al., 2018), blue crab urine is chemically distinguishable based on diet (Fig. 2.2), with the known urinary metabolites homarine and trigonelline contributing to this separation, as they were identified in the PC 1 loadings plot for the ^1H NMR spectral analysis (Fig. 2.3).

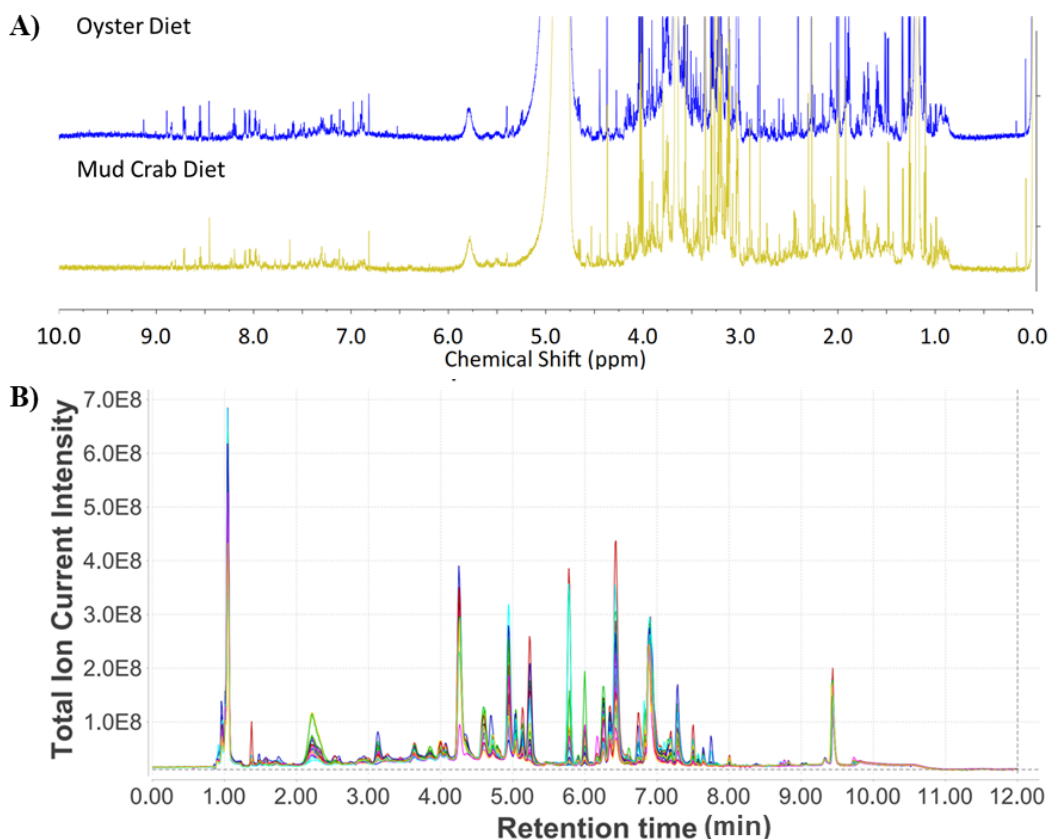


Figure 2.1 Complementary ^1H NMR and LC-MS spectra were acquired for 24 blue crab urine samples: mud crab diet (n=12) and oyster diet (n=12). A) Representative ^1H NMR spectra for urine of each blue crab diet: oyster (blue spectrum) and mud crab (gold spectrum). B) Overlaid LC-MS chromatograms for all 24 urine samples. Mass spectra were acquired using positive ionization electrospray mode.

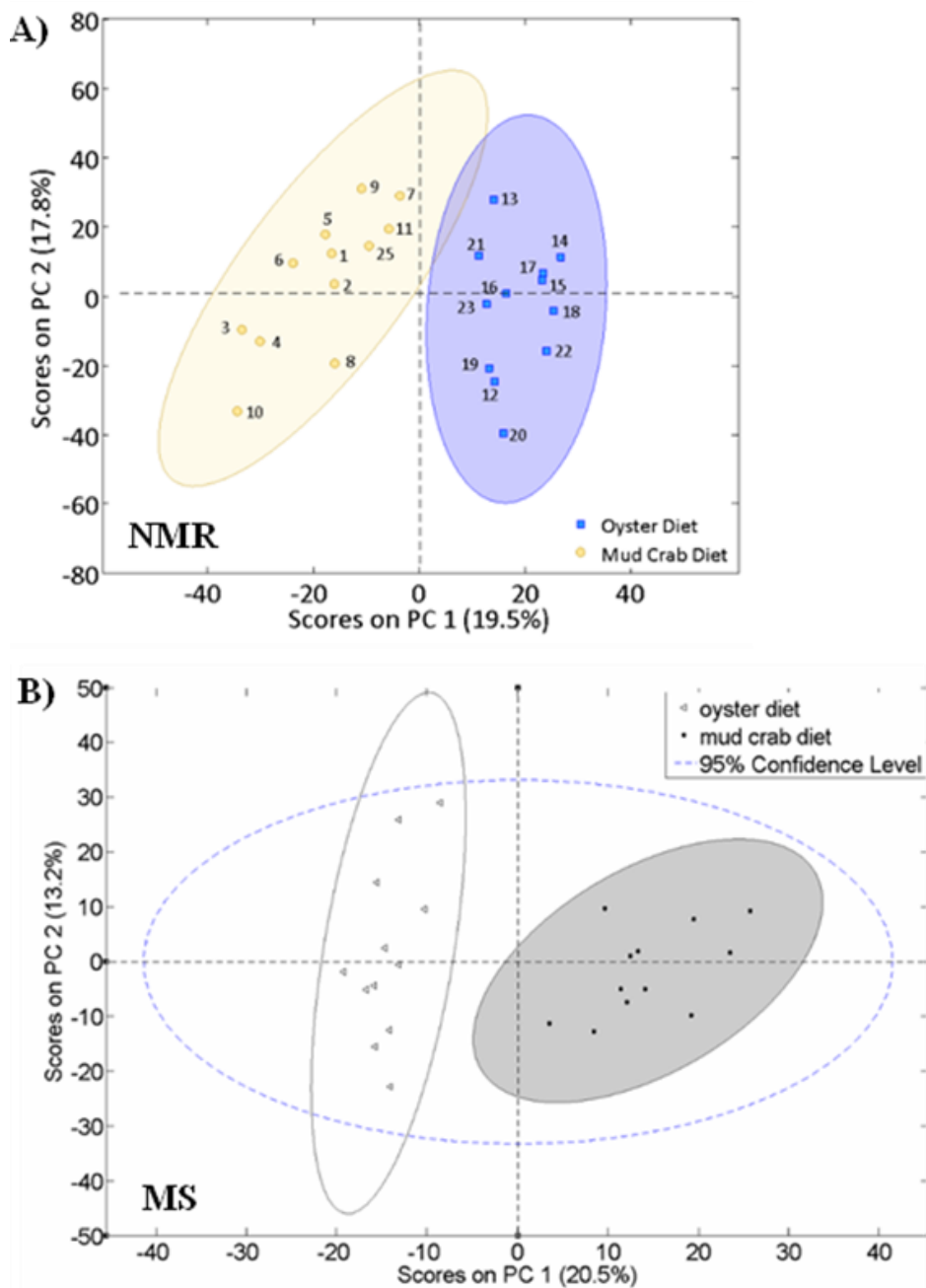


Figure 2.2 Principal component analyses of ^1H NMR (A) and LC-MS (B) blue crab urine metabolomics datasets. ^1H NMR and mass spectra were acquired for 24 urine samples: mud crab diet ($n = 12$) and oyster diet ($n = 12$). Strong separation of treatments for both models indicates distinct chemical profiles for urine of blue crabs fed different diets.

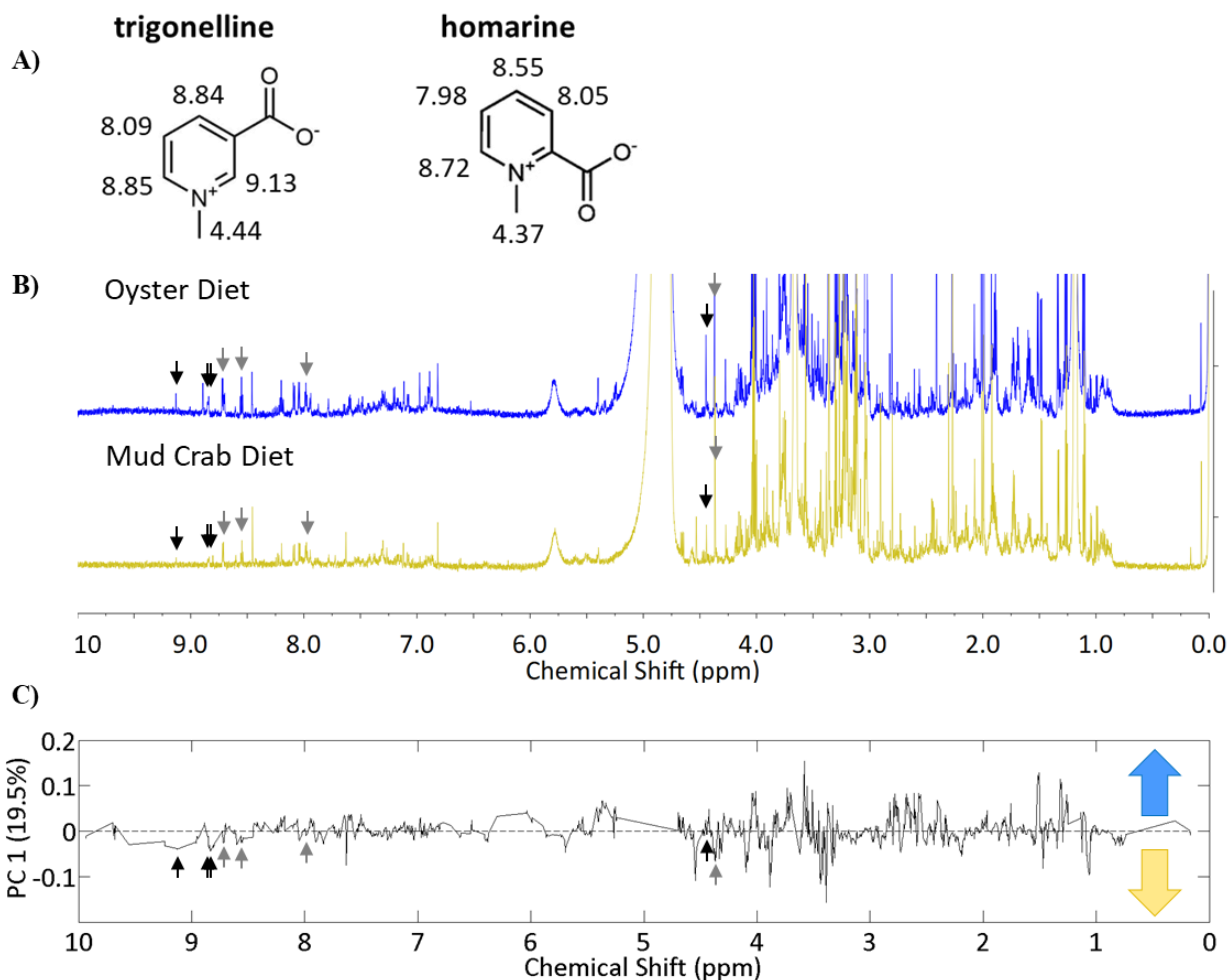


Figure 2.3 Trigonelline and homarine are two blue crab urine metabolites that contribute to distinct chemical profiles for blue crab urine of different diets. **A)** Structures of homarine and trigonelline with their ^1H NMR chemical shifts. Two representative ^1H NMR spectra (**B)** and the corresponding loadings plot (**C)** for the principal component analysis of the ^1H NMR blue crab urine metabolomics dataset. Black arrows point to peaks for trigonelline, and gray arrows point to peaks for homarine. Trigonelline and homarine peaks are negative in the loadings plot indicating that these features are enriched in the mud crab diet (yellow arrow). Feature enriched in the oyster diet are positive for PC 1 in the loadings plot (blue arrow).

PLS-R analyses revealed that urine potency, with respect to its ability to enhance oyster shell strength, was not diet-dependent. In other words, urine of blue crabs fed oysters was not more or less potent as a cue to oyster spat than urine of blue crabs fed mud crabs (Fig. 2.4). This was evident for PLS-R models of both ^1H NMR and MS data because blue

crab urine samples were not segregated by diet along the regression line (Fig. 2.4). This was in contrast to mud crabs' response to blue crab urine, whereby diet-dependent chemical differences in blue crab urine generally correlated with suppression of mud crab feeding (i.e., increased urine potency (Fig. 2.5) (Poulin et al., 2018). Interestingly, in the current study, oyster diet blue crab urine sample 12 was comparably potent (towards mud crabs) to the most fear-inducing mud crab diet urine samples (Fig. 2.5). This urine mixture was the second most potent overall for reducing mud crab feeding, and notably also caused oysters to make the strongest shells. Potency did not correlate with total concentration of urine metabolites (i.e., derived from the overall abundance of measurable chemical signals for each sample), rejecting the hypothesis that the most concentrated or chemically rich urine is typically most potent in fear-inducing assays. In addition, no single individual metabolite on its own significantly accounted for the fear-inducing properties of blue crab urine, as revealed by Pearson correlation coefficients (data not shown). Overall, it's clear that multiple compounds in blue crab urine are required to elicit fear-inducing effects in oyster spat and mud crabs.

2.4.2 Blue Crab Urine is Not a Source of Nutrients to Oyster Spat

Based on urine protein concentrations measured by interpolation from a standard curve, blue crab urine contained approximately 0.1% of the protein of in an equal volume of Algae Shellfish Diet, which was used to feed oyster spat in our experiments (data not shown). Thus, crab urine is not an appreciable nutrient source for juvenile oysters, leading us to reject the alternative hypothesis that oysters absorb nutrients from urine resulting in stronger shells.

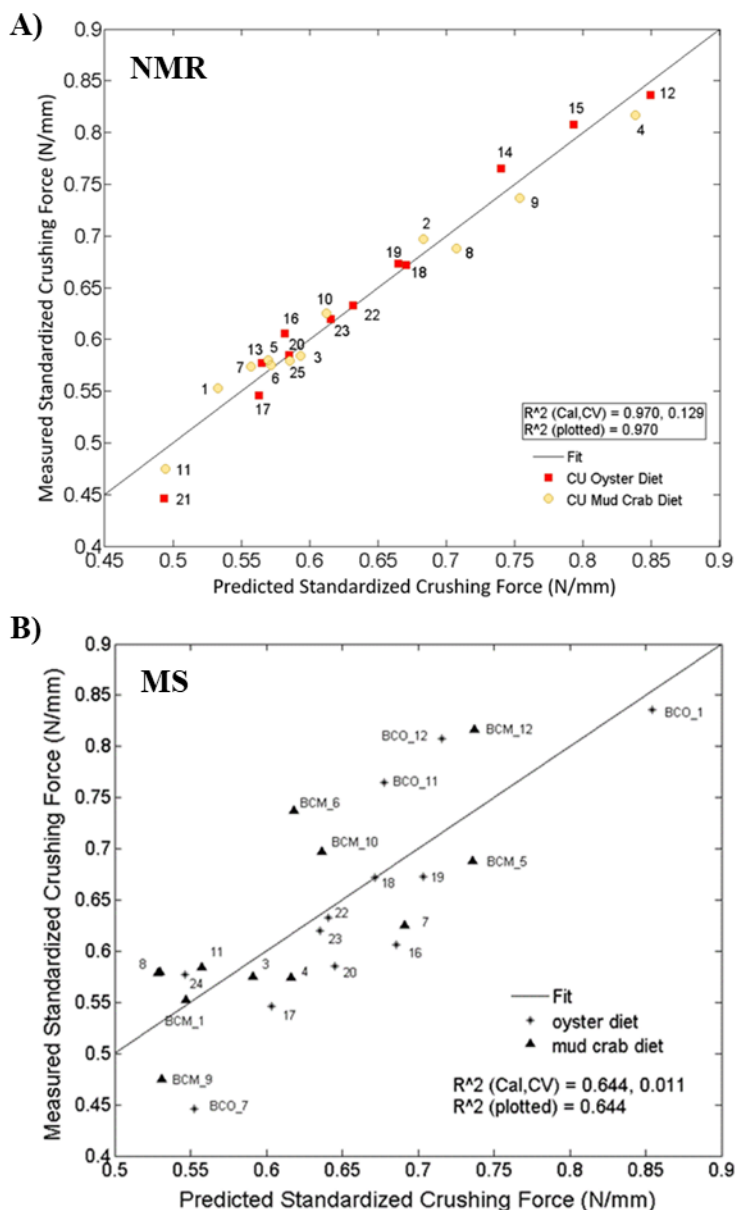


Figure 2.4 Partial least squares regression analyses for ^1H NMR (A) and MS (B) metabolomics datasets related to oyster shell strengthening. For both models, measured oyster shell standardized crushing force is regressed against spectroscopic chemical features to predict standardized crushing force values for each urine sample. Lines of best fit for the ^1H NMR and MS metabolomics models have R^2 values of 0.97 and 0.64 respectively, where higher R^2 values are indicative of a better predictive model.

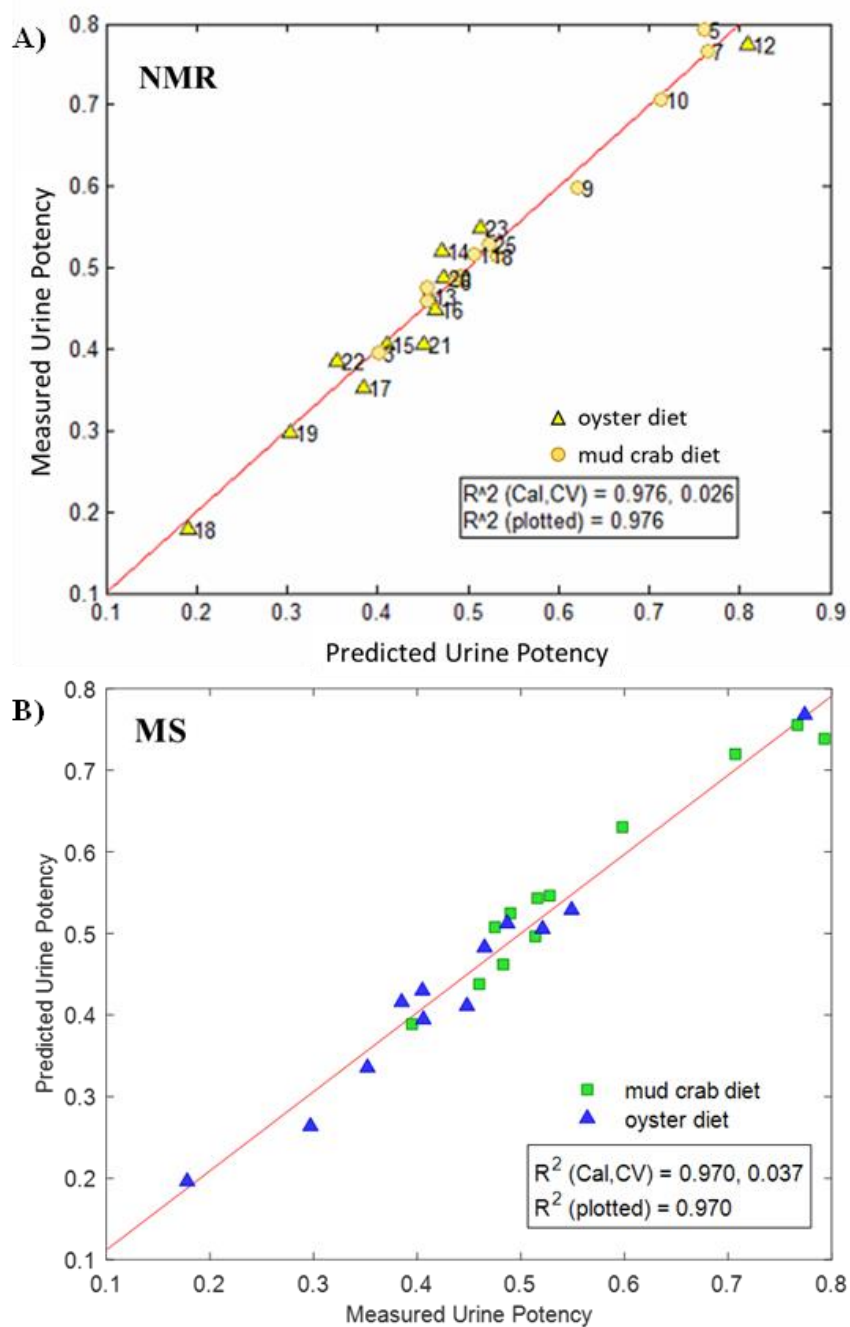


Figure 2.5 Partial least squares regression analyses for ^1H NMR (A) and MS (B) metabolomics datasets related to mud crab feeding suppression. For both models, measured urine potency is regressed against spectroscopic chemical features to predict urine potency values for each urine sample. Plotted lines of best fit are for the ^1H NMR and MS metabolomics calibrated models ($R^2 = 0.98$ and 0.97 respectively). Higher urine potency indicates reduced mud crab feeding and higher R^2 values are indicative of a better predictive model.

2.4.3 Blue Crab Urine Biomarkers Indicative of Predation Risk: Specific and Common Fear Cues Utilized by Multi-Trophic Prey

PLS-R analysis of the ^1H NMR metabolomics dataset revealed that trigonelline is a minor component of the cue blend that correlated with increasing oyster shell strength (Fig. 2.6). The presence of trigonelline in the VIP plot of this model supports previous results that oysters perceive trigonelline as a fear cue (Roney et al., 2023), although cross-validation for this model was poor (Fig. 2.4; R^2 (Cal) = 0.97; R^2 (CV) = 0.13). However, contrary to results from this same previous study, the PLS-R model did not identify homarine as a significant cue correlating with stronger oyster shells, suggesting that trigonelline is a more critical component of the fear-inducing blend for oysters than homarine. As these results indicated that homarine and trigonelline were perhaps less important fear-inducing cues towards oysters than other unidentified metabolites, 2D NMR spectroscopy of blue crab urine was explored to identify other metabolites with high VIP scores, but insufficient instrument sensitivity, spectral complexity, and low metabolite concentrations made this option impractical in the absence of purification efforts (data not shown).

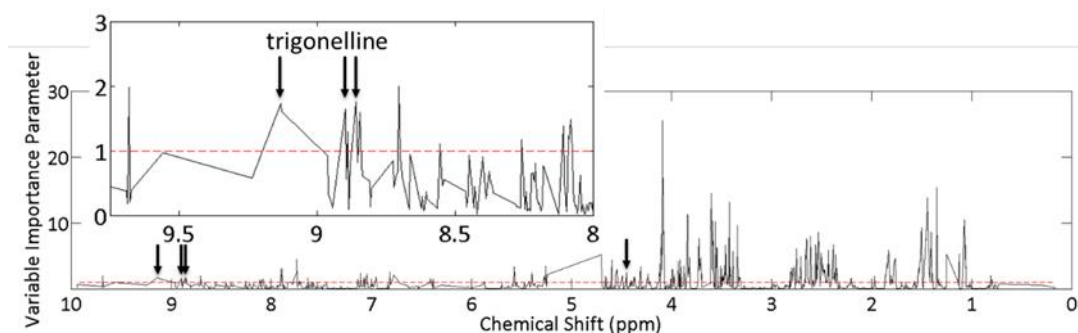


Figure 2.6 Variable importance parameter plot for the ^1H NMR metabolomics partial least squares regression analysis. Peaks above the dashed red line are chemical features corresponding to molecules whose concentrations positively correlate with oyster shell strength. Black arrows point to features corresponding to trigonelline.

Original PLS-R models generated from MS metabolomics data (Fig. 2.7; oyster shell strengthening assay, R^2 (CV) = 0.01; Fig. 2.5; mud crab feeding assay, R^2 (CV) = 0.04) were improved using variable selection, since by this method individual features are considered independent of each other. Genetic algorithm variable selection of MS features improved cross validated PLS-R models for predicting oyster shell strengthening and reduced mud crab feeding (Fig. 2.7; oyster shell strengthening assay, R^2 (CV) = 0.89; mud crab feeding assay, R^2 (CV) = 0.95), on average selecting a subset of variables representing approximately 8% of the total. These models pinpointed specific features in blue crab urine that may serve as biomarkers for increased oyster shell strength (Table 2.1) and reduced mud crab feeding (Table 2.2). Seven features were important for PLS-R models of fear responses for both prey (Table 2.3). These molecules are top candidates for common fear cues, as constituents of biological exudates important to multiple prey species seeking to avoid predation. Proposed molecular formulae for these spectral features are indicative of small nitrogenous compounds and organic acids (Tables 2.1, 2.2, and 2.3). Additionally, Pearson correlation coefficients were calculated for MS features, but values were low (≤ 0.59), indicating that individual variables did not, on their own, correlate well with oyster shell strengthening.

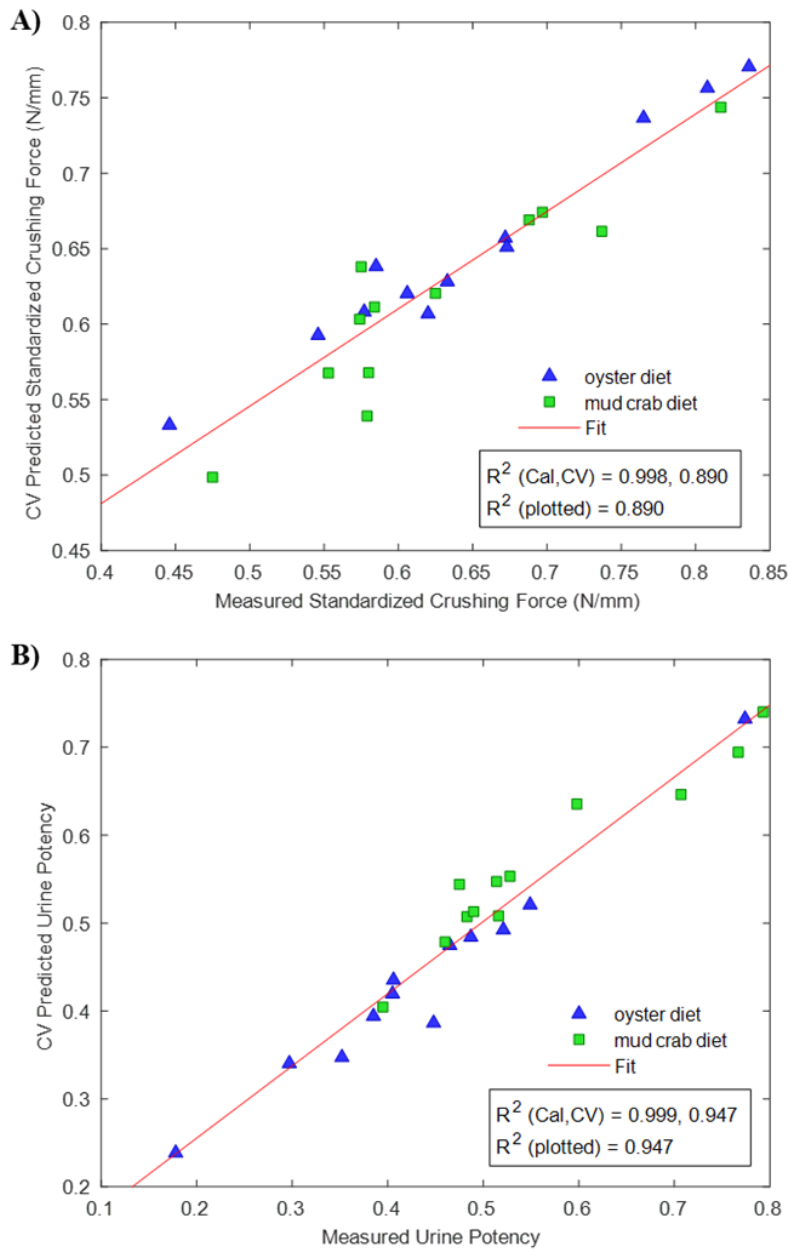


Figure 2.7 Partial least squares regression models for the oyster shell strengthening (A) and mud crab feeding (B) assays using the positive ion MS metabolomics dataset. Only two of the final eight models (i.e., four PLS-R models per bioassay) are shown. Urine potency, measured for oysters as increased shell strength and for mud crabs as decreased food consumption, were regressed against mass spectral features to predict the potency of each urine sample. Plotted lines of best fit are for the MS metabolomics cross-validated models ($R^2 = 0.89$ for the oyster shell strengthening assay and $R^2 = 0.95$ for the mud crab feeding assay). Higher urine potency indicates stronger oyster shells or reduced mud crab feeding; Higher R^2 values are indicative of a better predictive model.

Table 2.1 Top ten positive ion MS features that correlated with increased oyster shell strength. A list of 78 features was compiled by cross-comparing four PLS-R models generated for the oyster shell strengthening assay. These models were built using a subset of variables that were selected by genetic algorithm variable selection and are more robust for predicting oyster shell strength. Features are ordered by variable importance parameter (VIP) scores from highest to lowest, where higher scores indicate greater importance to the model.

Variables (m/z)	Retention Time (min)	Oyster Bioassay MS PLS-R Model Name ID	VIP Scores for Listed Oyster Bioassay MS PLS-R Model	Total Number of Models in Which Feature is Present	Average Normalized Peak Area for QCs	Molecular Formula Proposed by Compound Discoverer 3.3
155.08162	4.969	GAPQN6	3.319	4	5.65E+05	C7 H10 N2 O2
392.16018	1.549	GAPQN6	2.378	4	6.13E+04	C22 H21 N3 O4
230.14993	7.089	GAPQN6	2.051	3	5.20E+04	C10 H19 N3 O3
214.06858	1.4	GAPQN6	1.828	1	1.15E+05	C7 H13 N O5
309.13788	6.205	GAnoPQN11	1.791	1	2.98E+04	C14 H20 N4 O2 S
250.03794	1.463	GAnoPQN9 REPEAT	1.602	1	5.87E+05	C8 H11 N O6 S
276.12637	4.397	GAPQN6	1.547	4	5.20E+04	C12 H21 N O4 S
269.13837	1.022	GAPQN10	1.528	2	2.85E+05	C14 H20 O5
243.13396	4.813	GAPQN6	1.495	2	2.71E+05	C11 H18 N2 O4
234.1336	5.156	GAnoPQN11	1.427	1	3.65E+04	C10 H19 N O5

Table 2.2 Top ten positive ion MS features that correlated with reduced mud crab feeding. A list of 81 features was compiled by cross-comparing four PLS-R models generated for the mud crab feeding assay. These models were built using a subset of variables that were selected by genetic algorithm variable selection and are more robust for predicting reduced mud crab feeding. Features are ordered by variable importance parameter (VIP) scores from highest to lowest, where higher scores indicate greater importance to the model.

Variables (m/z)	Retention Time (min)	Mud Crab Bioassay MS PLS-R Model Name ID	VIP Scores from Mud Crab Bioassay MS PLS-R Model	Total Number of Models in Which Feature is Present	Average Normalized Peak Area for QCs	Molecular Formula Proposed by Compound Discoverer 3.3
222.11577	4.698	GAPQNM13	2.642	4	3.38E+06	C9 H19 N O3 S
295.16516	1.675	GAPQNM13	2.456	4	1.51E+05	C15 H22 N2 O4
173.09216	7.164	GAPQNM13	2.191	3	4.24E+04	C7 H12 N2 O3
236.0951	1.482	GAnoPQNM17	2.098	1	3.25E+04	C9 H17 N O4 S
172.13327	3.273	GAnoPQNM17	2.080	1	1.00E+06	C9 H17 N O2
245.2336	9.27	GAPQNM13	1.994	4	1.11E+05	C12 H28 N4 O
232.10982	6.928	GAPQNM20	1.957	1	1.80E+05	C10 H18 N O3 P
123.05548	1.754	GAPQNM13	1.645	2	7.07E+05	C6 H6 N2 O
454.09737	7.801	GAPQNM13	1.597	1	2.07E+04	C19 H19 N O12
195.07646	2.452	GAnoPQNM19 REPEAT	1.542	1	5.61E+04	C9 H10 N2 O3

Table 2.3 Seven positive ion MS features that correlated with both increased oyster shell strength and reduced mud crab feeding. This list was compiled by cross-comparison of all of the oyster and mud crab bioassay PLS-R models generated from features chosen by genetic algorithm variable selection. Features are ordered by variable importance parameter (VIP) for the oyster bioassay. Scores are ordered from highest to lowest, where higher scores indicate greater importance to the model.

Variables (m/z)	Retention Time (min)	Oyster Bioassay MS PLS-R Model Name ID	VIP Scores for Listed Oyster Bioassay MS PLS-R Model	Total Number of Oyster PLS-R Models in Which Feature is Present	Mud Crab Bioassay MS PLS-R Model Name ID	VIP Scores for Listed Mud Crab Bioassay MS PLS-R Model	Total Number of Mud Crab PLS-R Models in Which Feature is Present	Average Normalized Peak Area for QCs	Molecular Formula Proposed by Discoverer 3.3
276.10777	2.482	GA _{no} PQN11	0.960	1	GAPQNM _C 13	0.659	2	1.79E+05	C6 H14 N9 O2 P
229.15448	6.865	GAPQN10	0.960	1	GAPQNM _C 20	0.581	2	2.75E+06	C11 H20 N2 O3
173.09216	7.164	GAPQN10	0.860	1	GAPQNM _C 13	2.191	3	4.24E+04	C7 H12 N2 O3
176.12817	5.298	GA _{no} PQN9 REPEAT	0.836	1	GA _{no} PQNMC19 REPEAT	0.866	1	2.68E+05	C8 H17 N O3
257.18596	4.88	GAPQN6	0.799	3	GAPQNM _C 20	0.663	2	7.10E+04	C13 H24 N2 O3
183.11045	7.068	GA _{no} PQN9 REPEAT	0.776	2	GAPQNM _C 13	1.383	2	7.94E+05	C7 H16 N2 O2
187.10778	8.361	GAPQN10	0.156	2	GA _{no} PQNMC17	1.058	2	6.30E+04	C8 H16 N2 O4

2.5 Discussion

Chemical cues indicative of predation risk are inherently complex, as materials released by predators into the environment are typically blends comprised of both primary metabolites common to many or most species, and specialized metabolites associated with one or a few species. The current study supports this pattern through identification of seven chemical features which appear to be used by both oysters and mud crabs to detect blue crabs as potential predators (Table 2.3), as well as many more specialized urine biomarkers unique to assessing risk for individual prey species (Tables 2.1 and 2.2). Prey have evolved the ability to detect a plethora of chemical cues associated with their predators, but most studies fail to understand the complete ecological picture. A handful of marine studies have identified specific or multiple molecules from blends of predator-derived compounds. For example, anthopleurine, is a sea anemone alarm pheromone released by injured conspecifics and by nudibranchs (predators of sea anemones) in the immediate days following a predation event, alerting surviving sea anemone to withdraw their exposed tissues for protection (Howe & Harris, 1978; Howe & Sheikh, 1975). Additionally, phytoplankton respond to a blend of waterborne taurolipids known as copepodamides,

exuded by copepod predators, inducing a diverse set of anti-predation mechanisms (Grebner et al., 2019; Lindström et al., 2017; Selander et al., 2015). In estuarine reefs, homarine and trigonelline are two blue crab urine cues that alert mud crabs to cease foraging and seek refuge (Poulin et al., 2018) and oysters, as juvenile spat, to invest in long-term shell strengthening (Roney, Cepeda et al., 2023). However, neither of these blue crab cues were identified as dominant components of the fear-inducing blend by cross-validated PLS-R models in the current study (Fig. 2.7; Tables 2.1, 2.2, and 2.3). Instead, multiple other metabolites that remain to be fully characterized appear to be responsible for most of the induced antipredator resistance in mud crabs and oyster spat. Part of this difference could be due to metabolic differences influencing urine chemical variation between blue crabs in different environments and at different times. Urine is a chemically complex fluid, and although different blue crab metabolites appear to be most important in different studies, what has remained consistent is the potent effects of blue crab urine towards prey and the simultaneous importance of multiple metabolites in each case.

Elucidating the molecular structures of individual metabolites responsible for fear-inducing effects has so far been challenging, partly because of the many hundreds of metabolites each present in low abundance. However, variable selection applied to metabolomics datasets filters out some chemical noise, enabling models to be generated from a subset of cues that are biologically relevant. In the current study, genetic algorithm variable selection resulted in prioritization of fewer than 10% of the total number of features, suggesting that the majority of molecules in blue crab urine are not useful for alerting prey of nearby predators. This is not surprising as urine is a ubiquitous biological fluid released by many different organisms, not all of which are predators. For example, studies in terrestrial systems have shown that prey respond to urine of relevant carnivores, although not urine from herbivores (Nolte et al., 1994) or conspecifics (Fendt, 2006).

Predator diet also influences prey response in marine systems as is the case for mud crabs (Poulin et al., 2018), although results from the current study show greater overlap in potency for urine of blue crabs fed different diets. (Fig. 2.7). In part, this may be explained by the fact that homarine and trigonelline were not selected by genetic algorithm variable selection in relation to reduced mud crab feeding (Fig. 2.7B), likely because, as shown by previous analyses (Roney et al., 2023), concentrations of these metabolites measured in blue crab urine of this sample set were comparable for both diets and lower than in previous years. Additionally, since homarine and trigonelline concentrations in urine analyzed for the current study were not previously found to correlate with oyster shell strengthening (Roney, Cepeda et al., 2023) nor reduced mud crab feeding (data not shown), it makes sense that these metabolites do not appear in the corresponding PLS-R models (Fig. 2.7). These results support the following hypothesis: when homarine and trigonelline are very abundant, prey take notice, but in the absence of high concentrations of these cues, prey rely on other molecules to assess predation. These second-tier fear cues appear not to be diet-dependent, resulting in greater overlapping metabolite concentrations and in turn urine mixtures of different diets. As a result, particular urine mixtures appear to be especially potent towards both mud crabs and oyster spat due to appreciable concentrations of common fear cues.

Prey response to predator cues is nuanced, which is why prey utilize complex blends and rely on what is available. In many cases, individual metabolites do not adequately explain prey response, requiring sophisticated methods such as metabolomics to explore the chemical basis for induction of antipredator resistance. Results from the current study suggest that mud crabs, a mid-trophic level organism, detect cues related to predator diet when available (Fig. 2.5), while oysters, at a lower trophic level, focus on more general blends of urine cues common to many relevant predators irrespective of diet (Fig. 2.4 and 2.7A). This may be a more advantageous strategy for oysters since they are

immobile, unable to seek refuge, and more accessible to certain predators. Across diverse animal species, urine shares broad chemical similarities, including pungent sulfurous volatile molecules and low molecular weight polar water-soluble compounds including amines. One study found that fox urine-derived 3-methyl-3-butenyl methyl sulfide was aversive to hares (Sullivan & Crump, 1986), while another proposed that sulfur-containing metabolites are likely fear cues as they are prevalent in the urine of carnivores, which is particularly effective at repelling prey (Nolte et al., 1994). The composition of wolf urine has been studied extensively, identifying alkyl pyrazine analogs as important constituents of a blend used by mice (Osada et al., 2013) and deer (Osada et al., 2014) to sense and avoid predators. Rodents exhibit avoidance behavior in the presence of phenylethylamine, a metabolite prevalent in the urine of many carnivores, and multiple prey in oyster reefs exhibit anti-predatory responses to blue crab urine quaternary amine metabolites homarine and trigonelline (Poulin et al., 2018; Roney et al., 2023). Proposed molecular formulae for features identified by PLS-R models in this study suggest that additional fear cues important to blends used by oysters and mud crabs are polar nitrogen and oxygen-containing metabolites which remain to be fully characterized.

Animal metabolism and urine composition are influenced by age, sex, diet, genetics, and environmental conditions (Bouatra et al., 2013; Osada et al., 2015). These factors almost certainly affect metabolites released in the urine of blue crabs and in turn prey perception of risk, although we did not explore systemic metabolism in the current study. Additional research has shown that external stressors such as climate change and exposure to anthropogenic contaminants (i.e., metals, plastics, and pollutants) impact animal metabolism. However, it is unknown how these factors influence predator urine composition, or a cue's chemical stability in the environment. As oceans become more acidic, ambient concentrations of chemical cues and their efficacy may be altered, with potentially large ramifications for common fear cues used by many prey. When designing

future metabolomic experiments investigating chemically mediated predator-prey interactions, all of these variables should be collectively taken into consideration.

The current study lays the foundation for discovering new fear cues from complex biological fluids, especially in cases in which blends of multiple metabolites are required to elicit prey response. The specificity of the response relies on the molecular structure of each predator metabolite and its presumed interaction with a corresponding prey receptor. Even small differences in chemical structure, for example, even among compounds that share the same metabolite class or carbon skeleton are expected to dramatically affect biological activity. Genetic algorithm variable selection and metabolomics are methods that can be leveraged for unraveling the composition of complex chemical cue blends important to predator-prey interactions, especially in marine systems where identities of the majority of these chemical cues remain unknown. Many predator-prey systems could be explored via this approach, including *Nucella* snails responding to predatory green crabs (Large & Smee, 2013), oysters strengthening their shells after exposure to chemical cues from predatory snails (Ponce et al., 2020), and urine-mediated interactions between generalist predatory fish and various prey. Development of novel bioassays are needed in conjunction with the use of novel metabolomic methods to facilitate ground-breaking discoveries. Adjustments and improvements for metabolomics methods are constantly being developed and will continue to facilitate the identification of chemical cues that influence interactions between predators and prey.

CHAPTER 3. ASSESSING ALGAL BIOFUEL POND SYSTEM EXOMETABOLOMES: INSIGHTS FOR PROTECTION FROM PESTS

This chapter is adapted from the final report submitted to Sandia National Laboratories as part of the Laboratory Directed Research and Development (LDRD) Program. Algal biofuel pond system exometabolomes were explored as part of a collaborative project between scientists at Sandia National Laboratories and the Georgia Institute of Technology: Marisa R. Cepeda, Gabriella Chebli, Nolan H. Barrett, Carolyn L. Fisher, Todd W. Lane, Samuel Moore, Hailey Loehde-Woolard, Samantha Spano, William Buzzeo, Ethan Bar-Nur, and Julia Kubanek.

3.1 Abstract

Preliminary studies at Sandia National Laboratories (SNL) identified several bacterial consortia comprised of multiple marine bacterial species that protect biofuel-relevant microalgae from ubiquitous microscopic pests called rotifers. While bacterial consortia offered varying degrees of protection against rotifers, some may better protect against phagotrophic algae and pathogens such as chytrid fungi. It was hypothesized that specific species within these bacterial communities produce secondary metabolites that act as natural agents of biocontrol and this work explores co-culturing algae with protective marine bacteria as a zero-cost pest control solution. The goal of this project was to identify bacterial natural products that exhibit toxicity or deterrent effects against pests, towards the development of algal cultivation methods that can be optimized for co-culturing with the

identified protective bacteria. Proton nuclear magnetic resonance (^1H NMR) spectroscopy- and mass spectrometry (MS)-based metabolomics methods were used to obtain chemical profiles of bacterial consortia exometabolomes in order to identify putative defenses against algal pond threats. Statistical analysis of a small-scale pilot experiment indicated that lipid-soluble exometabolomes are influenced by bacteria, and more specifically that algal cultures with protective bacterial consortia have chemical profiles that are distinguishable from those with non-protective bacteria. Furthermore, SNL isolated 36 bacteria from unique sources (i.e., several protective bacterial consortia) and a bacterial extract library was generated to explore the toxicity effects of bacterial extracts on rotifers, phagotrophic algae, and chytrids. Screening of bacterial extracts generated from this isolate library indicated that 6 of 36 bacteria were significantly toxic to rotifers. However, several follow-up experiments failed to reproduce the observed toxicity, and Illumina next-generation sequencing results suggested that this was likely in part because many bacteria in the library were not clonal. Additional toxicity bioassays were conducted with 18 of the 36 bacterial isolates that had been exposed to rotifer and algal conditioned media to address the hypothesis that rotifer cues induce bacteria to produce anti-rotifer compounds. However, these extracts had no impact over rotifer mortality. Five of these isolates were tested at higher concentrations, with one isolate increasing the mortality rate of rotifers; however, this isolate was found to be an impure culture. A subset of these bacterial extracts was screened for growth-suppressing effects on the phagotrophic alga *Poteroochromonas malhamensis*. Initial experiments failed to indicate allelopathic effects of bacterial culture extracts; however stimulatory effects of media components were implicated in these results. Follow-up experiments with extracts of bacterial supernatants, instead of whole

cultures, reduced the stimulatory effects of the media, but little evidence of allelopathy was observed and there was no evidence that the presence of *P. malhamensis* induced antialgal metabolite production in these bacteria. Of the 36 bacterial supernatant extracts screened, two significantly suppressed the growth of this algal pest. However, one of the bacterial isolates found to decrease *P. malhamensis* growth consisted of multiple bacterial species and the purity status of the second is unknown. Moving forward, clonal bacterial isolates with reproducible growth and metabolite production will be key for developing methods to identify protective molecules, using rotifers as a model system. These methods can then be applied to additional target pests (e.g., chytrids) that threaten commercially valuable microalgal species.

3.2 Introduction

As fossil fuel reserves continue to be depleted and atmospheric carbon dioxide warms the planet, the need for renewable liquid fuel sources has increased. Liquid biofuels derived from microalgae biomass show the most promise because these algae are able to accumulate up to 75% of their dry weight in lipids (i.e., fuel molecule precursors) (Mubarak et al., 2015). In addition, they are an important alternative to current fuel sources because a large portion of the biomass produced by microalgae comes from carbon dioxide sequestered from the atmosphere (Falkowski et al., 1998). However, to make algal biofuels competitive with liquid fossil fuels, the cost of production needs to be greatly reduced (A. Sun et al., 2011) through optimization of growth conditions, conservation of resources (e.g., fresh water, land, etc.), and elimination of predator-induced “pond crashes” that result in algal biomass loss (Hamilton, 2014).

Although progress has been made toward determining optimal conditions for industrial microalgae cultivation (Hamilton, 2014), predators of microalgae (e.g. ,protists, copepods, rotifers, etc.) are ubiquitous in open-air ponds (Flynn et al., 2017). Once introduced into a pond, predators are capable of capitalizing on an almost limitless food source. Current methods to eliminate predators often involve the addition of pesticides, but this option is not ideal because of risks to environmental health and the need to add more compound after it gets consumed or degraded (Montemezzani et al., 2015). Examples of compounds that have been used previously as pesticides against predators in biofuel ponds include rotenone (Van Ginkel et al., 2015), quinine sulfate (C. Xu et al., 2015), and hypochlorite (Park et al., 2016), none of which are known to be naturally produced by microalgae or their associated bacteria. A potential source of protective compounds are bacteria, which produce complex secondary metabolites and benefit microalgae through nutrient exchange (Fuentes et al., 2016). Therefore, the biofuel industry could directly benefit from growing microalgae with bacterial consortia because bacteria provide microalgae with essential nutrients, improve their growth, and have the potential to protect them from predators.

Previous studies carried out by our collaborators at Sandia National Laboratories have already identified protective bacterial consortia that kill rotifers (*Brachionus plicatilis*), preventing their predation on microalgae (*Microchloropsis salina*) (Fisher et al., 2019). While observations of rotifers exposed to these bacterial consortia indicate that the interaction is chemically mediated, further work is needed to determine the exact protection mechanism. Rotifer death may be caused by exposure to molecules excreted by bacteria into the surrounding culture media, or alternatively rotifers may need to ingest bacterial

cells in order to be negatively impacted. The chemical profiles of algal cultures with and without protective bacteria are expected to be distinguishable based on distinct chemical features associated with protective molecules. These molecules may be either extracellularly released or intracellular bacterial secondary metabolites. Therefore, this project was divided into the following steps to bridge the current knowledge gap: 1) Chemically profile algal cultures with non-protective and protective bacterial consortia, 2) Identify aquatic bacterial isolates from select bacterial consortia, 3) Determine which bacterial isolates produce natural products that protect algal crops from predation by rotifers, phagotrophic algae, and chytrids to in turn prevent biofuel ponds from crashing.

3.3 Methods, results, and discussion

3.3.1 Chemical Profiling of Bacterial Consortia Exometabolomes

To explore whether bacteria exude protective secondary metabolites, we conducted multiple experiments to determine whether microalgal cultures with protective or non-protective bacterial consortia could be distinguished from each other through chemical profiling of their exometabolomes (i.e., metabolites present in conditioned media). In a pilot study conducted at SNL, *Microchloropsis salina* was cultured with protective and non-protective bacterial consortia or without bacteria (negative control). At Georgia Tech, natural products were extracted from conditioned algal culture media using solid phase extraction (SPE) and eluted with methanol. Two technical replicates were analyzed per treatment group and all samples were partitioned into lipid- and water-soluble fractions using a water-methanol-chloroform (9:10:15) mixture.

^1H NMR spectroscopy was used to generate chemical profiles for lipid- and water-soluble fractions of conditioned media from each of the two treatments and the no-bacteria control. Several dominant chemical features in ^1H NMR spectra were observed in all three treatments. To consider compounds beyond these most dominant ones, principal component analyses (PCA) were performed on spectra for both lipid- and water-soluble extracts to determine whether the treatment groups could be distinguished from each other based on differences among more minor chemical features (Fig. 3.1 and 3.2). PCA of ^1H NMR spectra for lipid-soluble extracts separated all three treatment groups from each other based on variation among their chemical features. The protective and non-protective bacterial treatments were separated by PC 1 which accounted for 43.8% of the variance between samples, while PC 2 separated both bacterial consortia treatments (protective and non-protective) from the no-bacteria control and explained 24.0% of the variance. These results indicate that the presence of bacteria affects the lipid-soluble exometabolome, and specifically the presence of protective bacterial consortia is associated with specific molecules that are distinguishable from those of non-protective bacteria. For PC analysis of the water-soluble extracts, PC 3 accounted for 14.8% of the variance between replicates and separated the no-bacteria control from the treatment with non-protective bacteria indicating that the presence of bacteria affects the chemical profile of the water-soluble exometabolome. PC 1 accounted for 46.7% of the variance, suggesting that algal cultures with protective bacteria are chemically distinct from those with non-protective bacteria or no bacteria. However, since PC 1 only separated one of the two protective samples from the other treatments, analysis of additional replicates is needed to confirm this. While the majority of metabolites in both the water-soluble and lipid-soluble exometabolomes are

likely algal in origin, it is most likely bacterial metabolites that distinguish the protective treatment from the no bacteria and non-protective treatments. These results were sufficiently promising to support expansion of the project to analyze a larger group of treatments and replicates.

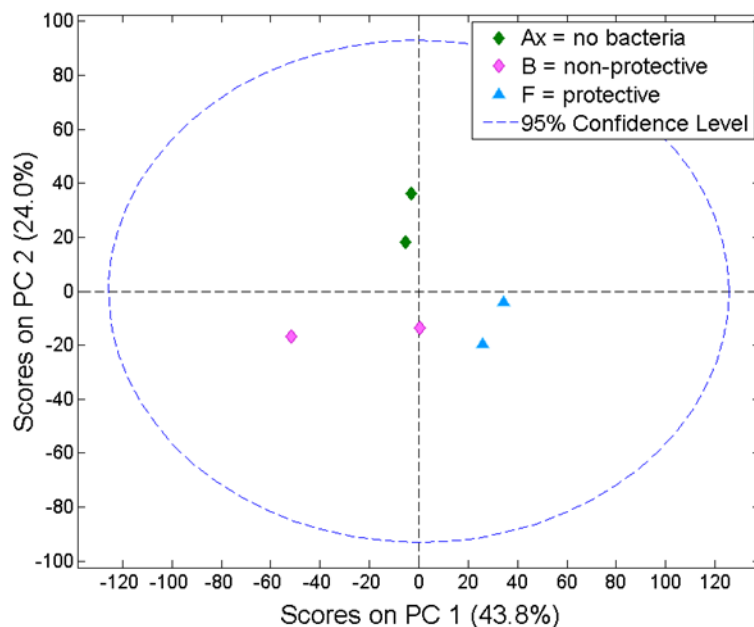


Figure 3.1 Principal component analysis (PCA) of ¹H NMR spectral data acquired for lipid-soluble algal culture conditioned media extracts, in the presence and absence of bacteria. Two technical replicates were tested per sample type: no bacteria (green diamond), non-protective bacteria (consortium “B”, pink diamond), protective bacteria (consortium “F”, blue triangle). Bacterial metabolites most likely distinguish the protective treatment from the non-protective and no bacteria treatments along the PC 1 axis.

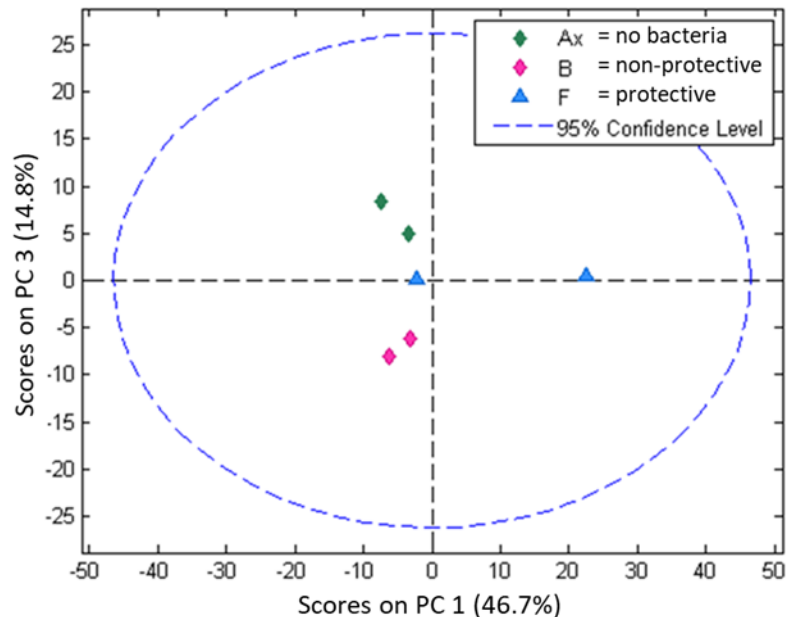


Figure 3.2 A principal component analysis of ^1H NMR spectral data acquired for water-soluble algal culture conditioned media extracts. Two technical replicates were tested per sample type: no bacteria (green diamond), non-protective (pink diamond), protective (blue triangle). Bacterial metabolites separated one of the two protective treatment technical replicates from the non-protective and no bacteria treatments along the PC 1 axis. Distinct metabolites in the second technical replicate were likely too dilute to distinguish it from the other treatments.

Given that MS is a more sensitive, yet complementary spectroscopic method to NMR spectroscopy for metabolomics analysis, we developed an LCMS-based chemical profiling method to distinguish the exometabolomes of algal cultures with and without protective bacteria. Lipid- and water-soluble fractions of the same pilot study samples used to acquire ^1H NMR spectra were recombined and dissolved in water prior to liquid chromatographic (LC) separation (TSKgel Amide-80 column) and electrospray ionization (ESI) ion trap MS analysis. MS chemical profiles of algal cultures without bacteria or with protective bacterial consortia are distinguishable for both positive (Fig. 3.3a) and negative ionization modes (Fig. 3.3b).

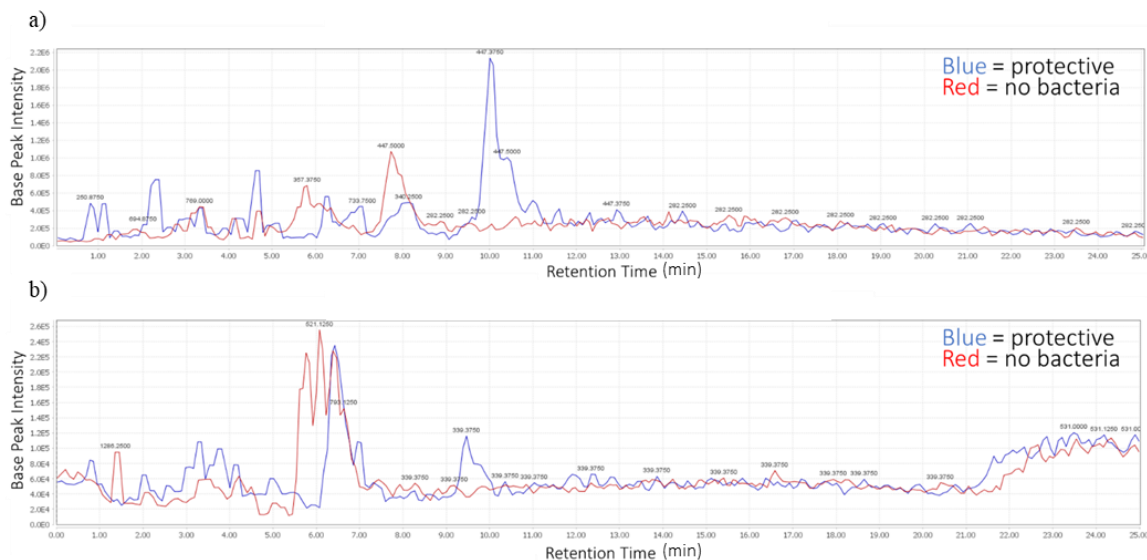


Figure 3.3 Base peak chromatograms from LCMS analysis of algal culture extracts
a) Positive mode base peak ion chromatograms for extracts of algal cultures grown with a protective bacterial consortia (blue) or no bacteria (red). **b) Negative mode base peak ion chromatograms for extracts of algal cultures grown with a protective bacterial consortia (blue) or no bacteria (red).**

A larger experiment was performed employing a 6×2 factorial design with six algal-bacterial treatments including one bacteria-free control (i.e., algae grown without a bacterial consortium), each either exposed or not exposed to rotifers. Bacterial consortia were considered to be protective in the presence of rotifers if the algal growth endpoint, measured by relative fluorescence, was significantly greater than that of the bacteria-free control with rotifers. Samples from all twelve treatments ($n=3$ replicates of each) were extracted using SPE and metabolites were eluted using methanol. Dried extracts were dissolved in deuterated dimethyl sulfoxide (DMSO- d_6) to acquire ^1H NMR spectra at 800 MHz. ^1H NMR spectra for all sample extracts were compared to a spectrum of the bacteria-free control extract (representative spectra shown in Fig. 3.4). Almost all dominant peaks in these NMR spectra for the different treatment groups were also present in the bacteria-free control, indicating that they likely correspond to microalgal metabolites. The

remaining dominant peaks were present in the bacteria-free control in the presence of rotifers indicating that these peaks either correspond to molecules produced by rotifers or by algae in the presence of rotifers, rather than by bacteria. The sole treatment whose extracts contained more than four additional peaks were associated with the least protective consortium, both in the presence and absence of rotifers. Examples of these peaks are circled in red in Figure 3.4. However, since these peaks are present in the least protective sample, it is unlikely that they correspond to protective molecules. If the most protective consortium samples contain extracellularly released protective bacterial metabolites contributing to algal protection, it is likely that the current extraction protocol is not appropriate for their identification (e.g., the protective compounds could be biomacromolecules such as proteins) or that the metabolites are produced at concentrations below the limit of detection for ^1H NMR spectroscopy.

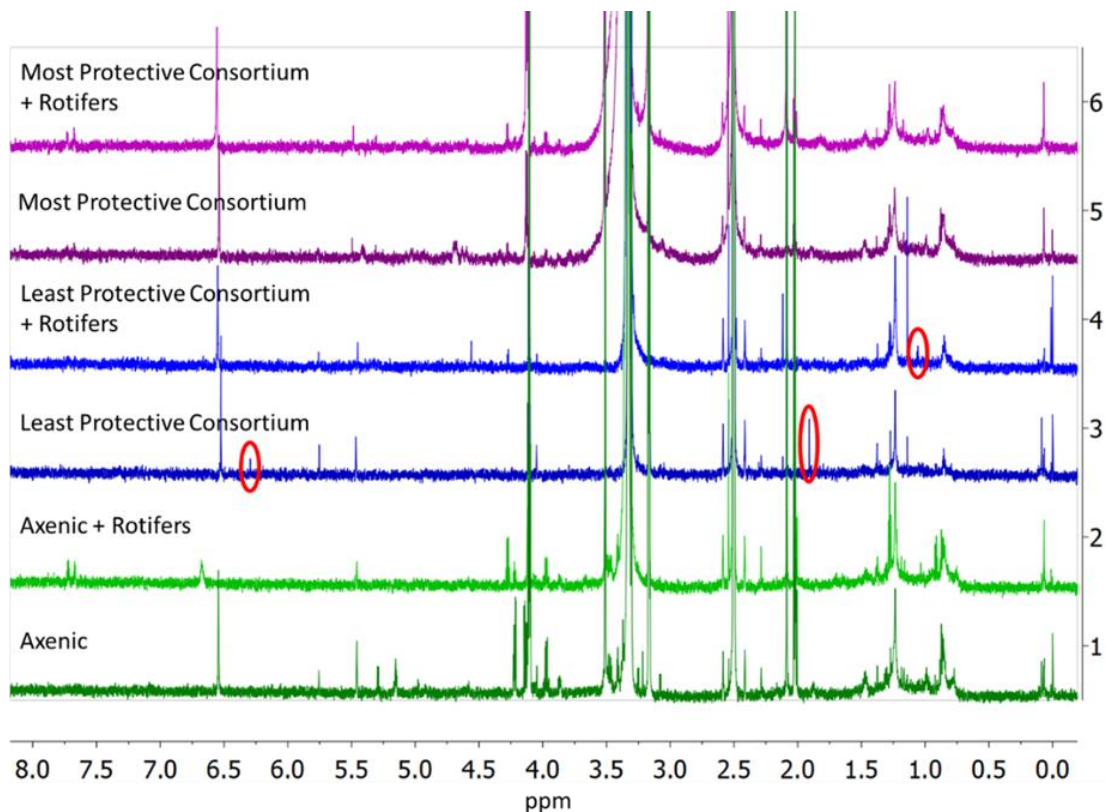


Figure 3.4 ^1H NMR spectra of algal culture-conditioned media extracts: no bacteria (dark green), no bacteria + rotifers (light green), least protective consortium (navy blue), least protective consortium + rotifers (royal blue), most protective consortium (dark purple), and most protective consortium + rotifers (light purple). Although many bacterial consortia were tested in this experiment, only the no bacteria, most protective consortia, and least protective consortia treatments are shown because they are representative of the entire data set. Red circles draw attention to signals associated with molecules arising from exposure to bacteria.

Since ^1H NMR spectroscopy was not adequate to detect chemical features unique to exometabolomes of algal cultures with the most protective bacterial consortia, LCMS was used to further characterize these extracts. Two samples (one strongly protective and one moderately protective algal-bacterial culture conditioned media extract) were chosen for the initial method development using C_{18} reversed phase LC and neither of these samples were from cultures that contained rotifers. While chromatograms for both samples each had a few broad peaks, distinct metabolites eluted early (~ 2 min) and mass spectra for

the labeled peaks (A and B) revealed more distinct chemical features (red circles) for the strongly protective algal-bacterial culture conditioned media extract (**Fig. 3.5**). As expected, MS spectra contained a greater number of spectral features, however the majority were present in all samples, unique features were at intensities comparable to the noise, and the most abundant molecules detected were plastics. Features of interest in the strongly protective consortium sample include m/z signals 140.9, 167.23, 169.12, and 202.36, and in the moderately protective consortium m/z signal 554.84. However, higher sample volumes and larger replicate numbers are needed to confirm that these signals are reproducible and unique to protective samples.

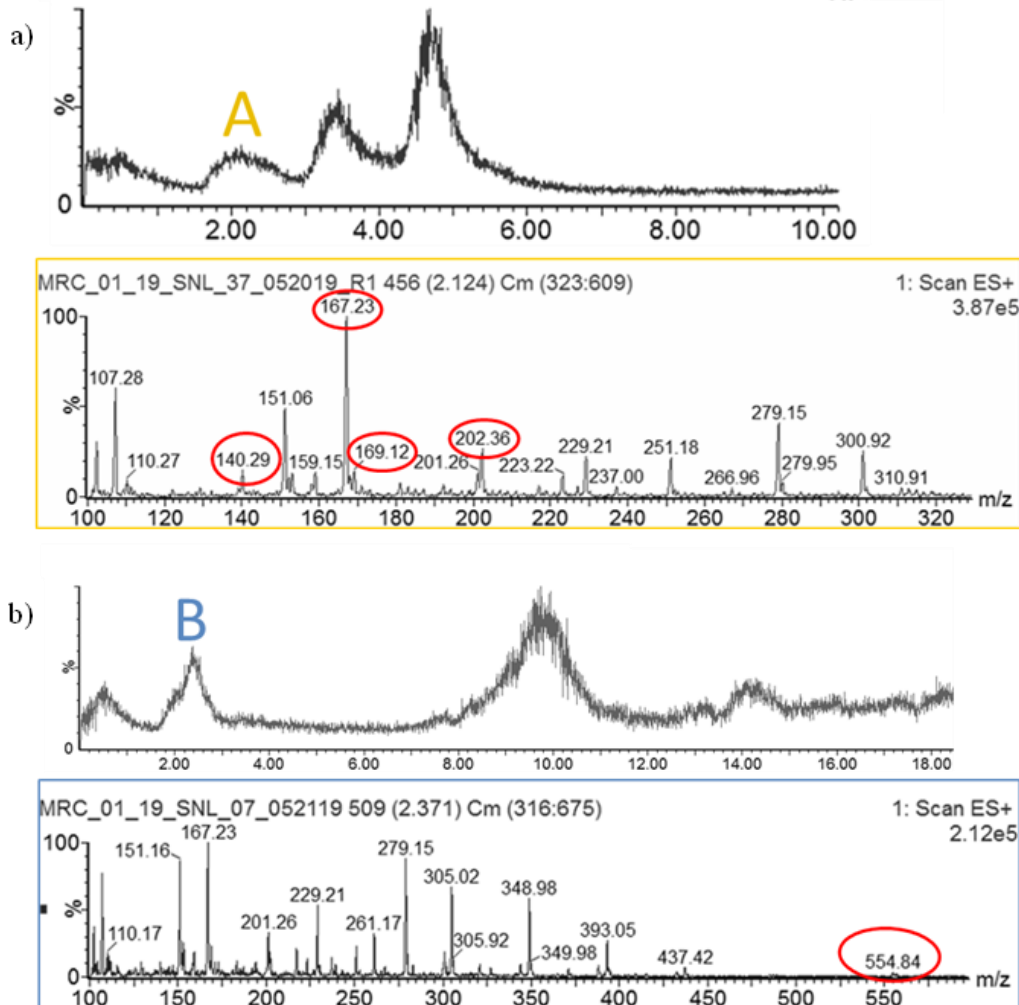


Figure 3.5 a) Liquid chromatography (LC) chromatogram for an algal-bacterial (strongly protective) culture conditioned media extract. The mass spectrum for peak A (gold outline) shows m/z signals for distinct metabolites (red circles). b) LC chromatogram for an algal-bacterial (moderately protective) culture conditioned media extract. The mass spectrum for peak A (blue outline) shows m/z signals for distinct metabolites (red circles).

3.3.2 A Comparison of SPE Methods for Extracting Algal Culture Conditioned Media

To get a broader scope of the types of metabolites present in algal-bacterial culture conditioned media, a pilot study was designed to compare culture extracts obtained by different SPE methods. *M. salina* microalgae were cultivated at SNL with *Alteromonas macleodii* bacteria to investigate their potential as a probiotic and determine whether they

protect microalgae from rotifer predation. Three different algal culture treatments (algae + rotifers, algae + bacteria, and algae + bacteria + rotifers) and a negative control (axenic) were monitored approximately every 24 hours by measuring relative fluorescence (Fig. 3.6). Growing *A. macleodii* with *M. salina* microalgae provided neither a probiotic nor protective effect; however, unsurprisingly, microalgae grew better in the absence of rotifers than microalgae exposed to rotifer predation. We proceeded by focusing on the algae + rotifers and algae + bacteria + rotifers samples to determine the best SPE method for extracting bacterial metabolites that would allow us to distinguish between cultures grown with and without bacteria. Since experimental relative fluorescence end point values were lower than in previous experiments, larger sample volumes (~95 mL) were extracted using three different SPE methods (C₈, PPL, and StrataX) that retain molecules spanning a range of polarities.

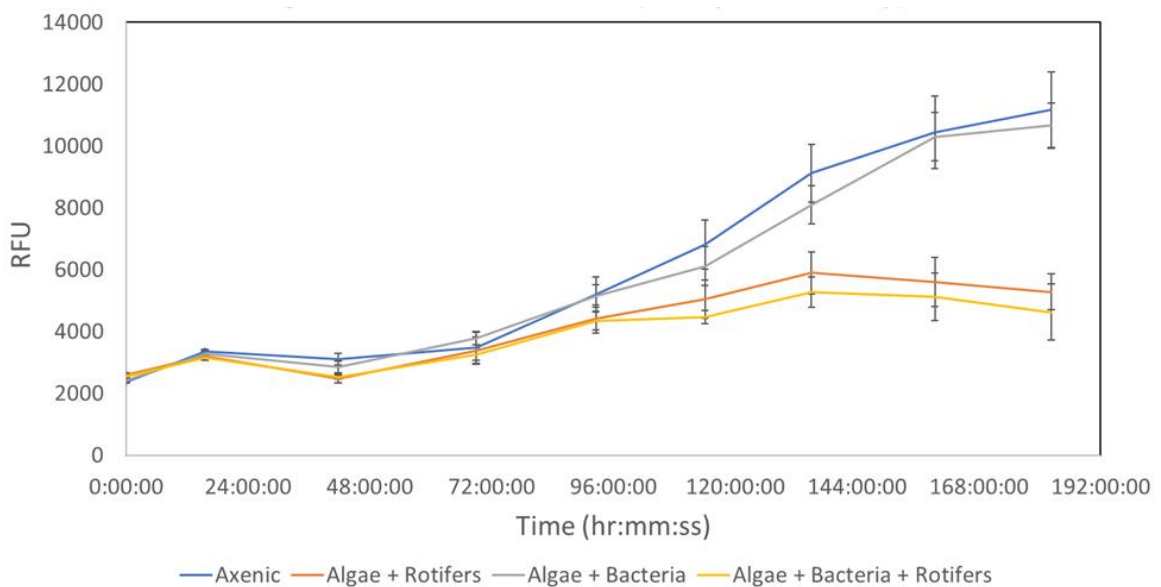


Figure 3.6 Algal growth curves for the *M. salina* and *A. macleodii* co-culture experiment: Axenic (blue), algae + rotifers (orange), algae + bacteria (grey), and algae + bacteria + rotifers (gold).

For LCMS chemical profiling of algae + rotifers and algae + bacteria + rotifers conditioned media extracts, positive ionization mode data were acquired using both hydrophilic interaction liquid chromatography (HILIC) and reversed phase liquid chromatography methods. Principal component analyses for both HILIC and reversed phase data sets were performed using the Thermo Scientific Compound Discoverer software and showed that samples shared more similarities if they were extracted using the same SPE method (Figs. 3.7 and 3.8). For the PCA of MS data acquired using reversed phase C₁₈ liquid chromatography (Fig. 3.7), PC 1 explained 67.8% of the variance between samples, while PC 2 explained 15.4% of the variance. The corresponding loadings plot shows individual molecular masses (gray dots) that contribute to the separation of samples in the PCA plot. The samples with the greatest number of associated molecular masses were those extracted using StrataX cartridges, followed by C₈ and then PPL. Thus, it was resolved that in future, we would use StrataX cartridges to extract important exometabolome metabolites from conditioned media samples in preparation for reversed phase LCMS.

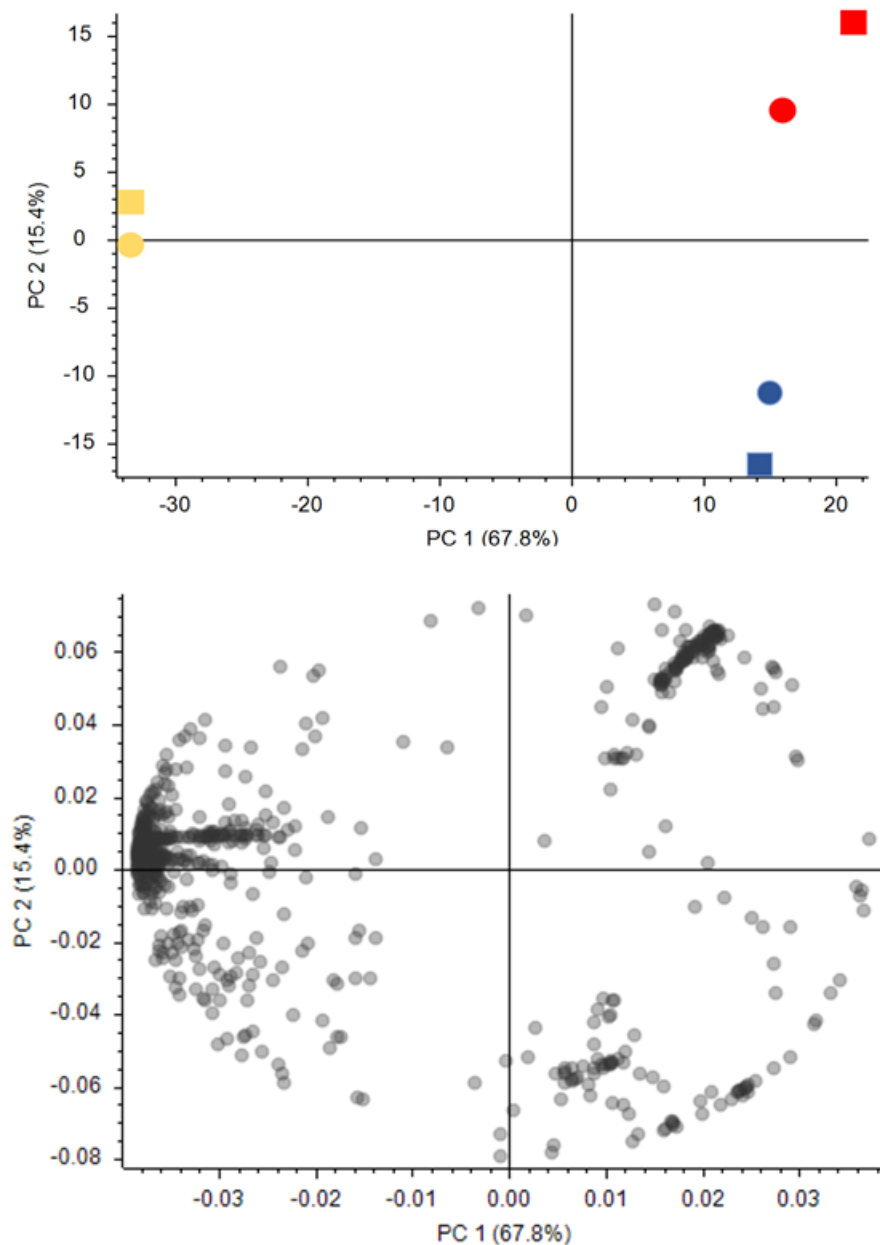


Figure 3.7 Top) Principal component analysis (PCA) of reversed phase C18 LCMS data acquired for algae + rotifers and algae + bacteria + rotifers conditioned media extracts. Three different solid phase extraction (SPE) methods are represented by red (C8), blue (PPL), or yellow (StrataX) shapes. Extracts from cultures grown with bacteria are represented as squares while those of extracts for cultures grown without bacteria are represented as circles. Bottom) Loadings plot where each point represents an individual molecular mass with a corresponding retention time.

For the PCA of MS data acquired using normal phase BEH HILIC (Fig. 3.8), PC 1

accounted for 61.2% of the variance between samples and PC 2 accounted for 16.3% of the variance. While the loadings plot for the HILIC PCA displayed a similar trend to that for the reversed phase analysis, the HILIC chromatography resolved a greater number of distinct chemical features for samples extracted using the StrataX cartridges. In addition, a greater number of chemical features spread across PC 2 may indicate that in future studies these features could be used to distinguish between StrataX extracts for algal cultures grown in the presence or absence of bacteria. However, this greater chemical diversity in the loadings plot for the normal phase LC-MS analysis should be treated with caution because it may be that it corresponds to irrelevant features that Compound Discoverer could not successfully filter out of the dataset as in the case for the reversed phase analysis. This aside, these results still indicated that we should use StrataX cartridges in preparation for BEH HILIC LCMS to ensure that we maximize chemical diversity in our analyses.

Results from that pilot study indicate that the SPE LCMS pipeline is suitable for analyzing algal-bacterial culture conditioned media. While PCA does not suggest that either reversed or normal phase liquid chromatography is better for separating molecules within each of the extracts, both datasets suggest that StrataX is the best SPE method for maximizing chemical diversity. In future studies, additional replicates are needed to produce more powerful PCA outcomes to establish whether the SPE LC-MS pipeline distinguishes extracts from algal cultures grown with or without bacteria in a statistically significant manner.

In an effort to simplify our metabolomic workflow, we designed and conducted an experiment in collaboration with the Systems Mass Spectrometry Core at Georgia Tech to determine whether conditioned algal culture media samples could be analyzed directly

without the need for an extraction step. HILIC high resolution MS data were acquired in both positive and negative ionization modes for three types of conditioned algal culture media samples: 1) samples that were never extracted, 2) samples that were extracted using SPE, and 3) the flow-through of samples that were extracted using SPE (i.e., compounds not retained by SPE). The three SPE methods that were tested in order of most to least non-polar were C8, PPL, and StrataX. For PCA of both positive and negative ionization mode data, samples statistically clustered according to the processing method. An example of this is shown in Figure 3.9 with the HILIC positive ionization mode data. In addition, within the group of samples that were generated from SPE, samples separated based on the three different SPE cartridge types. PC 1 in both the positive and negative ionization mode PCA plots separated SPE samples from the non-extracted and flow-through samples, indicating that the flow-through may share more features with samples that were never extracted. While very few features were associated with the flow-through samples, a large number of features were associated with both the non-extracted and SPE extracted samples (Fig. 3.9B). Therefore, this experiment suggests that conditioned algal culture media samples can be analyzed using LC-MS without prior SPE, however metabolites that are more dilute may not be detected.

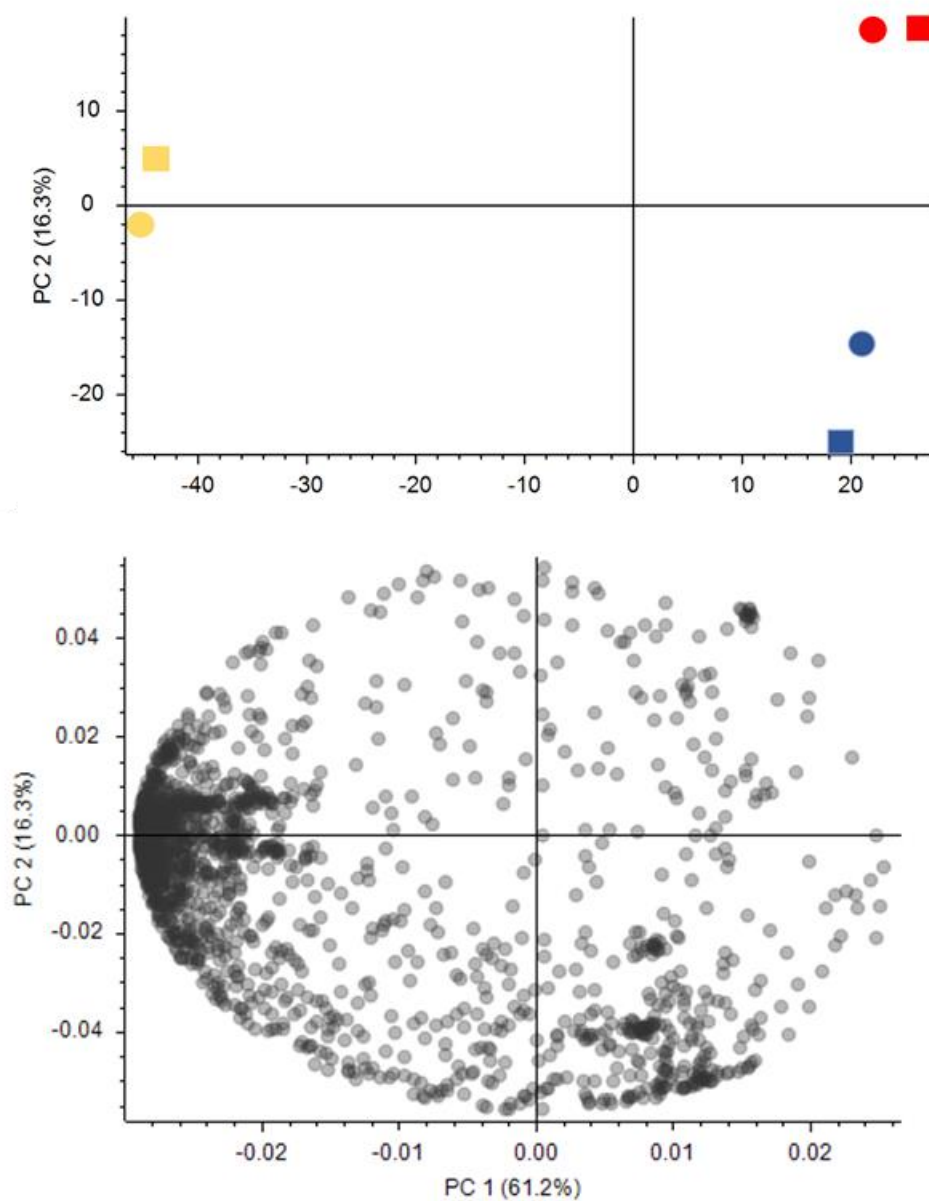


Figure 3.8 Top) Principal component analysis (PCA) of normal phase BEH HILIC LCMS data acquired for algae + rotifers and algae + bacteria + rotifers conditioned media extracts. Three different solid phase extraction (SPE) methods are represented by red (C8), blue (PPL), or yellow (StrataX) shapes. Extracts from cultures grown with bacteria are represented as squares while those of extracts for cultures grown without bacteria are represented as circles. Bottom) Loadings plot where each point represents an individual molecular mass with a corresponding retention time.

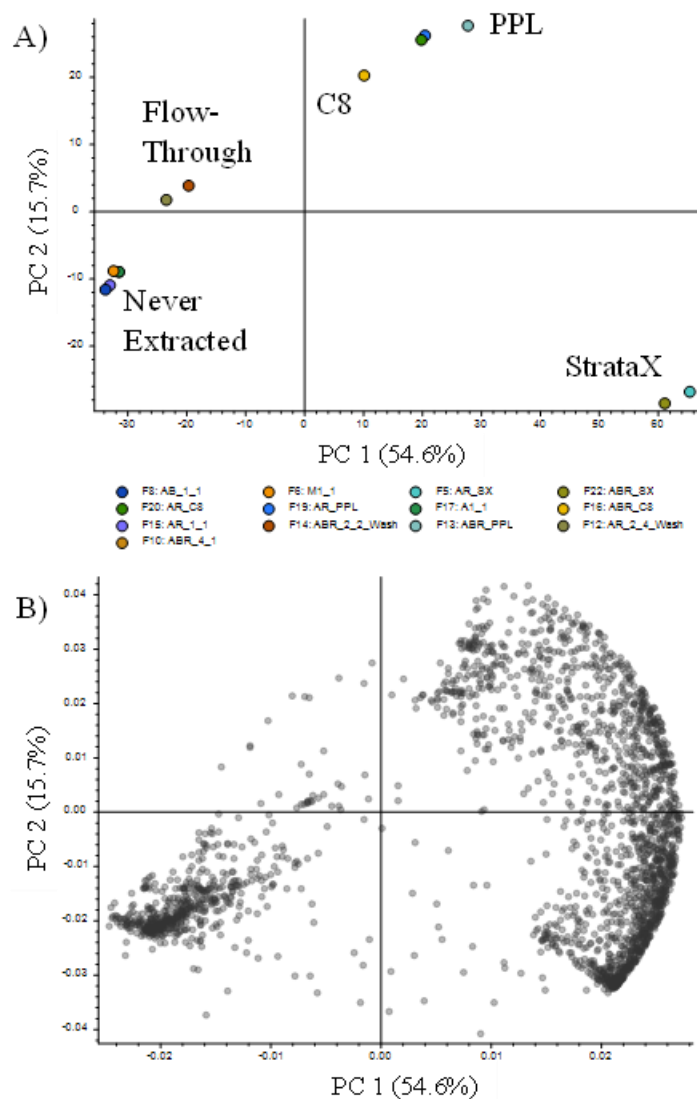


Figure 3.9 A) Principal component analysis (PCA) for HILIC positive ionization mode LCMS data. PC 1 on the x axis and PC 2 on the y axis represent 54.6% and 15.7% of the variance among samples respectively B) Loadings plot of chemical features that correspond with samples in the PCA plot. Each feature is a molecular mass with a corresponding retention time and how they group results in the separation of treatment groups.

3.3.3 Anti-rotifer Natural Products from Aquatic Bacterial Isolates

Previous challenges related to poor reproducibility and low concentration of metabolites associated with algal-bacterial consortia paved the way for the design of new

experiments focusing on 36 bacterial isolates, each tested separately. SNL isolated these bacteria from five unique sources based on observations suggestive of their potential to produce protective natural products: bacterial consortia associated with dead rotifers, a live rotifer culture, and an outdoor pond at Arizona State University where the algal crop survived while algae in nearby ponds did not. At Georgia Tech, to leverage the protective potential of these bacteria, a natural product extract library was created from two major experiments whereby bacteria were either grown in isolation or in the presence of waterborne cues from the rotifer *Brachionus manjavacas*. Strain numbers used in the current report are those provided by Dr. Carolyn Fisher at SNL. We aimed to test the overarching hypothesis that individual bacterial strains produce natural products that kill rotifers, and the secondary hypothesis that the presence of rotifers induce production of anti-rotifer natural products in bacteria.

For the first experiment, single cultures of each bacterium were generated in marine media, lysed with 0.1 mm ceramic beads to ensure cell rupture, and extracted twice with ethyl acetate. (Preliminary experiments with additional solvents, such as dichloromethane, to extract bacteria produced similar results.) These extracts were then dissolved in dimethyl sulfoxide (DMSO) and screened in a rotifer toxicity assay slightly modified from previous studies (Kubanek et al., 2007; Snell & Persoone, 1989). Each well in a 24-well plate contained 6-8 rotifers, *M. salina* (850,000 cells mL⁻¹), and 10 µL of treatment or control solutions dissolved in DMSO. Extracts were tested at half-fold of the concentration of the original bacterial culture (by volume), a concentration close to the maximum of what is realistically achievable for algal raceway pond applications while still higher than undetectable levels in previous algal-bacterial co-culture experiments (Fisher et al., 2019).

For this initial bacterial extract screening, all treatments and controls were tested in triplicate wells (Fig. 3.10). Six of 36 extracts were significantly more toxic to rotifers than their corresponding DMSO negative control ($p < 0.05$), as was the $\sim 0.75 \mu\text{M}$ rotenone positive control ($p < 0.05$). The toxicity of bacterial extract #10 was comparable to that of the rotenone positive control, making it the most promising for future investigation. However, bacterial extract #3 was also reasonably toxic, followed by extracts for isolates #4, #6, #18, and #26 which all had comparably lower bioactivities. Extracts for bacterial isolates #2, #9, #20, and #23 did not result in any notable rotifer mortality, nor did the remainder of the 36 bacterial extracts tested (Fig. 3.10).

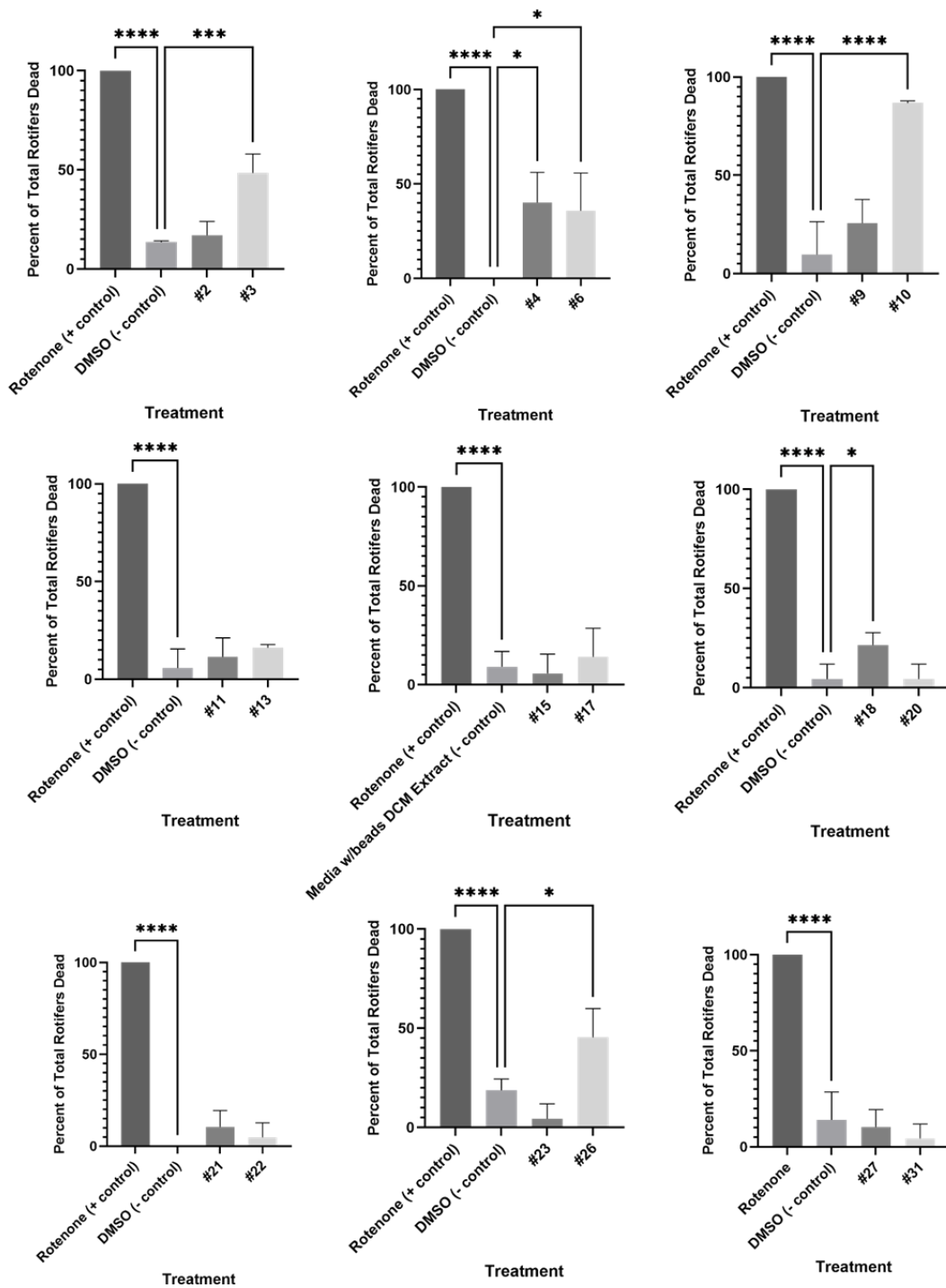


Figure 3.10 24-hour rotifer toxicity assay initial screening results. One graph is shown for each 24-well plate assay. Asterisks denote when extracts of bacterial isolates (n = 3) were significantly more toxic than the corresponding negative control (n = 3; p < 0.05). The toxicity of the isolate 10 extract was comparable to that of the rotenone positive control (~0.75 μ M). Of all the extracts generated, isolate 10 was the most toxic, followed by isolate #3.

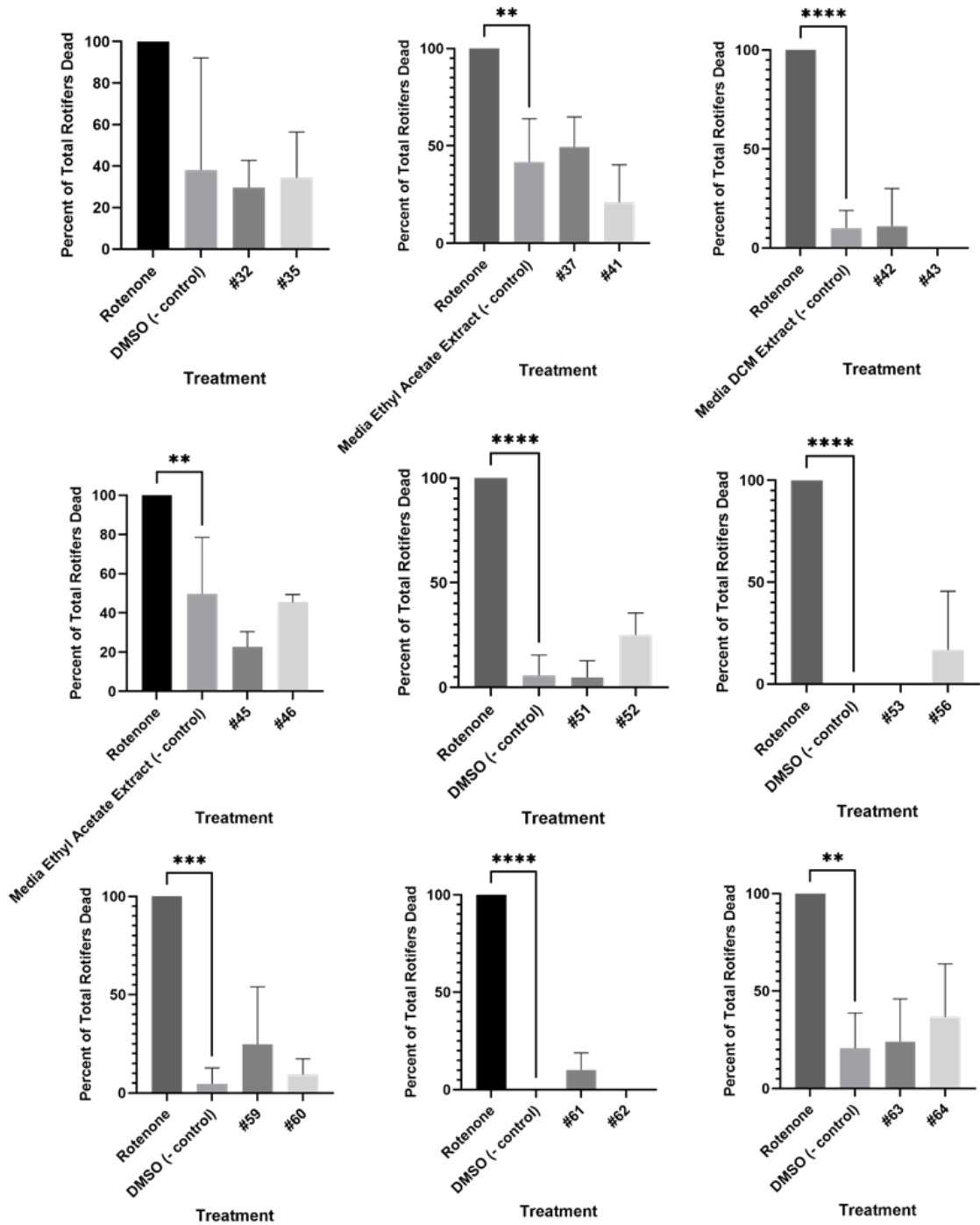


Figure 3.10 (continued)

Given that six bacterial extracts were toxic to rotifers in the initial screening, the corresponding bacterial isolates were recultured (n = 3 independent replicate cultures), and

extracted as previously described to reproduce our original findings. Surprisingly, the average rotifer mortality observed was below 25% for all treatments, and none were significantly different from the marine media extract negative control ($p > 0.05$) (Fig. 3.11).

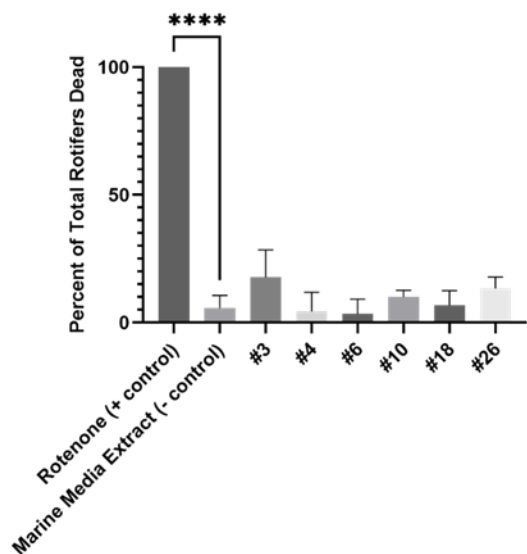


Figure 3.11 24-hour rotifer toxicity assay follow-up experiment. Bacterial extracts for isolates #3, #4, #6, #10, #18, and #26 were generated in biological triplicate and screened for rotifer toxicity in a 24-well plate assay. Previously observed rotifer toxicity was not reproducible for any of the bacterial isolates. However, toxicity observed for both the rotenone positive control and marine media extract negative control was as expected.

3.3.4 *Sanger and Illumina Next Generation Sequencing to Identify Aquatic Bacterial Isolates*

Because of the inability to reproduce some experimental findings, we hypothesized that some isolates might not be clonal, and even potentially mixtures of a small number of bacterial species, potentially resulting in variable bacterial growth, inconsistent metabolite production, and in turn irreproducible rotifer toxicity. In order to investigate this, DNA from all 36 bacterial isolates was extracted, amplified, and purified

in preparation for several sequencing experiments.

Illumina next generation (NG) sequencing results for a selective subset of the 36 bacterial isolates, complemented by previously acquired Sanger sequencing data for all samples, provided critical insights about the purity and overall species diversity for bacteria that were previously assumed to be clonal isolates. The primers used for 16S rRNA coding region amplification (27F and 1492R) for Sanger sequencing capture the whole 16S region so in comparing the whole 16S sequences to the V2 subregion of the 16S rRNA coding region used for NG sequencing (and given that the reference database used by the 16S Metagenomics app in BaseSpace), the classifications derived from the Sanger sequenced data are more likely to be accurate to the most basal level. Many of the bacteria have only recently been discovered and not been analyzed for secondary metabolism and so their potential is above average. Since Sanger sequencing only allows for classification analysis of the most abundant DNA sequence in a sample, NG sequencing was essential to understanding a sample's bacterial composition in its entirety. Nine isolates were selected for further investigation by NG sequencing based on previous rotifer bioassay experiments which suggested they had reasonable potential to serve as biocontrol agents in algal cultivation systems (i.e., the six bacteria resulting in statistically significant toxicity to rotifers and three additional bacteria that possibly resulted in false negative results). All bacterial constituents of each particular sample were quantified relative to each other, and further analysis allowed for family, genus, and, in some cases, species level classification (Table 3.1).

Table 3.1 Validation of strain purity for nine bacterial samples. Sequencing of 16S rDNA revealed that four of nine bacterial samples consisted of multiple strains or species. The criteria for strain purity used here are as follows: 1) the percent of total reads for a single species must be greater than 98.5% and 2) no other single classification category may have a percent of total reads greater than 0.2%. Classification of 16S rDNA sequences (greater than 0.2% of total reads) from illumina Next Generation sequence analysis is synthesized from both Sanger and illumina Next Generation sequence comparison with reference libraries NCBI Blast and "RefSeq RDP 16S v3 May 2018 DADA2 32 BP" used by illumina in the 16S Metagenomics application, respectively. The illumina sequencing was performed on the V2 region of the 16S rDNA coding region and does not perfectly predict the classification of the bacteria with 100% certainty. This table was created by Nolan Barrett.

Sample ID #	Pure Isolate?	Genus & Species	Family	Subclassification Notes	Environments	Secondary Metabolites known from these taxa	References
3	Yes	<i>Epibacterium mobile</i> (formerly <i>Ruegeria mobilis</i>)	Rhodobacterales	<i>Roseobacter</i> clade	Marine coastal pelagic (Matallana-Surget et al 2018); Geographically ubiquitous in tropical and temperate marine environments (Gram 2010)	Tropodithietic acid - tropolone with dithiete moiety (Gram 2010)	(Gram et al., 2010; Matallana-Surget et al., 2018)
4	Yes	<i>Epibacterium mobile</i> (formerly <i>Ruegeria mobilis</i>)	Rhodobacterales	<i>Roseobacter</i> clade	Marine coastal pelagic (Matallana-Surget et al 2018); Geographically ubiquitous in tropical and temperate marine environments (Gram 2010)	Tropodithietic acid (Gram 2010)	(Gram et al., 2010; Matallana-Surget et al., 2018)
6	Yes	<i>Epibacterium mobile</i> (formerly <i>Ruegeria mobilis</i>)	Rhodobacterales	<i>Roseobacter</i> clade	Marine coastal pelagic (Matallana-Surget et al 2018); Geographically ubiquitous in tropical and temperate marine environments (Gram 2010)	Tropodithietic acid (Gram 2010)	(Gram et al., 2010; Matallana-Surget et al., 2018)
10	Yes	<i>Epibacterium mobile</i> (formerly <i>Ruegeria mobilis</i>)	Rhodobacterales	<i>Roseobacter</i> clade	Marine coastal pelagic (Matallana-Surget et al 2018); Geographically ubiquitous in tropical and temperate marine environments (Gram 2010)	Tropodithietic acid (Gram 2010)	(Gram et al., 2010; Matallana-Surget et al., 2018)
18	No	<i>Pseudomonas</i> sp., <i>P. kunmingensis</i> , <i>Pseudomonas</i> sp. (JQ762275), and unclassified Rhodobacterales	<i>Pseudomonas</i> adaceae and Rhodobacterales		Marine and terrestrial, <i>P. kunmingensis</i> is from a phosphate mine (Xie 2014)	Quinolines, quinolones, variety of alkaloids, and variety of halogenated compounds (Isnanetyo 2009)	(Isnanetyo & Kamei, 2009; Xie et al., 2014)

Table 3.1 (continued)

26	No	<i>Rheinheimera baltica</i> , <i>R. aquimaris</i> , <i>Rheinheimera</i> sp., and unclassified Rhodobacteraceae	Chromatiaceae and Rhodobacteraceae		Marine, pelagic (Brettar 2002)	<i>R. baltica</i> , glaukothalin (Grossart 2009); <i>R. aquimaris</i> , antiquroum sensing diketopiperazines (Sun 2016)	(Brettar et al., 2002; Grossart et al., 2009; S. Sun et al., 2016)
32	No	<i>Paracoccus</i> sp. (JX126474), unclassified Rhodobacteraceae, <i>Paenirhodobacter enshiensis</i> (JN797511), <i>Roseicitreum antarcticum</i> (FJ196006), <i>Paracoccus aquimaris</i> (NR_148324.1), <i>Paracoccus</i> sp., <i>Rheinheimera baltica</i> , <i>Roseovarius pacificus</i> (DQ120726), <i>Ruegeria arenilitoris</i> (JQ807219), <i>Paracoccus solventivorans</i> (AY014175), and <i>Thalassococcus halodurans</i> (DQ397336)	Rhodobacteraceae and Chromatiaceae		<i>P. enshiensis</i> is from sewage outlet soil (wang 2014), <i>R. antarcticum</i> from sandy intertidal sediment of Antarctica (Yu 2011), <i>P. aquimaris</i> from seawater (kim 2015), <i>R. pacificus</i> from deep sea sediment (wang 2009), <i>P. solventivorans</i> (Siller 1996), <i>T. halodurans</i> from marine sponge (Lee 2007)	No secondary metabolites described for most of these species.	(Kim & Lee, 2015; Lee et al., 2007; Siller et al., 1996; B. Wang et al., 2009; D. Wang et al., 2014; Yu et al., 2011)

Table 3.1 (continued)

37	No	<i>Epibacterium mobile</i> (formerly <i>Ruegeria mobilis</i>), <i>Rheinheimera baltica</i>	Rhodobacterales and Chromatiaceae		Marine coastal pelagic (Matallana-Surget et al 2018); Geographically ubiquitous in tropical and temperate marine environments (Gram 2010); Marine pelagic (Brettar 2002)	<i>E. mobile</i> , tropodithietic acid (Gram 2010); <i>R. baltica</i> , glaukothalin (Grossart 2009)	(Brettar et al., 2002; Gram et al., 2010; Grossart et al., 2009; Matallana-Surget et al., 2018)
46	Yes	<i>Epibacterium mobile</i> (formerly <i>Ruegeria mobilis</i>)	Rhodobacterales	<i>Roseobacter</i> clade	Marine coastal pelagic (Matallana-Surget et al 2018); Geographically ubiquitous in tropical and temperate marine environments (Gram 2010)	Tropodithietic acid (Gram 2010)	(Gram et al., 2010)

From NG sequencing analyses, five of the nine selected samples (i.e., isolates #3, #4, #6, #10, and #46) were determined to consist of a single species under the following criteria: 1) the percent of total reads for a single species was greater than 98.5% and 2) no other single classification category contributed a percent of total reads greater than 0.2%. The remaining four of the nine sequenced samples contained a variety of 16S rDNA sequences and could not be considered single strains or species. Through integration of NG and previously acquired Sanger sequencing data, tentative classifications were made of the 16S genes associated with each sample. Given these more recent findings, plausible alternative reasons for irreproducible bioactivity include, but are not limited to, highly variable bacterial growth or the possibility that #10 contains multiple competing strains of the same species. Regardless of the cause, the variable bioactivity of sample #10 and other pure bioactive isolates remains elusive.

Of the nine samples of particular interest, all identified bacterial species are known to be found in marine environments, and are thus not likely to have arisen from lab contamination but rather from mixed communities and populations within the original

bacterial samples. The Rhodobacteraceae family was highly represented especially by *Epibacterium mobile* (formerly *Ruegeria mobilis*) in the *Roseobacter* clade but other members of this family were also observed (Matallana-Surget et al., 2018).⁴ Members of the families Pseudomonadaceae and Chromatiaceae were also represented, especially in samples that were clearly impure. For the remaining 27 cultures, only Sanger sequencing data was collected so only the most abundant species within each sample could be confirmed and not all of these were classifiable to the species level. The families represented by the most abundant 16S rDNA sequences per each sample were Rhodobacteraceae, Erythrobacteraceae, Pseudoalteromonadaceae, Flavobacteriaceae, Chromatiaceae, Alteromonadaceae, Vibrionaceae, and Pseudomonadaceae (Table 3.2). When taken together, most of the 36 bacterial samples contained species belonging Rhodobacteraceae followed by Chromatiaceae and Vibrionaceae, with isolate #10 standing out as the most interesting due to its confirmed purity (i.e., it is a single species) and previously observed exceptional rotifer toxicity which was well above that of extracts generated from all other bacterial samples. The microbes in this collection represent a diverse group of marine bacterial families with potential to produce bioactive molecules relevant for these studies.

Table 3.2. The bacterial families represented in the 36 bacterial samples are all found in the marine environment and known to produce a wide array of potentially useful secondary metabolites. This table was created by Nolan Barrett.

Bacterial Family	Environmental Range	Secondary Metabolites known for these taxa	References
Rhodobacteraceae	Both marine and non marine environments	Indole derivatives, tropone derivatives, indigoidine, NRPs	(Martens et al., 2007; Pujalte et al., 2014; Simon et al., 2017)
Erythrobacteraceae	Both marine and non marine environments	Notable for their terpenoids but also produce an array of compounds in the other major biosynthetic classes.	(Cho et al., 2021; L. Xu et al., 2020)
Pseudoalteromonadaceae	Widespread in marine environment, often symbionts	Wide variety of compounds including pentabromopseudilin, korormycin, thiomarinol A, bromo-alterochromides A and B, and tambjamine YP1	(Bowman, 2007; Gram et al., 2010; Ivanova et al., 2014)
Flavobacteriaceae	Both marine and non marine environments	Wide variety of compounds NRPs, terpenoids, polyketides, alkaloids	(Gavriilidou et al., 2020)
Chromatiaceae	Both marine and non marine environments, including many extreme environments	Elemental sulfur, bacteriochlorophyll, carotenoids, vitamin B12, poly-beta-hydroxybutyrate, molecular hydrogen	(Imhoff, 2014)
Alteromonadaceae	Widespread in marine environment	Wide variety of compounds including thiomarinol, alteramide A, quinolone and pyrone derivatives	(Gram et al., 2010; López-Pérez & Rodriguez-Valera, 2014)

Table 3.2 (continued)

Vibrionaceae	Widespread in marine environment	Wide variety of compounds NRPs, terpenoids, polyketides, alkaloids	(Gram et al., 2010; Mansson et al., 2011)
Pseudomonadaceae	Marine, aquatic, terrestrial, and pathogens to many organisms	Well known for their metabolites for quorum sensing but also produce phenazine derivatives, rhizoxin analogues, cyclic lipopeptides, and a new class of alkyl-substituted aromatic acids, among other natural product groups.	(Cousin, 1999; Shahid et al., 2018)

3.3.5 Aquatic Bacterial Natural Product Induction in Response to Rotifer Cues

We had originally hypothesized that ecological challenge from rotifer cues induces production of bioactive natural products and that unique metabolites are up-regulated by only a select group of bacteria. In total, 111 unique extracts were generated from 36 bacterial isolates as described in Figure 3.12. To generate the rotifer filtrate, rotifers were fed *M. salina* for 24 hours, carefully filtered from seawater with a sieve, and algae were removed via centrifugation. For the algal control treatment, fresh artificial seawater was exposed to algae during the feeding period, but never exposed to rotifers. These samples were also centrifuged to remove algal cells, and for both the rotifer and algal filtrate samples removal of algae was confirmed via microscopy. Live bacterial cultures were exposed to chemical cues from the conditioned media of rotifers fed *M. salina*, conditioned media of an *M. salina* culture, or artificial seawater. Dense cultures were lysed with ceramic beads using an OMNI International Bead Ruptor Elite tissue homogenizer and

extracted twice with ethyl acetate in glass scintillation vials. Extracts from half of the bacterial isolates were screened in the 24-well rotifer toxicity assay following the previously described procedure.

Following the initial screening of induced bacterial extracts from 18 of the 36 isolates, additional experiments were conducted on a subset of bacterial extracts at higher concentrations. Rotifer toxicity bioassays were conducted in 24-well plates over 24 hours with 10-12 rotifers per replicate. Rotifers were exposed to these induced extracts (Fig. 3.12) at 3x and 6x the concentration that was used in the previously described rotifer toxicity bioassays, resulting in concentrations of 1.5-fold and 3-fold the original bacterial culture concentration. Rotifers were counted via microscopy 24 hours after bacterial extract exposure.

Extracts from 18 of the bacterial isolates that had been grown in the presence of rotifer conditioned media, algal conditioned media, or artificial seawater were screened against rotifers in a 24-hour toxicity bioassay. None of the 18 extracts, regardless of the conditions in which the bacteria were grown, significantly killed rotifer compared to the negative marine media control (Fig. 3.13). The positive and negative controls were compared to each other, and treatments from the same bacterial isolate were compared to each other and to the positive and negative controls. The rotenone positive control significantly induced rotifer mortality compared to all other treatments within each 24-well plate experimental setup ($n = 3$; $p < 0.001$). The rotifer and algal filtrate-exposed bacterial extract in isolate #2 caused greater rotifer mortality than its artificial seawater control counterpart (Fig. 3.13) ($n = 3$; $p = 0.024$); however, it was not statistically significant from the negative control ($n = 3$; $p > 0.05$). Overall, there was no evidence that these bacteria

produced anti-rotifer compounds either constitutively or when exposed to rotifer and algal conditioned media.

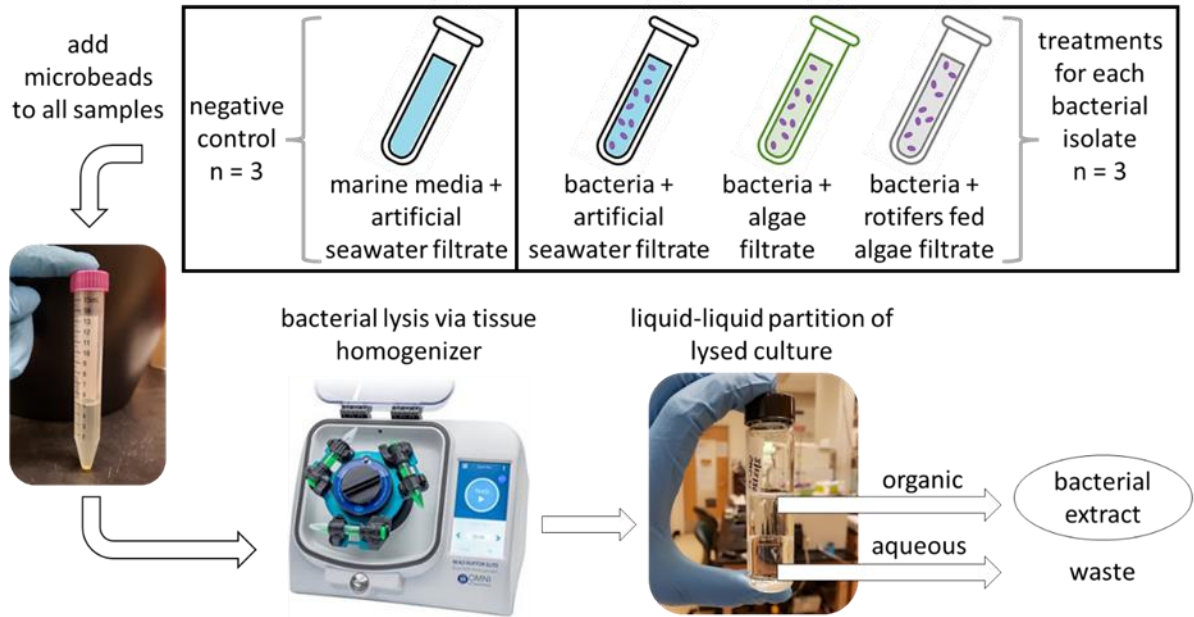


Figure 3.12 Induction Experiment. 36 bacterial isolates were grown in the presence of rotifer conditioned media, algal conditioned media, or artificial seawater. Induced bacteria were lysed with ceramic beads in a tissue homogenizer and extracted by liquid-liquid partitioning of the whole culture. Ethyl acetate bacterial extracts were screened in a 24-well rotifer toxicity assay.

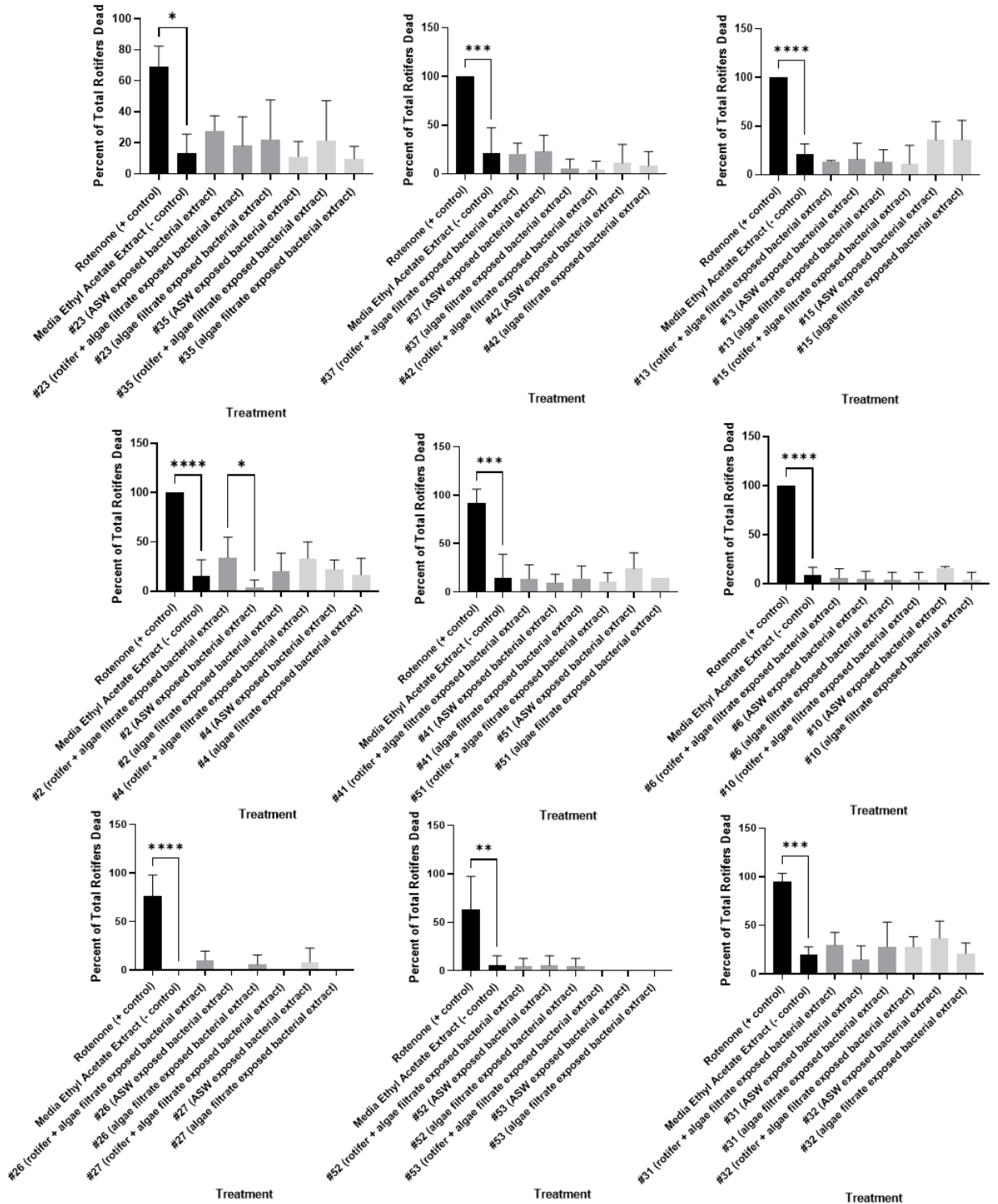


Figure 3.13 24-hour rotifer toxicity assay utilizing induced bacterial extracts screening results. One graph is shown for each 24-well plate assay. Asterisks denote both the positive control rotenone (~0.75 μ M) being significantly more toxic than the

marine media extract negative control and when treatments from the same isolate were significantly different from one of the other treatments (n = 3; p ≤ 0.05). Of all the extracts screened, the only significant difference within a set of isolate treatments was the rotifer and algal filtrate exposed bacterial extract in isolate #2 inducing greater rotifer mortality than the artificial seawater control counterpart (n = 3; p = 0.024); however, it was not statistically significant from the negative control (n = 3; p > 0.05). (* = p ≤ 0.05; ** p ≤ 0.01; * = p ≤ 0.001; **** p ≤ 0.0001).**

3.3.6 Testing Higher Concentrations of Bacterial Extracts for Rotifer Mortality

To determine whether high concentrations of bacterial extracts may induce a higher mortality rate in rotifers, a subset of extracts were chosen for future investigation both based on bacterial diversity and on the initial bacterial extract screening results from Figure 3.10. These bacterial isolates were #3 (*Epibacterium mobile*), #4 (*Ruegeria* sp.) #9 (*Erythrobacter* sp.), #26 (*Rheinheimera baltica*; impure isolate) and #64 (*Vibrio* sp.). These bacterial isolates were tested at a “low” concentration (3x the concentration of the original screening) and a “high” concentration (6x the concentration of the original screening) In 4 of the 5 isolates, there were no significant differences between any of the treatments and the negative marine media control, nor were there any significant differences within the three “low” or three “high” treatments or pairwise between the “low” and corresponding “high” treatments (Fig. 3.14). The three high concentration treatments from isolate #26 bacterial extracts did significantly induce rotifer mortality compared to the negative control (n = 3; p = 0.0002, 0.020, and 0.0009). However, given the previous inability to reproduce isolate #26 results (Figs. 3.10 and 3.11) and isolate #26’s status as an impure culture based on next gen Illumina sequencing results, pursuing isolate #26 further raises multiple challenges, such as parsing out this polyculture into monocultures and retesting each new isolate to traceback to a potentially toxic bacterial strain against rotifers.

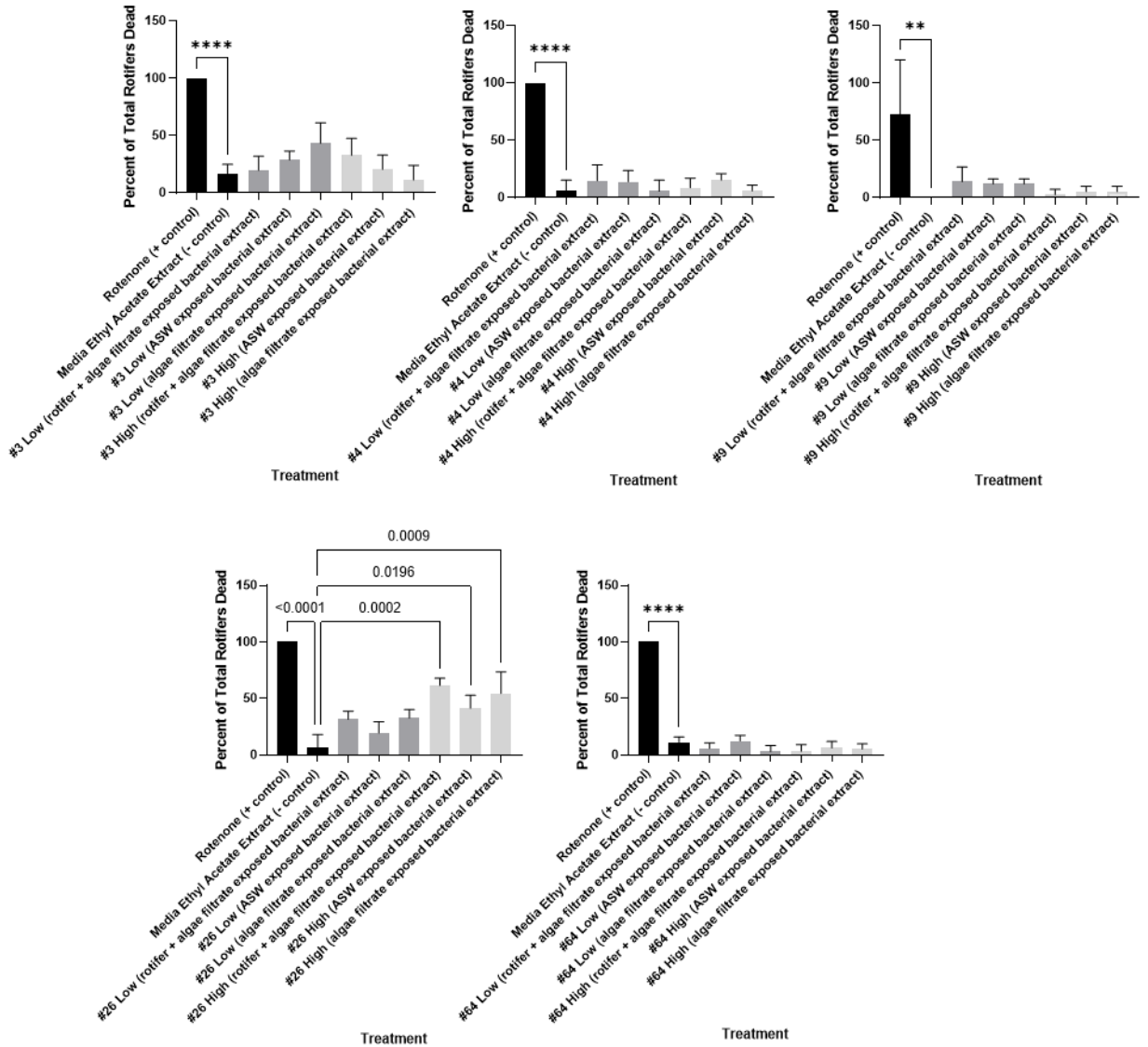


Figure 3.14 24-hour rotifer toxicity assay utilizing induced bacterial extracts at increased concentrations screening results. One graph is shown for each 24-well plate assay. Asterisks denote both the positive control rotenone ($\sim 0.75 \mu\text{M}$) being significantly more toxic than the marine media extract negative control and when treatments from the same isolate were significantly different from one or the other treatments ($n = 3$; $p < 0.05$). Extracts were screened at a low (1.5-fold the original bacterial culture concentration) or high (3-fold the original bacterial culture concentration) concentration. Of all the extracts screened, the only significant differences were found in isolate #26, where the high concentrations of all 3 treatments were statistically different than the negative marine media control ($n = 3$, p values notes on graph). (* = $p \leq 0.05$; ** $p \leq 0.01$; *** = $p \leq 0.001$; **** $p \leq 0.0001$).

3.3.7 Natural Products from Aquatic Bacterial Isolates for Controlling Phagotrophic Algae

The phagotrophic alga *Poterioochromonas malhamensis* is a known pest of lipid-rich *Chlorella* species cultivated for biofuel which is why it was selected as a model for screening bacterial extracts against unwanted algal pests (Ma et al., 2018). It was hypothesized that some of the 36 aquatic bacteria produce natural products that suppress growth of phagotrophic algae and that some are induced only after exposure to the phagotrophic alga. Therefore, similarly to the experimental design described for the induction experiment targeting rotifers, all 36 bacterial isolates were cultured in the presence of pest cues from lysed *P. malhamensis* algal cells in an effort to activate interesting metabolite production and in turn induce bioactivity. An algal growth inhibition assay was developed to screen for bacterial extracts bioactive against *P. malhamensis* (Fig. 3.15).

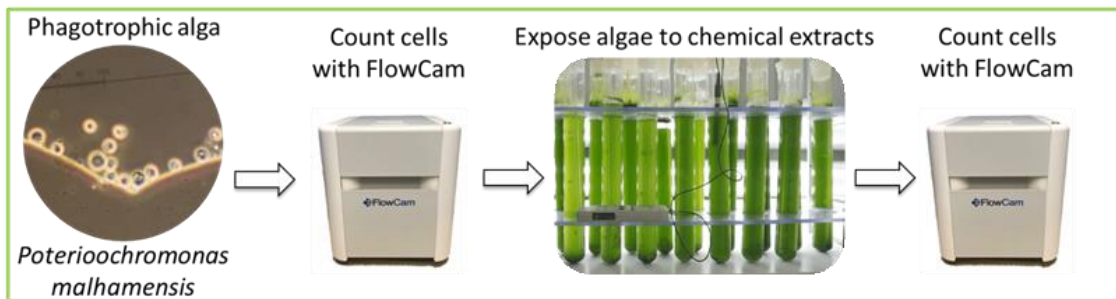


Figure 3.15 Phagotrophic alga *Poterioochromonas malhamensis* bioassay. Algae were enumerated using a FlowCam and exposed to chemical extracts in 10 mL culture tubes. Cells will be counted with a FlowCam before and after exposure to determine bioactivity.

3.3.8 Generation of Bacterial Extracts to Screen for Anti-phagotrophic alga Activity

I. Bacterial extract generation

IA. Bacterial cell extract generation

Bacterial cultures were grown 35 ppt marine media for 24 or 48 hours depending on the growth rate of the isolate at 21 °C in a 12/12 light dark cycle (n = 3). Optical density measurements were recorded to standardize the inoculum concentration for the bacterial induction experiments. A new set of bacterial cultures were inoculated from previous cultures and were exposed to *P. malhamensis* cell lysate to induce the production of bioactive secondary metabolites by the bacteria against *P. malhamensis* (n = 3). A second set of bacterial cultures were grown without exposure to *P. malhamensis* cell lysate to determine whether induced bacterial extracts impact the growth of *P. malhamensis* differently than non-induced bacterial extracts. All cultures were prepared in biological triplicate and incubated under the same conditions as previously described. After 24 or 48 hours of growth, the bacterial cells were lysed with 0.1 mm ceramic beads using the OMNI International Bead Ruptor Elite tissue homogenizer to ensure cell rupture, extracted with ethyl acetate (2 x 5 mL), and dried by rotary evaporation. Marine media with and without *P. malhamensis* cell lysate was also extracted following the same procedure to serve as controls for the *P. malhamensis* growth inhibition assays.

IB. Bacterial supernatant extract generation

Bacterial isolates were grown in the same manner as in IA for the induced and non-induced treatments, however supernatant extracts were generated using different methods. Bacterial cells were pelleted via centrifugation (3000 rpm for 10 minutes) and the

supernatant was pipetted off. The supernatant was extracted with ethyl acetate (2 x 5 mL) and dried by rotary evaporation. Marine media with and without *P. malhamensis* cell lysate was also extracted following this procedure to serve as controls for the *P. malhamensis* growth inhibition assays.

II. *P. malhamensis* cell lysate generation

To prepare *P. malhamensis* lysate, the alga was grown in freshwater *Ochromonas* medium to early exponential phase (60,000 cells/mL) at 21 °C in a 12/12 light dark cycle. This concentration mimics *P. malhamensis* having a strong presence in an algal pond but not yet dominating the community. Cells were pelleted at 3000 rpm for 10 minutes. The supernatant was discarded, and the algal cells were rinsed twice with deionized water. The cells were resuspended in marine media and lysed with 0.1 mm ceramic beads using the OMNI International Bead Ruptor Elite tissue homogenizer to ensure cell rupture. Cell debris were removed by centrifugation and this lysate-conditioned marine media was used to culture the previously described bacterial cultures.

III. *P. malhamensis* growth inhibition bioassays:

The following growth inhibition bioassay was conducted twice, once for the cellular extracts generated in IA and again for the supernatant extracts generated in IB. Bacterial and marine media control extracts that represented 5 ml of liquid culture were resuspended in 100 µL DMSO and screened for inhibition of *P. malhamensis* growth utilizing a Fluid Imaging FlowCam, an instrument that combines digital imaging, flow cytometry, and microscopy, to enumerate cells following exposure to extracts of a subset

of bacterial isolates. The goal of these first experiments was to determine whether the extract from bacteria that grew exposed to *P. malhamensis* cell lysate impacted the growth of *P. malhamensis* differently than the extract from bacteria that grew without *P. malhamensis* exposure (i.e., induced vs non-induced). A subset of bacteria was selected based on the Sanger sequencing data so that multiple genera were tested. These bacterial genera included *Rugeria* sp., *Epibacterium mobile*, *Rhodobacteraceae*, and *Paracoccus* sp. The starting *P. malhamensis* concentrations were ~30,000 cells/ml. The growth inhibition bioassays took place in 10 ml culturing tubes, and 30 μ L of the dissolved bacterial extract was added to each test tube in biological triplicate with a total algal culture of 3 ml. The final concentration was half-fold the original bacterial culture and equal to the bacterial extract concentration used in the rotifer toxicity assays, as this is a concentration close to the maximum of what is realistically achievable for algal raceway pond applications while still higher than undetectable levels in previous algal-bacterial co-culture experiments (Fisher et al., 2019). The cultures were incubated for 72 hours at 22 °C in a 12/12 hour light/dark cycle. Cells were enumerated via flow cytometry on the FlowCam using an 80 μ m field of view flow cell and the following settings: 10x objective, autoimage rate of 20 frames/second, 0.150 ml/minute flow rate, and a particule filter of 2-20 μ m . Cells from each biological replicate were counted twice and the average of these two counts was used to calculate *P. malhamensis*' growth rate over 72 hours.

For the comprehensive screening of all 36 bacterial isolate supernatant extracts against *P. malhamensis*, bacterial extracts were prepared following the protocol in IB for the non-induced treatments. Growth inhibition bioassays were conducted as described

earlier, but in sets. Groups of three bacterial isolate extracts were paired with one marine media control to maintain statistical power.

No bacterial cellular or supernatant extracts were found to suppress growth of *P. malhamensis*, and exposure of these bacteria to *P. malhamensis* lysate did not appear to induce antimicrobial defenses. Overall, *P. malhamensis* experienced increased growth when cultured with cellular bacterial extracts (Fig. 3.16). There was no statistically significant difference between the induced and non-induced treatments for all five of the bacterial isolates tested in this experiment ($n = 3$; $p > 0.05$). Nor was there a statistically significant difference between the two controls or each control, or the induced control and the induced treatments, or the non-induced control and the non-induced treatments (Figs. 3.16 and 3.17).

For the *P. malhamensis* cultures exposed to extracted bacterial cells, the greatest difference was between non-induced bacterial isolate #6 and the non-induced control, and between non-induced #2 and the non-induced control ($p = 0.12$ and $p = 0.13$, respectively). However, all the induced vs non-induced comparisons were more similar ($p > 0.70$). There was substantial variation between biological replicates (indicated by the error bars in Fig. 3.16). The exact reason for such variation is unclear. Of the five bacterial isolates tested, isolate #32 was found to be a mixture of multiple genera (Table 3.1), and thus the lack of consistency among biological replicates may have been due to different strain assemblages in the culture. Isolate #2 did not undergo next generation (NG) Illumina sequencing and potentially was a polyculture. Bacterial isolates #4, #6, and #10 were found to be clonal by next gen sequencing. Extracting whole-cell bacterial cultures likely created nutrient-rich extracts, which increased overall growth in *P. malhamensis* compared to the controls that

did not contain these bacterially derived nutrients. For this set of experiments, optical density measurements were not acquired for the bacterial cultures prior to extraction. Despite being inoculated with the same concentration of starter culture and strategically randomized in the incubator (Methods IA), the possibility exists that the biological replicates varied somewhat in initial cell density, compounding the variation in the nutrient-rich extract to which *P. malhamensis* was exposed.

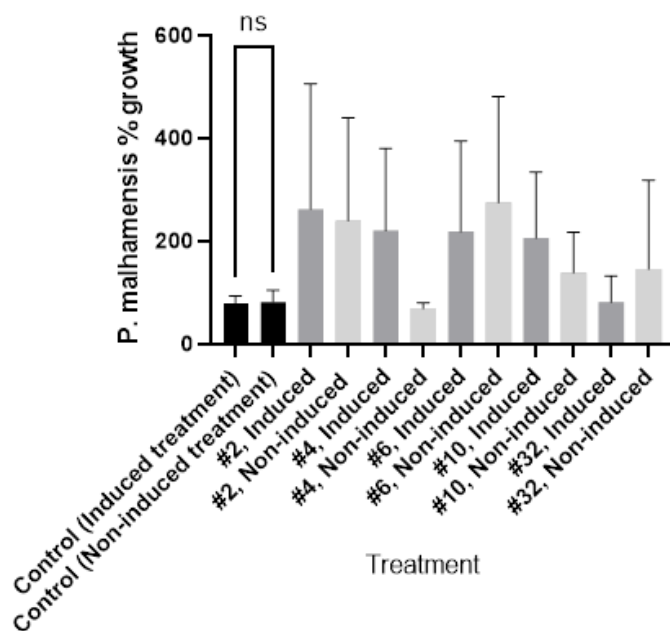


Figure 3.16 72-hour *P. malhamensis* growth inhibition assay initial screening results from the bacterial cellular extract induced versus non-induced experiment. Bacterial isolates (#2, #4, #6, #10, #32) were cultured in the presence (induced) and absence (non-induced) of *P. malhamensis* lysate to produce bacterial cell extracts corresponding to each isolate. *P. malhamensis* was grown exposed to these bacterial extracts, and growth rate was determined via flow cytometry. Induced and non-induced samples from the same isolate were compared to each other, and all non-induced samples were compared to the non-induced control while all induced samples were compared to the induced control. The two controls were compared to each other. There was no statistical significance between any of these comparisons ($n = 3$; $p > 0.05$). The greatest difference was between non-induced #6 and the noninduced control and non-induced #2 and the non-induced control ($p = 0.12$ and $p = 0.13$, respectively). However, all the induced vs non-induced comparisons were more similar ($p > 0.70$). Data acquisition and analysis were performed by Gabriella Chebli.

Nutrient stimulation from bacterial cell extracts may have overpowered inhibitory effects of bacterially derived natural products. To test this hypothesis, the induction experiment was repeated with supernatant extracts, rather than whole culture extracts, using the same bacterial isolates (Method 1B, Fig. 3.17). Overall, there was less variation among biological replicates and less growth enhancement among the treatments compared to both controls compared to the growth inhibition assay conducted with bacterial cell extracts (Figs. 3.16 and 3.17). The same comparisons were made as before: induced and non-induced isolates were compared to each other, and the induced treatments were compared to the induced control while the non-induced treatments were compared to the non-induced control. The only statistically significant outcome was the slight stimulation of *P. malhamensis* by induced isolate #2 treatment versus the relevant media control ($n = 3$; $p = 0.038$). There was no statistical significance among the other comparisons ($n = 3$; $p = 0.12 - 0.89$) (Fig. 3.17). The more uniform growth rates between biological replicates and bacterial supernatant extract treatments and controls supports that whole cell bacterial extracts stimulated *P. malhamensis* growth in the earlier experiment (Figs. 3.16 and 3.17). Exposure of bacteria to *P. malhamensis* cell lysate did not induce the production of anti-algal natural products, nor was there any evidence that these bacterial isolates produce anti-algal natural products constitutively. This subset of bacteria tested represents multiple genera within the bacterial consortium (Methods III), all of which are present at least once more in the other 32 bacterial isolates to be tested. The induced treatments did not decrease *P. malhamensis* growth compared to their non-induced counterparts or the controls and, compared to the controls, at times increased *P. malhamensis* growth. Considering these results, supernatant extracts were generated for the remaining bacterial isolates, and these

were screened against *P. malhamensis* without the induction portion of these previous two experiments.

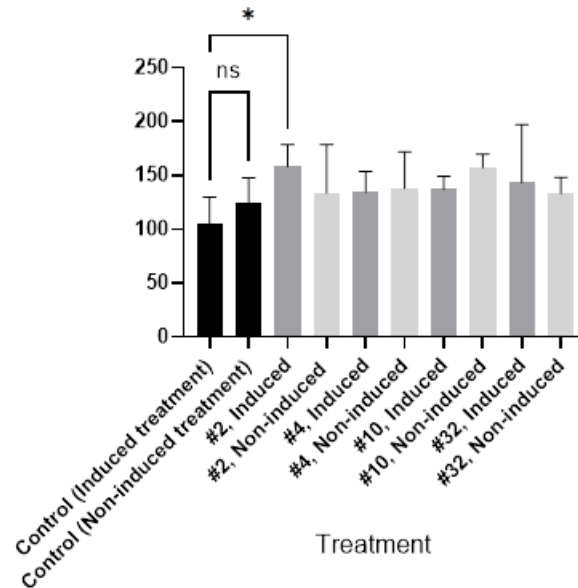


Figure 3.17 72-hour *P. malhamensis* growth inhibition assay initial screening results from the bacterial supernatant extract induced versus non-induced experiment. Bacterial isolates (#2, #4, #10, #32) were cultured in the presence (induced) and absence (non-induced) of *P. malhamensis* lysate to produce bacterial supernatant extracts corresponding to each isolate. *P. malhamensis* was grown exposed to these bacterial extracts, and growth rate was determined via flow cytometry. Induced and non-induced samples from the same isolate were compared to each other, and all non-induced samples were compared to the non-induced control while all induced samples were compared to the induced control. The two controls were compared to each other. The only statistically significant comparison was between the induced isolate #2 treatment and its respective control (n = 3; p = 0.038). There was no statistical significance between the other comparisons (n = 3; p = 0.12 to 0.89). Data acquisition and analysis were performed by Gabriella Chebli.

The supernatant extracts from 36 bacterial isolates were screened against *P. malhamensis* with most bacterial isolates having no impact over the growth rate of *P. malhamensis* (Fig. 3.18). Isolates #59, #61, and #62 increased *P. malhamensis* growth rate (n = 3 each; p = 0.022, 0.0019, 0.0031, respectively) compared to marine media extract controls. These three bacterial isolates did not undergo NG Illumina sequencing, and thus

their identity as a monoculture or polyculture is unclear. Sanger sequencing data indicates the genera *Ruegeria* sp. (#59 and #61) and *Vibrio* sp. (#62) were most prominent in the samples of these bacterial cultures analyzed for sequencing. It is possible that these strains, and the other strains showing no significant impact, do not produce algicidal metabolites impacting *P. malhamensis* growth. It is also possible that due to most of the cultures not being pure, a single strain that potentially produced inhibitory compounds did not adequately dominate the bacterial community to inhibit *P. malhamensis*. Most interestingly, bacterial isolates #26 and #63 decreased growth of *P. malhamensis* ($n = 3$ each; $p = 0.0022, 0.042$, respectively) (Fig. 3.18), with #26 likely including the bacterial genus *Rheinheimera* sp. and #63 *Vibrio* sp. *Vibrio* spp. are a especially common marine bacteria, and it is not surprising that one species may enhance algal growth rate, and another from the same genus may slightly inhibit algal growth rate (Natrah et al., 2014). Studying these bacterial isolates further would likely include multiple challenges due to isolate #26 being an impure culture and the likelihood that the other isolates of interest—including isolate #63 which was not sequenced using Illumina NG sequencing—are also polycultures, given the irreproducible results observed in the rotifer toxicity bioassays. Additionally, few studies have investigated the natural microbiome of *P. malhamensis*, especially with regards to the specific genera in this study, perhaps due to the disconnect in habitats between this freshwater alga and these marine-derived bacteria. Nevertheless, these results and this study provide insight into the potential of utilizing bacterially derived metabolites to inhibit the growth rate of certain algal species or in the opposite case, increasing the growth rate of potentially beneficial algal species.

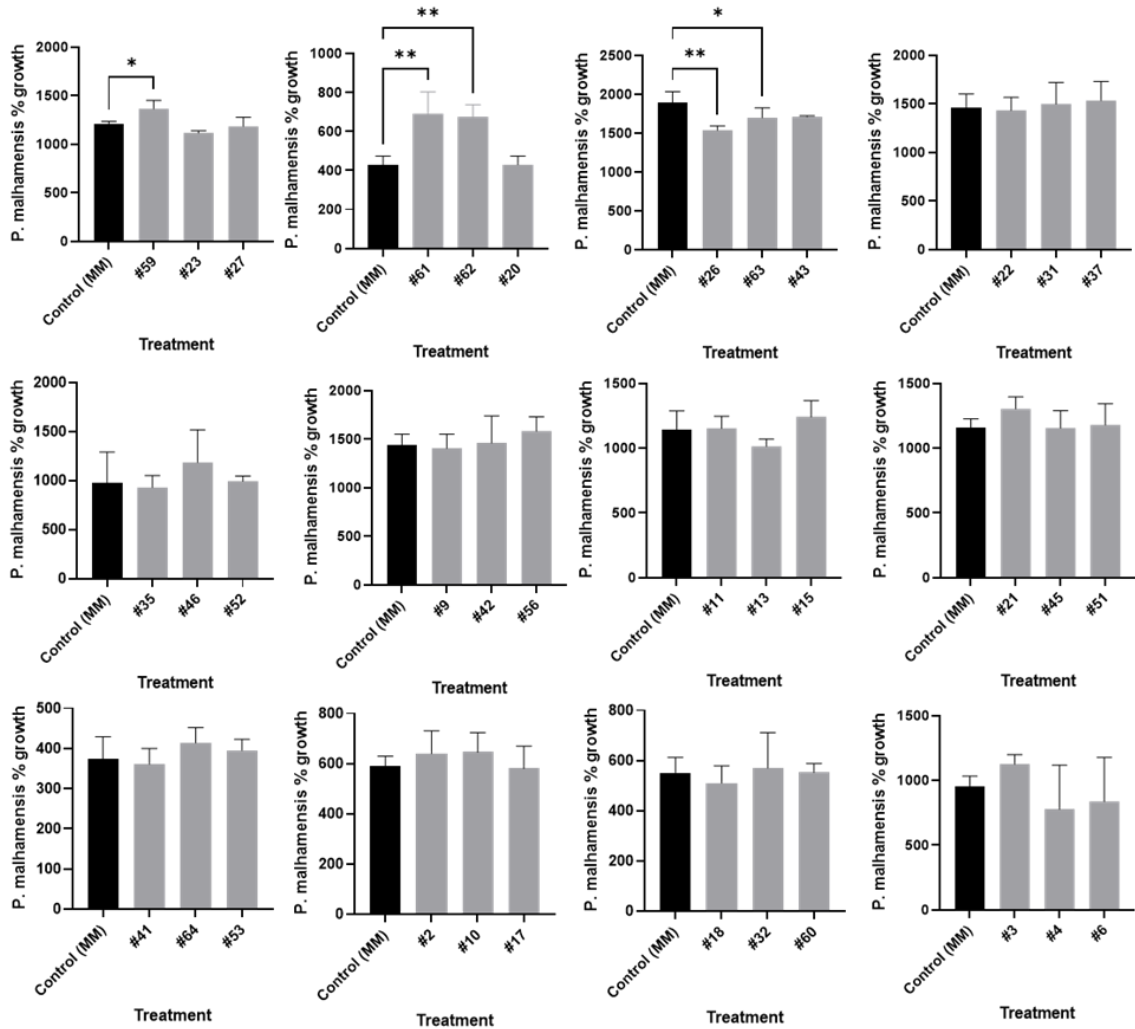


Figure 3.18 72-hour *P. malhamensis* growth inhibition assay screening results where *P. malhamensis* was exposed to bacterial supernatant from 36 different bacterial isolates. *P. malhamensis* was grown exposed to these bacterial supernatant extracts, and growth rate was determined via flow cytometry. One graph is shown for each assay “set,” consisting of three bacterial isolates and one marine media control. Asterisks denote when extracts of bacterial isolates (n = 3) had a significantly greater impact on growth than the corresponding control (n = 3; p < 0.05 for * and p < 0.01 for **). Isolates #63 and #26 decreased the growth rate of *P. malhamensis* compared to the marine media control (p = 0.042, 0.0022, respectively), whereas isolates #59, #61, and #62 increased *P. malhamensis* growth rate (p = 0.022, 0.0019, 0.0031, respectively). Data acquisition and analysis were performed by Gabriella Chebli.

3.3.9 Anti-chytrid Natural Products from Aquatic Bacterial Isolates

The freshwater green alga *Haematococcus pluvialis* is primarily cultivated in mass culture to produce astaxanthin, a commercially valuable antioxidant and dietary supplement, however crops are often decimated by chytrid infection (Gutman et al., 2009). For this reason, known parasites of *H. pluvialis*, chytrids JEL0821 *Paraphysoderma sederbokerensis* and JEL0842 *Rhizophyidium* sp., were purchased from the Collection of Zoosporic Eufungi at the University of Michigan (CZEUM) with the intent of developing another bioassay to screen the previously generated bacterial natural product extract library. Given the biological and consequent chemical diversity of this bacterial library, it was hypothesized that select isolates produce molecules toxic to chytrids.

To our knowledge, a model chytrid has yet to be isolated from an ecologically relevant source for biofuel investigations (i.e., an *M. salina* algal raceway pond), and while the species that were purchased are not known to infect algae cultivated for biofuel, they were selected to explore their potential as model organisms. Maintaining liquid cultures of both species at Georgia Tech revealed that they grew extremely slowly at all conditions used (i.e., liquid PmTG and YPD media, at 23 °C or 30 °C), and even under the growth conditions recommended by CZEUM. While *P. sederbokerensis* grew noticeably faster than *Rhizophyidium* sp. in liquid cultures, both species did poorly at 30 °C regardless of the media type (i.e., we observed reduced growth and a noticeable increase in cellular debris). On average, a 3-5 mL culture took about 3 months to reach a visibly noticeable higher density, even after manipulating temperature and nutrient conditions, making both organisms poor candidates for a model system exploring bacteria-chytrid interactions for the protection of algal biofuels. While a model organism approach assumes that related

organisms share fundamental similarities, our efforts to culture these chytrids in the lab strongly suggest that these organisms are very specialized, especially with regard to morphology and physiology. Therefore, the chytrids selected are not predictive of other fungal parasites and are not suited for algal biofuel studies requiring a model organism. Given this, the algal biofuel community would strongly benefit from collaborating with mycologists to identify a model chytrid for future studies.

3.4 Conclusions

Bacterial consortia have useful environmental properties, but mixtures of different species are subject to problems associated with lack of reproducibility and low concentration of metabolites from any single bacterial constituent within a mixed community. Our initial experiments with bacterial consortia did not yield extracts with adequate concentrations of compounds to enable robust metabolomics analysis, although differences in chemical profiles were observed based on presence or absence of bacteria.

Bacterial isolates from aquatic environments have the potential to be useful as sources of natural products to protect biofuels, for example killing or deterring rotifer grazers. Several occurrences of bacterial isolates producing extractable materials that were toxic to rotifers were observed, but these were not consistently reproducible even when conditions were near-identical. Our bacterial library consisted of some isolates that appeared to represent a single species (maybe even a single strain), but also many that were mixtures of two or more species. It would be necessary to acquire clonal cultures, for the sake of reproducibility and to be able to associate a natural product with its producer bacterial strain, in order to better assess the potential of bacteria to protect microalgae against pests

found in biofuel ponds. This bacterial library represents diverse taxonomic groups, including some taxa that are known secondary metabolite producers and also some rare species, creating opportunities for future development.

CHAPTER 4. CONCLUSIONS AND FUTURE DIRECTIONS

The number of chemical cues that mediate interactions in biological systems is vast, yet the identities of the majority of these molecules remain unknown. Commendable efforts made by chemists and ecologists have resulted in the discovery of many cues essential for various purposes including, but not limited to, defense, finding food, avoiding predation, and choosing a mate. This thesis explores chemical cues that mediate predator-prey interactions for two distinct marine systems: oyster reefs and algal biofuel ponds.

Cues used by marine prey for assessment of predation risk must be waterborne, but inorganic salts in seawater present unique challenges for isolation and compound identification. New approaches are still needed to overcome the presence of salts which interfere with preferred analytical methods (i.e., mass spectrometry and ^1H NMR spectroscopy). As chapter 3 focused on algal exometabolomes, a thorough exploration of cue isolation from seawater was conducted to assess different extraction methods for compatibility with a metabolomics workflow. However, results revealed that downstream spectroscopic analyses were biased by these different sample preparation methods, indicating that multiple complementary sample preparation methods are needed to capture the full chemical richness of a biological sample which will later be related back to biological activity. Chapters 1 and 2 circumvented the problem of salts, by acquiring biological fluids directly from their source, a strategy which should be implemented when possible to facilitate cue isolation and identification. While urine may seem like an obvious choice for metabolomics analysis, other biological fluids such as blood and hemolymph should be explored for potential kairomones as molecules exuded from injury are clearly

related to predation risk.

Determining the source of a cue is comparatively less challenging than solving the structures of specific molecules, with the majority of metabolomics studies annotating only a small fraction of an organism's metabolome. As spectroscopic instrumentation continues to improve in sensitivity and resolution alongside development of sophisticated statistical tools, more reliable biomarkers can be identified for non-model systems, and perhaps be used to establish new model systems for ecological studies. Continual interest in development of metabolomics tools is essential for the discovery of important chemical cues in diverse ecological systems. However, it is critical that the field continue to standardize methods to ensure best practices and reproducibility. As is demonstrated in chapter 3, machine learning and robust statistics will be critical for generating models from spectral features (i.e., cue blends) that are the most predictive of biological phenomena.

In the context of the chemical ecology of predation risk, the results of this thesis emphasize that cues are often complex blends that elicit nuanced biological responses from different species. While measured effects (e.g., oyster shell strengthening and mud crab foraging suppression) are often subtle, they have the potential for large scale non-consumptive effects at the community and ecosystem levels. More specifically, the successful utilization of chemical cues by prey to assess risk and avoid predation results in notable ecosystem changes. A systems biology approach would be ideal for exploring these systems more holistically, prioritizing identification of sensory receptors used for detection of chemical cues by non-model species. Understanding of the molecular and cellular mechanisms required for chemical detection can be facilitated by genome sequencing, bioinformatics, and development of culturable cell lines for ecologically important species

which are often not yet available. This represents a future avenue for chemical ecology research.

Understanding how chemical cues mediate life processes allows for controlled manipulation of biological systems. Various industries including crop cultivation, farming, and pest management may leverage chemical cues as tools to obtain a preferred outcome by improving the survival and reproduction of economically valuable species. For example, knowledge of chemical cues that manipulate oyster growth could be used to improve oyster farming or reef restoration projects by increasing their survival. In the case of microalgal crops, knowledge of chemical cues could be used to manipulate and increase the production of biofuels or biopharmaceuticals. Hence successes from collaborations between chemists and ecologists leading to identification of chemical cues also harbors great potential for broader impacts in conservation biology and development of clean energy.

**APPENDIX A. SUPPLEMENTARY FIGURES AND TABLES FOR
CHAPTER 1**

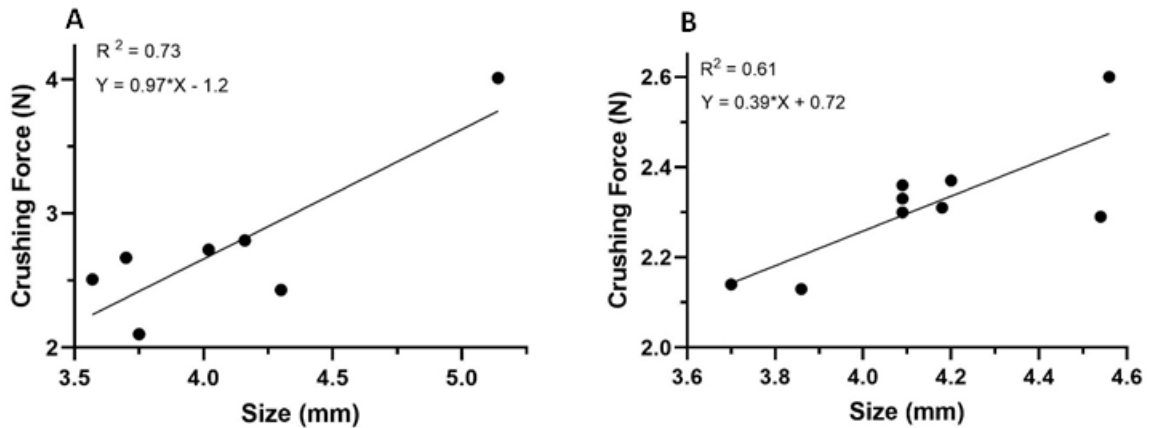


Figure A1 A simple linear regression of the average spat size and crushing force per replicate in the predator water (A) and seawater (B) treatments from 2020 predator cue bioassay experiment. The relationship between size and crushing force follows a significantly positive linear relationship for both the positive and negative controls (PW, $P = 0.01$ and SW, $P = 0.02$), indicating that stronger individuals often have a larger shell. Because of this evidence for a linear relationship, we use standardized crushing force (crushing force/size) to report changes in shell strength from our series of experiments.

Table A1 pH and salinity values recorded with Orion Star™ A121 Portable pH Meter during June – Sept. 2020 bioassay experiments. Values were recorded directly before water changes in each aquarium.

Treatment	pH Avg \pm SD	Salinity Avg \pm SD
Trigonelline	8.35 \pm 0.13	21.00 \pm 0.53
Homarine	8.37 \pm 0.15	21.03 \pm 0.59
Trigonelline + Homarine	8.37 \pm 0.23	21.06 \pm 0.53
Seawater	8.38 \pm 0.17	20.83 \pm 0.48
Blue Crab Urine (Mud Crab Diet)	8.33 \pm 0.16	20.81 \pm 0.49
Blue Crab Urine (Oyster Diet)	8.33 \pm 0.23	20.92 \pm 0.53
Predator Water	8.34 \pm 0.19	20.76 \pm 0.69

Table A2 The number of blue crab individuals making up urine treatment mixtures for blue crabs fed an oyster diet and mud crab diet. All blue crabs were between 11-19 cm size and were fed the appropriate diet for one week before urine extraction began.

Blue Crab Urine Replicate	# of Individuals in Mixture (Oyster Diet)	# of Individuals in Mixture (Mud Crab Diet)
1	5	6
2	6	6
3	12	6
4	3	4
5	3	3
6	4	3
7	4	3
8	5	5
9	5	4

Table A3 Concentrations of homarine and trigonelline for the dose response experiment and number of replicates for each dose. Replicates were excluded from analysis if they experienced high mortality of oyster spat (less than 6 spat alive). Concentrations of homarine and trigonelline for the homarine + trigonelline dose response curve are the same as those used for the dose response curves of the individual cues. Single asterisks (*) indicate the natural concentration upper limits for homarine and trigonelline in blue crab urine (oyster diet). Double asterisks () indicate that these doses were excluded from additional statistical analyses because they exceeded the natural concentration range.**

Homarine		Trigonelline		Homarine + Trigonelline
Concentration (μM)	Replicates	Concentration (μM)	Replicates	Replicates
0.85	3	0.24	3	3
2.7	1	0.74	4	4
8.5	4	2.4	3	2
27	3	7.4	3	4
85*	3	24*	3	4
270**	4	74 **	2	3
850 **	2	240 **	4	3

Table A4 Concentrations and corresponding volumes of blue crab urine doses used in the 2022 urine dose response experiment. Urine was collected and pooled from 22 crabs that ranged 13 – 18 cm in size and each crab produced 1.31 ± 0.18 mL on average. Cue concentration estimates are based on the assumption that in 1 mL of blue crab urine, the concentrations of homarine and trigonelline are 13 ± 21 μ M and 3.6 ± 6.9 μ M, respectively, as quantified from urine in the 2020 predator cue bioassay. Asterisks (*) indicate that urine was diluted to the appropriate concentration (based on trigonelline values) and dosed using a 1 mL aliquot volume.

Homarine (μM)	Trigonelline (μM)	Urine Volume (mL)
65.00	23	5
16.25	5.75	1.25
4.06	1.44	0.313*
1.02	0.36	0.078*
0.25	0.09	0.020*
0.06	0.02	0.005*
0.02	0.01	0.001*
0.004	0.001	0.0003*

REFERENCES

- Alseekh, S., Aharoni, A., Brotman, Y., Contrepois, K., D'Auria, J., Ewald, J., C. Ewald, J., Fraser, P. D., Giavalisco, P., Hall, R. D., Heinemann, M., Link, H., Luo, J., Neumann, S., Nielsen, J., Perez de Souza, L., Saito, K., Sauer, U., Schroeder, F. C., ... Fernie, A. R. (2021). Mass spectrometry-based metabolomics: A guide for annotation, quantification and best reporting practices. *Nature Methods*, 18(7), Article 7. <https://doi.org/10.1038/s41592-021-01197-1>
- Andersen, C. M., & Bro, R. (2010). Variable selection in regression—A tutorial. *Journal of Chemometrics*, 24(11–12), 728–737. <https://doi.org/10.1002/cem.1360>
- Aru, V., Balling Engelsen, S., Savorani, F., Culurgioni, J., Sarais, G., Atzori, G., Cabiddu, S., & Cesare Marincola, F. (2017). The Effect of Season on the Metabolic Profile of the European Clam *Ruditapes decussatus* as Studied by ¹H-NMR Spectroscopy. *Metabolites*, 7(3), 36. <https://doi.org/10.3390/metabo7030036>
- Ashihara, H. (2008). Trigonelline (N-methylnicotinic acid) Biosynthesis and its Biological Role in Plants. *Natural Product Communications*, 3(9), 1934578X0800300906. <https://doi.org/10.1177/1934578X0800300906>
- Ashihara, H., Ludwig, I. A., Katahira, R., Yokota, T., Fujimura, T., & Crozier, A. (2015). Trigonelline and related nicotinic acid metabolites: Occurrence, biosynthesis, taxonomic considerations, and their roles in planta and in human health. *Phytochemistry Reviews*, 14(5), 765–798. <https://doi.org/10.1007/s11101-014-9375-z>
- Baldwin, I. T. (1998). Jasmonate-induced responses are costly but benefit plants under attack in native populations. *Proceedings of the National Academy of Sciences*, 95(14), 8113–8118. <https://doi.org/10.1073/pnas.95.14.8113>
- Bauvais, C., Bonneau, N., Blond, A., Pérez, T., Bourguet-Kondracki, M.-L., & Zirah, S. (2017). Furanoterpene Diversity and Variability in the Marine Sponge *Spongia officinalis*, from Untargeted LC-MS/MS Metabolomic Profiling to Furanolactam Derivatives. *Metabolites*, 7(2), 27. <https://doi.org/10.3390/metabo7020027>
- Bayona, L. M., de Voogd, N. J., & Choi, Y. H. (2022). Metabolomics on the study of marine organisms. *Metabolomics*, 18(3), 17. <https://doi.org/10.1007/s11306-022-01874-y>

- Belgrad, B. A., Knudson, W., Roney, S. H., Walton, W. C., Lunt, J., & Smee, D. L. (2023). Induced defenses as a management tool: Shaping individuals to their environment. *Journal of Environmental Management*, 338, 117808. <https://doi.org/10.1016/j.jenvman.2023.117808>
- Belgrad, B. A., Smee, D. L., & Weissburg, M. J. (2023). Predator signaling of multiple prey on different trophic levels structures trophic cascades. *Ecology*, e4050. <https://doi.org/10.1002/ecy.4050>
- Berking, S. (1987). Homarine (N-methylpicolinic acid) and trigonelline (N-methylnicotinic acid) appear to be involved in pattern control in a marine hydroid. *Development*, 99(2), 211–220. <https://doi.org/10.1242/dev.99.2.211>
- Berlinck, R. G. S., Crnkovic, C. M., Gubiani, J. R., Bernardi, D. I., Ióca, L. P., & Quintana-Bulla, J. I. (2021). The isolation of water-soluble natural products – challenges, strategies and perspectives. *Natural Product Reports*. <https://doi.org/10.1039/D1NP00037C>
- Bharti, S. K., & Roy, R. (2012). Quantitative ¹H NMR spectroscopy. *TrAC Trends in Analytical Chemistry*, 35, 5–26. <https://doi.org/10.1016/j.trac.2012.02.007>
- Böcker, S. (2017). Searching molecular structure databases using tandem MS data: Are we there yet? *Current Opinion in Chemical Biology*, 36, 1–6. <https://doi.org/10.1016/j.cbpa.2016.12.010>
- Bouatra, S., Aziat, F., Mandal, R., Guo, A. C., Wilson, M. R., Knox, C., Bjorndahl, T. C., Krishnamurthy, R., Saleem, F., Liu, P., Dame, Z. T., Poelzer, J., Huynh, J., Yallou, F. S., Psychogios, N., Dong, E., Bogumil, R., Roehring, C., & Wishart, D. S. (2013). The Human Urine Metabolome. *PLOS ONE*, 8(9), e73076. <https://doi.org/10.1371/journal.pone.0073076>
- Bowman, J. P. (2007). Bioactive Compound Synthetic Capacity and Ecological Significance of Marine Bacterial Genus *Pseudoalteromonas*. *Marine Drugs*, 5(4), 220–241.
- Boysen, A. K., Carlson, L. T., Durham, B. P., Groussman, R. D., Aylward, F. O., Ribalet, F., Heal, K. R., White, A. E., DeLong, E. F., Armbrust, E. V., & Ingalls, A. E. (2021). Particulate Metabolites and Transcripts Reflect Diel Oscillations of Microbial Activity in the Surface Ocean. *MSystems*, 6(3), e00896-20. <https://doi.org/10.1128/mSystems.00896-20>

- Brettar, I., Christen, R., & Höfle, M. G. (2002). *Rheinheimera baltica* gen. Nov., sp. Nov., a blue-coloured bacterium isolated from the central Baltic Sea. *International Journal of Systematic and Evolutionary Microbiology*, 52(Pt 5), 1851–1857. <https://doi.org/10.1099/00207713-52-5-1851>
- Bristow, M. L., Gabor, C., & Huertas, M. (2019). Conspecific Chemical Cues Modulate Reproductive Physiology and Behavior in a Live-Bearing Fish. *The FASEB Journal*, 33(S1), 1b429–1b429. https://doi.org/10.1096/fasebj.2019.33.1_supplement.1b429
- Broadhurst, D., Goodacre, R., Jones, A., Rowland, J. J., & Kell, D. B. (1997). Genetic algorithms as a method for variable selection in multiple linear regression and partial least squares regression, with applications to pyrolysis mass spectrometry. *Analytica Chimica Acta*, 348(1), 71–86. [https://doi.org/10.1016/S0003-2670\(97\)00065-2](https://doi.org/10.1016/S0003-2670(97)00065-2)
- Broadhurst, D., Goodacre, R., Reinke, S. N., Kuligowski, J., Wilson, I. D., Lewis, M. R., & Dunn, W. B. (2018). Guidelines and considerations for the use of system suitability and quality control samples in mass spectrometry assays applied in untargeted clinical metabolomic studies. *Metabolomics*, 14(6), 72. <https://doi.org/10.1007/s11306-018-1367-3>
- Brönmark, C., & Miner, J. G. (1992). Predator-Induced Phenotypical Change in Body Morphology in Crucian Carp. *Science*, 258(5086), 1348–1350.
- Cao, L., Guler, M., Tagirdzhanov, A., Lee, Y.-Y., Gurevich, A., & Mohimani, H. (2021). MolDiscovery: Learning mass spectrometry fragmentation of small molecules. *Nature Communications*, 12(1), Article 1. <https://doi.org/10.1038/s41467-021-23986-0>
- Carr, W. E. S., Netherton, III., J. C., Gleeson, R. A., & Derby, C. D. (1996). Stimulants of Feeding Behavior in Fish: Analyses of Tissues of Diverse Marine Organisms. *The Biological Bulletin*, 190(2), 149–160. <https://doi.org/10.2307/1542535>
- Castillo, S., Gopalacharyulu, P., Yetukuri, L., & Orešič, M. (2011). Algorithms and tools for the preprocessing of LC–MS metabolomics data. *Chemometrics and Intelligent Laboratory Systems*, 108(1), 23–32. <https://doi.org/10.1016/j.chemolab.2011.03.010>
- Chang, H.-Y., Colby, S. M., Du, X., Gomez, J. D., Helf, M. J., Kechris, K., Kirkpatrick, C. R., Li, S., Patti, G. J., Renslow, R. S., Subramaniam, S., Verma, M., Xia, J., &

- Young, J. D. (2021). A Practical Guide to Metabolomics Software Development. *Analytical Chemistry*, 93(4), 1912–1923. <https://doi.org/10.1021/acs.analchem.0c03581>
- Chen, H., Zheng, Y., Zhan, J., He, C., & Wang, Q. (2017). Comparative metabolic profiling of the lipid-producing green microalga *Chlorella* reveals that nitrogen and carbon metabolic pathways contribute to lipid metabolism. *Biotechnology for Biofuels*, 10(1), 153. <https://doi.org/10.1186/s13068-017-0839-4>
- Cho, S.-H., Jeong, Y., Lee, E., Ko, S.-R., Ahn, C.-Y., Oh, H.-M., Cho, B.-K., & Cho, S. (2021). Assessment of *Erythrobacter* Species Diversity through Pan-Genome Analysis with Newly Isolated *Erythrobacter* sp. 3-20A1M. *Journal of Microbiology and Biotechnology*, 31(4), 601–609. <https://doi.org/10.4014/jmb.2012.12054>
- Cousin, M. A. (1999). PSEUDOMONAS | Introduction. In R. K. Robinson (Ed.), *Encyclopedia of Food Microbiology* (pp. 1864–1867). Elsevier. <https://doi.org/10.1006/rwfm.1999.1290>
- Cronin, G., & Hay, M. E. (1996). Induction of Seaweed Chemical Defenses by Amphipod Grazing. *Ecology*, 77(8), 2287–2301. <https://doi.org/10.2307/2265731>
- Dawson, H. M., Heal, K. R., Boysen, A. K., Carlson, L. T., Ingalls, A. E., & Young, J. N. (2020). Potential of temperature- and salinity-driven shifts in diatom compatible solute concentrations to impact biogeochemical cycling within sea ice. *Elementa: Science of the Anthropocene*, 8, 25. <https://doi.org/10.1525/elementa.421>
- Deland, J.-P., Gries, R., Gries, G., Judd, G. J. R., & Roitberg, B. D. (1993). Sex pheromone components of the fruit-tree leaf roller, *Archips argyrospilus* (Walker) (Lepidoptera: Tortricidae), in British Columbia. *Journal of Chemical Ecology*, 19(12), 2855–2864. <https://doi.org/10.1007/BF00980587>
- Dickson, D. M. J., & Kirst, G. O. (1986). The role of β -dimethylsulphoniopropionate, glycine betaine and homarine in the osmoacclimation of *Platymonas subcordiformis*. *Planta*, 167(4), 536–543. <https://doi.org/10.1007/BF00391230>
- Dieterle, F., Ross, A., Schlotterbeck, G., & Senn, H. (2006). Probabilistic Quotient Normalization as Robust Method to Account for Dilution of Complex Biological Mixtures. Application in ¹H NMR Metabonomics. *Analytical Chemistry*, 78(13), 4281–4290. <https://doi.org/10.1021/ac051632c>

- Dove, A. D. M., Leisen, J., Zhou, M., Byrne, J. J., Lim-Hing, K., Webb, H. D., Gelbaum, L., Viant, M. R., Kubanek, J., & Fernández, F. M. (2012). Biomarkers of Whale Shark Health: A Metabolomic Approach. *PLOS ONE*, 7(11), e49379. <https://doi.org/10.1371/journal.pone.0049379>
- Dührkop, K., Fleischauer, M., Ludwig, M., Aksenov, A. A., Melnik, A. V., Meusel, M., Dorrestein, P. C., Rousu, J., & Böcker, S. (2019). SIRIUS 4: A rapid tool for turning tandem mass spectra into metabolite structure information. *Nature Methods*, 16(4), Article 4. <https://doi.org/10.1038/s41592-019-0344-8>
- Dusenbery, D. B. (2001). Physical Constraints in Sensory Ecology. In F. G. Barth & A. Schmid (Eds.), *Ecology of Sensing* (pp. 1–17). Springer. https://doi.org/10.1007/978-3-662-22644-5_1
- Eason, A., Powell, A., Roney, S., Lin, C., Russell, C., Belgrad, B., & Smee, D. L. (2021). Timing of Predation Risk During Early Development Influences Oyster Shell Morphology. *Gulf and Caribbean Research*, 32, SC1–SC5. <https://doi.org/10.18785/gcr.3201.13>
- Erb, M., & Kliebenstein, D. J. (2020). Plant Secondary Metabolites as Defenses, Regulators, and Primary Metabolites: The Blurred Functional Trichotomy. *Plant Physiology*, 184(1), 39–52. <https://doi.org/10.1104/pp.20.00433>
- Falkowski, P. G., Barber, R. T., & Smetacek, V. (1998). Biogeochemical Controls and Feedbacks on Ocean Primary Production. *Science*, 281(5374), 200–206. <https://doi.org/10.1126/science.281.5374.200>
- Fendt, M. (2006). Exposure to Urine of Canids and Felids, but not of Herbivores, Induces Defensive Behavior in Laboratory Rats. *Journal of Chemical Ecology*, 32(12), 2617–2627. <https://doi.org/10.1007/s10886-006-9186-9>
- Ferland-Raymond, B., March, R. E., Metcalfe, C. D., & Murray, D. L. (2010). Prey detection of aquatic predators: Assessing the identity of chemical cues eliciting prey behavioral plasticity. *Biochemical Systematics and Ecology*, 38(2), 169–177. <https://doi.org/10.1016/j.bse.2009.12.035>
- Ferrari, M. C. O., Wisenden, B. D., & Chivers, D. P. (2010). Chemical ecology of predator–prey interactions in aquatic ecosystems: A review and prospectus. *Canadian Journal of Zoology*, 88(7), 698–724. <https://doi.org/10.1139/Z10-029>

- Ferrero, D. M., Lemon, J. K., Fluegge, D., Pashkovski, S. L., Korzan, W. J., Datta, S. R., Spehr, M., Fendt, M., & Liberles, S. D. (2011). Detection and avoidance of a carnivore odor by prey. *Proceedings of the National Academy of Sciences*, *108*(27), 11235–11240. <https://doi.org/10.1073/pnas.11033171108>
- Fiehn, O., Robertson, D., Griffin, J., van der Werf, M., Nikolau, B., Morrison, N., Sumner, L. W., Goodacre, R., Hardy, N. W., Taylor, C., Fostel, J., Kristal, B., Kaddurah-Daouk, R., Mendes, P., van Ommen, B., Lindon, J. C., & Sansone, S.-A. (2007). The metabolomics standards initiative (MSI). *Metabolomics*, *3*(3), 175–178. <https://doi.org/10.1007/s11306-007-0070-6>
- Fisher, C. L., Ward, C. S., Lane, P. D., Kimbrel, J. A., Sale, K. L., Stuart, R. K., Mayali, X., & Lane, T. W. (2019). Bacterial communities protect the alga *Microchloropsis salina* from grazing by the rotifer *Brachionus plicatilis*. *Algal Research*, *40*, 101500. <https://doi.org/10.1016/j.algal.2019.101500>
- Flynn, K. J., Kenny, P., & Mitra, A. (2017). Minimising losses to predation during microalgae cultivation. *Journal of Applied Phycology*, *29*(4), 1829–1840. <https://doi.org/10.1007/s10811-017-1112-8>
- Fraker, M. E. (2008). The dynamics of predation risk assessment: Responses of anuran larvae to chemical cues of predators. *Journal of Animal Ecology*, *77*(4), 638–645. <https://doi.org/10.1111/j.1365-2656.2008.01386.x>
- Fuentes, J. L., Garbayo, I., Cuaresma, M., Montero, Z., González-Del-Valle, M., & Vílchez, C. (2016). Impact of Microalgae-Bacteria Interactions on the Production of Algal Biomass and Associated Compounds. *Marine Drugs*, *14*(5), 100. <https://doi.org/10.3390/md14050100>
- Gavriilidou, A., Gutleben, J., Versluis, D., Forgiarini, F., van Passel, M. W. J., Ingham, C. J., Smidt, H., & Sipkema, D. (2020). Comparative genomic analysis of Flavobacteriaceae: Insights into carbohydrate metabolism, gliding motility and secondary metabolite biosynthesis. *BMC Genomics*, *21*(1), 569. <https://doi.org/10.1186/s12864-020-06971-7>
- Gebser, B., & Pohnert, G. (2013). Synchronized Regulation of Different Zwitterionic Metabolites in the Osmoadaptation of Phytoplankton. *Marine Drugs*, *11*(6), 2168–2182. <https://doi.org/10.3390/md11062168>
- Gibson, R., Lau, C.-H. E., Loo, R. L., Ebbels, T. M. D., Chekmeneva, E., Dyer, A. R., Miura, K., Ueshima, H., Zhao, L., Daviglus, M. L., Stamler, J., Van Horn, L.,

- Elliott, P., Holmes, E., & Chan, Q. (2020). The association of fish consumption and its urinary metabolites with cardiovascular risk factors: The International Study of Macro-/Micronutrients and Blood Pressure (INTERMAP). *The American Journal of Clinical Nutrition*, *111*(2), 280–290. <https://doi.org/10.1093/ajcn/nqz293>
- Gillard, J., Frenkel, J., Devos, V., Sabbe, K., Paul, C., Rempt, M., Inzé, D., Pohnert, G., Vuylsteke, M., & Vyverman, W. (2013). Metabolomics Enables the Structure Elucidation of a Diatom Sex Pheromone. *Angewandte Chemie International Edition*, *52*(3), 854–857. <https://doi.org/10.1002/anie.201208175>
- Godard, R., Wannamaker, C., & Bowers, B. (1998). Responses of Golden Shiner Minnows to Chemical Cues from Snake Predators. *Behaviour*, *135*(8), 1213–1228. <https://doi.org/10.1163/156853998792913447>
- Gomez-Diaz, C., & Benton, R. (2013). The joy of sex pheromones. *EMBO Reports*, *14*(10), 874–883. <https://doi.org/10.1038/embor.2013.140>
- Gram, L., Melchiorson, J., & Bruhn, J. B. (2010). Antibacterial activity of marine culturable bacteria collected from a global sampling of ocean surface waters and surface swabs of marine organisms. *Marine Biotechnology (New York, N.Y.)*, *12*(4), 439–451. <https://doi.org/10.1007/s10126-009-9233-y>
- Grebner, W., Berglund, E. C., Berggren, F., Eklund, J., Harðadóttir, S., Andersson, M. X., & Selander, E. (2019). Induction of defensive traits in marine plankton—New copepodamide structures. *Limnology and Oceanography*, *64*(2), 820–831. <https://doi.org/10.1002/lno.11077>
- Griffen, B. D., Toscano, B. J., & Gatto, J. (2012). The role of individual behavior type in mediating indirect interactions. *Ecology*, *93*(8), 1935–1943. <https://doi.org/10.1890/11-2153.1>
- Gromski, P. S., Muhamadali, H., Ellis, D. I., Xu, Y., Correa, E., Turner, M. L., & Goodacre, R. (2015). A tutorial review: Metabolomics and partial least squares-discriminant analysis – a marriage of convenience or a shotgun wedding. *Analytica Chimica Acta*, *879*, 10–23. <https://doi.org/10.1016/j.aca.2015.02.012>
- Grossart, H.-P., Thorwest, M., Plitzko, I., Brinkhoff, T., Simon, M., & Zeeck, A. (2009). Production of a Blue Pigment (Glaukothalin) by Marine *Rheinheimera* spp. *International Journal of Microbiology*, *2009*, 701735. <https://doi.org/10.1155/2009/701735>

- Grunseich, J. M., Aguirre, N. M., Thompson, M. N., Ali, J. G., & Helms, A. M. (2021). Chemical Cues from Entomopathogenic Nematodes Vary Across Three Species with Different Foraging Strategies, Triggering Different Behavioral Responses in Prey and Competitors. *Journal of Chemical Ecology*, 47(10–11), 822–833. <https://doi.org/10.1007/s10886-021-01304-8>
- Gutman, J., Zarka, A., & Boussiba, S. (2009). The host-range of *Paraphysoderma sedebokerensis*, a chytrid that infects *Haematococcus pluvialis*. *European Journal of Phycology*, 44(4), 509–514. <https://doi.org/10.1080/09670260903161024>
- Hahn, M. A., Effertz, C., Bigler, L., & von Elert, E. (2019). 5 α -cyprinol sulfate, a bile salt from fish, induces diel vertical migration in *Daphnia*. *ELife*, 8, e44791. <https://doi.org/10.7554/eLife.44791>
- Hamilton, C. E. (2014). *Exploring the Utilization of Complex Algal Communities to Address Algal Pond Crash and Increase Annual Biomass Production for Algal Biofuels* (DOE/EE--1060, 1220809; p. DOE/EE--1060, 1220809). <https://doi.org/10.2172/1220809>
- Hammill, E., Petchey, O., & Anholt, B. (2010). Predator Functional Response Changed by Induced Defenses in Prey. *The American Naturalist*, 176, 723–731. <https://doi.org/10.1086/657040>
- Harborne, J. B. (2001). Twenty-five years of chemical ecology. *Natural Product Reports*, 18(4), 361–379. <https://doi.org/10.1039/B005311M>
- Hartmann, T. (2008). The lost origin of chemical ecology in the late 19th century. *Proceedings of the National Academy of Sciences*, 105(12), 4541–4546. <https://doi.org/10.1073/pnas.0709231105>
- Harvell, C. D. (1990). The Ecology and Evolution of Inducible Defenses. *The Quarterly Review of Biology*, 65(3), 323–340.
- Hay, M. E. (1996). Marine chemical ecology: What's known and what's next? *Journal of Experimental Marine Biology and Ecology*, 200(1), 103–134. [https://doi.org/10.1016/S0022-0981\(96\)02659-7](https://doi.org/10.1016/S0022-0981(96)02659-7)
- Hay, M. E. (2009). Marine Chemical Ecology: Chemical Signals and Cues Structure Marine Populations, Communities, and Ecosystems. *Annual Review of Marine Science*, 1(1), 193–212. <https://doi.org/10.1146/annurev.marine.010908.163708>

- Hay, M. E. (2014). Challenges and Opportunities in Marine Chemical Ecology. *Journal of Chemical Ecology*, 40(3), 216–217. <https://doi.org/10.1007/s10886-014-0393-5>
- Heal, K. R., Durham, B. P., Boysen, A. K., Carlson, L. T., Qin, W., Ribalet, F., White, A. E., Bundy, R. M., Armbrust, E. V., & Ingalls, A. E. (2021). *Marine Community Metabolomes Carry Fingerprints of Phytoplankton Community Composition*. 6(3), e01334-20. <https://doi.org/10.1128/mSystems.01334-20>
- Hermes, D. A., & Mattson, W. J. (1992). The Dilemma of Plants: To Grow or Defend. *The Quarterly Review of Biology*, 67(3), 283–335. <https://doi.org/10.1086/417659>
- Hesse, A., Classen, A., Knoll, M., Timmermann, F., & Vahlensieck, W. (1986). Dependence of urine composition on the age and sex of healthy subjects. *Clinica Chimica Acta*, 160(2), 79–86. [https://doi.org/10.1016/0009-8981\(86\)90126-9](https://doi.org/10.1016/0009-8981(86)90126-9)
- Howe, N. R., & Harris, L. G. (1978). Transfer of the sea anemone pheromone, anthopleurine, by the nudibranch *Aeolidia papillosa*. *Journal of Chemical Ecology*, 4(5), 551–561. <https://doi.org/10.1007/BF00988919>
- Howe, N. R., & Sheikh, Y. M. (1975). Anthopleurine: A sea anemone alarm pheromone. *Science (New York, N.Y.)*, 189(4200), 386–388. <https://doi.org/10.1126/science.238286>
- Imhoff, J. F. (2014). The Family Chromatiaceae. In E. Rosenberg, E. F. DeLong, S. Lory, E. Stackebrandt, & F. Thompson (Eds.), *The Prokaryotes: Gammaproteobacteria* (pp. 151–178). Springer. https://doi.org/10.1007/978-3-642-38922-1_295
- Isnansetyo, A., & Kamei, Y. (2009). Bioactive substances produced by marine isolates of *Pseudomonas*. *Journal of Industrial Microbiology and Biotechnology*, 36(10), 1239–1248. <https://doi.org/10.1007/s10295-009-0611-2>
- Ivanova, E. P., Ng, H. J., & Webb, H. K. (2014). The Family Pseudoalteromonadaceae. In E. Rosenberg, E. F. DeLong, S. Lory, E. Stackebrandt, & F. Thompson (Eds.), *The Prokaryotes: Gammaproteobacteria* (pp. 575–582). Springer. https://doi.org/10.1007/978-3-642-38922-1_229
- Kats, L. B., & Dill, L. M. (1998). The scent of death: Chemosensory assessment of predation risk by prey animals. *Écoscience*, 5(3), 361–394. <https://doi.org/10.1080/11956860.1998.11682468>

- Kawamata, M., Kon-ya, K., & Miki, W. (1994). Trigonelline, an Antifouling Substance Isolated from an Octocoral *Dendronephthya* sp. *Fisheries Science*, 60(4), 485–486. <https://doi.org/10.2331/fishsci.60.485>
- Kiesecker, J. M., Chivers, D. P., & Blaustein, A. R. (1996). The use of chemical cues in predator recognition by western toad tadpoles. *Animal Behaviour*, 52(6), 1237–1245. <https://doi.org/10.1006/anbe.1996.0271>
- Kim, K., & Lee, S.-S. (2015). *Paracoccus aquimaris* sp. Nov., isolated from seawater. *Antonie Van Leeuwenhoek*, 108(4), 871–877. <https://doi.org/10.1007/s10482-015-0541-0>
- Kubaneck, J., Snell, T. W., & Pirkle, C. (2007). Chemical defense of the red tide dinoflagellate *Karenia brevis* against rotifer grazing. *Limnology and Oceanography*, 52(3), 1026–1035. <https://doi.org/10.4319/lo.2007.52.3.1026>
- Kuhl, C., Tautenhahn, R., Böttcher, C., Larson, T. R., & Neumann, S. (2012). CAMERA: An Integrated Strategy for Compound Spectra Extraction and Annotation of Liquid Chromatography/Mass Spectrometry Data Sets. *Analytical Chemistry*, 84(1), 283–289. <https://doi.org/10.1021/ac202450g>
- Kuhlisch, C., & Pohnert, G. (2015). Metabolomics in chemical ecology. *Natural Product Reports*, 32(7), 937–955. <https://doi.org/10.1039/C5NP00003C>
- Laforsch, C., Beccara, L., & Tollrian, R. (2006). Inducible defenses: The relevance of chemical alarm cues in *Daphnia*. *Limnology and Oceanography*, 51(3), 1466–1472. <https://doi.org/10.4319/lo.2006.51.3.1466>
- Lapan, E. A. (1975). Studies on the chemistry of the octopus renal system and an observation on the symbiotic relationship of the dicyemid mesozoa. *Comparative Biochemistry and Physiology Part A: Physiology*, 52(4), 651–657. [https://doi.org/10.1016/S0300-9629\(75\)80018-1](https://doi.org/10.1016/S0300-9629(75)80018-1)
- Large, S. I., & Smee, D. L. (2013). Biogeographic variation in behavioral and morphological responses to predation risk. *Oecologia*, 171(4), 961–969. <https://doi.org/10.1007/s00442-012-2450-5>
- Lass, S., & Spaak, P. (2003). Chemically induced anti-predator defences in plankton: A review. *Hydrobiologia*, 491(1), 221–239. <https://doi.org/10.1023/A:1024487804497>

- Laughlin, R. A. (1982). Feeding Habits of the Blue Crab, *Callinectes Sapidus* Rathbun, in the Apalachicola Estuary, Florida. *Bulletin of Marine Science*, 32(4), 807–822.
- Lee, O. O., Tsoi, M. M. Y., Li, X., Wong, P.-K., & Qian, P.-Y. (2007). *Thalassococcus halodurans* gen. Nov., sp. Nov., a novel halotolerant member of the Roseobacter clade isolated from the marine sponge *Halichondria panicea* at Friday Harbor, USA. *International Journal of Systematic and Evolutionary Microbiology*, 57(Pt 8), 1919–1924. <https://doi.org/10.1099/ijs.0.64801-0>
- Leonard, G. H., Bertness, M. D., & Yund, P. O. (1999). Crab Predation, Waterborne Cues, and Inducible Defenses in the Blue Mussel, *Mytilus Edulis*. *Ecology*, 80(1), 1–14. [https://doi.org/10.1890/0012-9658\(1999\)080\[0001:CPWCAI\]2.0.CO;2](https://doi.org/10.1890/0012-9658(1999)080[0001:CPWCAI]2.0.CO;2)
- Liebal, U. W., Phan, A. N. T., Sudhakar, M., Raman, K., & Blank, L. M. (2020). Machine Learning Applications for Mass Spectrometry-Based Metabolomics. *Metabolites*, 10(6), Article 6. <https://doi.org/10.3390/metabo10060243>
- Lima, S. L. (1998). Nonlethal Effects in the Ecology of Predator-Prey Interactions. *BioScience*, 48(1), 25–34. JSTOR. <https://doi.org/10.2307/1313225>
- Lindström, J., Grebner, W., Rigby, K., & Selander, E. (2017). Effects of predator lipids on dinoflagellate defence mechanisms—Increased bioluminescence capacity. *Scientific Reports*, 7(1), Article 1. <https://doi.org/10.1038/s41598-017-13293-4>
- Long, J. D., & Hay, M. E. (2006). Fishes learn aversions to a nudibranch's chemical defense. *Marine Ecology Progress Series*, 307, 199–208. <https://doi.org/10.3354/meps307199>
- López-Pérez, M., & Rodriguez-Valera, F. (2014). The Family Alteromonadaceae. In E. Rosenberg, E. F. DeLong, S. Lory, E. Stackebrandt, & F. Thompson (Eds.), *The Prokaryotes: Gammaproteobacteria* (pp. 69–92). Springer. https://doi.org/10.1007/978-3-642-38922-1_233
- Ludwig, C., & Günther, U. L. (2011). MetaboLab—Advanced NMR data processing and analysis for metabolomics. *BMC Bioinformatics*, 12(1), 366. <https://doi.org/10.1186/1471-2105-12-366>
- Ma, M., Gong, Y., & Hu, Q. (2018). Identification and feeding characteristics of the mixotrophic flagellate *Poterioochromonas malhamensis*, a microalgal predator

isolated from outdoor massive *Chlorella* culture. *Algal Research*, 29, 142–153. <https://doi.org/10.1016/j.algal.2017.11.024>

Maerz, J. C., Panebianco, N. L., & Madison, D. M. (2001). Effects of Predator Chemical Cues and Behavioral Biorhythms on Foraging, Activity of Terrestrial Salamanders. *Journal of Chemical Ecology*, 27(7), 1333–1344. <https://doi.org/10.1023/A:1010309108210>

Mansson, M., Gram, L., & Larsen, T. O. (2011). Production of Bioactive Secondary Metabolites by Marine Vibrionaceae. *Marine Drugs*, 9(9), 1440–1468. <https://doi.org/10.3390/md9091440>

Martens, T., Gram, L., Grossart, H.-P., Kessler, D., Müller, R., Simon, M., Wenzel, S. C., & Brinkhoff, T. (2007). Bacteria of the Roseobacter clade show potential for secondary metabolite production. *Microbial Ecology*, 54(1), 31–42. <https://doi.org/10.1007/s00248-006-9165-2>

Matallana-Surget, S., Werner, J., Wattiez, R., Lebaron, K., Intertaglia, L., Regan, C., Morris, J., Teeling, H., Ferrer, M., Golyshin, P. N., Gerogiorgis, D., Reilly, S. I., & Lebaron, P. (2018). Proteogenomic Analysis of Epibacterium Mobile BBCC367, a Relevant Marine Bacterium Isolated From the South Pacific Ocean. *Frontiers in Microbiology*, 9. <https://www.frontiersin.org/articles/10.3389/fmicb.2018.03125>

Mathias, A. P., Ross, D. M., & Schachter, M. (1960). The distribution of 5-hydroxytryptamine, tetramethylammonium, homarine, and other substances in sea anemones. *The Journal of Physiology*, 151(2), 296–311.

May, M. A., Bishop, K. D., & Rawson, P. D. (2017). NMR Profiling of Metabolites in Larval and Juvenile Blue Mussels (*Mytilus edulis*) under Ambient and Low Salinity Conditions. *Metabolites*, 7(3), 33. <https://doi.org/10.3390/metabo7030033>

McClintock, J. B., Baker, B. J., Hamann, M. T., Yoshida, W., Slattery, M., Heine, J. N., Bryan, P. J., Jayatilake, G. S., & Moon, B. H. (1994). Homarine as a feeding deterrent in common shallow-water antarctic lamellarian gastropod *Marseniopsis mollis*: A rare example of chemical defense in a marine prosobranch. *Journal of Chemical Ecology*, 20(10), 2539–2549. <https://doi.org/10.1007/BF02036190>

Meinwald, J., Leal, W. S., & Kubanek, J. (2018). Molecules as Biotic Messengers. *ACS Omega*, 3(4), 4048–4053. <https://doi.org/10.1021/acsomega.8b00268>

- Misra, B. B. (2021). New software tools, databases, and resources in metabolomics: Updates from 2020. *Metabolomics*, *17*(5), 49. <https://doi.org/10.1007/s11306-021-01796-1>
- Montemezzani, V., Duggan, I. C., Hogg, I. D., & Craggs, R. J. (2015). A review of potential methods for zooplankton control in wastewater treatment High Rate Algal Ponds and algal production raceways. *Algal Research*, *11*, 211–226. <https://doi.org/10.1016/j.algal.2015.06.024>
- Mubarak, M., Shaija, A., & Suchithra, T. V. (2015). A review on the extraction of lipid from microalgae for biodiesel production. *Algal Research*, *7*, 117–123. <https://doi.org/10.1016/j.algal.2014.10.008>
- Muslin, O. (2017). *Quantification of Osmolytes in the Sargasso Sea Surface Layer Water Column* (Oregon State University). Oregon State University. https://ir.library.oregonstate.edu/concern/graduate_thesis_or_dissertations/t435gh40k
- Nakaoka, M. (2000). Nonlethal Effects of Predators on Prey Populations: Predator-Mediated Change in Bivalve Growth. *Ecology*, *81*(4), 1031–1045. [https://doi.org/10.1890/0012-9658\(2000\)081\[1031:NEOPOP\]2.0.CO;2](https://doi.org/10.1890/0012-9658(2000)081[1031:NEOPOP]2.0.CO;2)
- Natrah, F. M. I., Bossier, P., Sorgeloos, P., Yusoff, F. Md., & Defoirdt, T. (2014). Significance of microalgal–bacterial interactions for aquaculture. *Reviews in Aquaculture*, *6*(1), 48–61. <https://doi.org/10.1111/raq.12024>
- Newell, R. I. E., Kennedy, V. S., & Shaw, K. S. (2007). Comparative vulnerability to predators, and induced defense responses, of eastern oysters *Crassostrea virginica* and non-native *Crassostrea ariakensis* oysters in Chesapeake Bay. *Marine Biology*, *152*(2), 449–460. <https://doi.org/10.1007/s00227-007-0706-0>
- Nolte, D. L., Mason, J. R., Epple, G., Aronov, E., & Campbell, D. L. (1994). Why are predator urines aversive to prey? *Journal of Chemical Ecology*, *20*(7), 1505–1516. <https://doi.org/10.1007/BF02059876>
- Núñez-Pons, L., & Avila, C. (2015). Natural products mediating ecological interactions in Antarctic benthic communities: A mini-review of the known molecules. *Natural Product Reports*, *32*(7), 1114–1130. <https://doi.org/10.1039/C4NP00150H>

- O'Connor, N. E., Grabowski, J. H., Ladwig, L. M., & Bruno, J. F. (2008). Simulated Predator Extinctions: Predator Identity Affects Survival and Recruitment of Oysters. *Ecology*, *89*(2), 428–438. <https://doi.org/10.1890/06-2029.1>
- Osada, K., Miyazono, S., & Kashiwayanagi, M. (2014). Pyrazine analogs are active components of wolf urine that induce avoidance and fear-related behaviors in deer. *Frontiers in Behavioral Neuroscience*, *8*, 276. <https://doi.org/10.3389/fnbeh.2014.00276>
- Osada, K., Miyazono, S., & Kashiwayanagi, M. (2015). The scent of wolves: Pyrazine analogs induce avoidance and vigilance behaviors in prey. *Frontiers in Neuroscience*, *9*. <https://www.frontiersin.org/article/10.3389/fnins.2015.00363>
- Park, S., Van Ginkel, S. W., Pradeep, P., Igou, T., Yi, C., Snell, T., & Chen, Y. (2016). The Selective Use of Hypochlorite to Prevent Pond Crashes for Algae-Biofuel Production. *Water Environment Research*, *88*(1), 70–78. <https://doi.org/10.2175/106143015X14362865227670>
- Peckarsky, B. L. (1980). Predator-Prey Interactions between Stoneflies and Mayflies: Behavioral Observations. *Ecology*, *61*(4), 932–943. <https://doi.org/10.2307/1936762>
- Peckarsky, B. L., Taylor, B. W., McIntosh, A. R., McPeck, M. A., & Lytle, D. A. (2001). Variation in Mayfly Size at Metamorphosis as a Developmental Response to Risk of Predation. *Ecology*, *82*(3), 740–757. [https://doi.org/10.1890/0012-9658\(2001\)082\[0740:VIMSAM\]2.0.CO;2](https://doi.org/10.1890/0012-9658(2001)082[0740:VIMSAM]2.0.CO;2)
- Playdon, M. C., Sampson, J. N., Cross, A. J., Sinha, R., Guertin, K. A., Moy, K. A., Rothman, N., Irwin, M. L., Mayne, S. T., Stolzenberg-Solomon, R., & Moore, S. C. (2016). Comparing metabolite profiles of habitual diet in serum and urine. *The American Journal of Clinical Nutrition*, *104*(3), 776–789. <https://doi.org/10.3945/ajcn.116.135301>
- Pohnert, G., Steinke, M., & Tollrian, R. (2007). Chemical cues, defence metabolites and the shaping of pelagic interspecific interactions. *Trends in Ecology & Evolution*, *22*(4), 198–204. <https://doi.org/10.1016/j.tree.2007.01.005>
- Ponce, M., Belgrad, B., Walton, W., & Smee, L. (2020). Nursery Exposure of Oyster Spat to Different Predators Strengthens Oyster Shells. *Gulf and Caribbean Research*, *31*, SC36–SC40. <https://doi.org/10.18785/gcr.3101.14>

- Poulin, R. X., Lavoie, S., Siegel, K., Gaul, D. A., Weissburg, M. J., & Kubanek, J. (2018). Chemical encoding of risk perception and predator detection among estuarine invertebrates. *Proceedings of the National Academy of Sciences*, *115*(4), 662–667. <https://doi.org/10.1073/pnas.1713901115>
- Poulin, R. X., & Pohnert, G. (2019). Simplifying the complex: Metabolomics approaches in chemical ecology. *Analytical and Bioanalytical Chemistry*, *411*(1), 13–19. <https://doi.org/10.1007/s00216-018-1470-3>
- Poulson-Ellestad, K. L., Jones, C. M., Roy, J., Viant, M. R., Fernández, F. M., Kubanek, J., & Nunn, B. L. (2014). Metabolomics and proteomics reveal impacts of chemically mediated competition on marine plankton. *Proceedings of the National Academy of Sciences*, *111*(24), 9009–9014. <https://doi.org/10.1073/pnas.1402130111>
- Prince, E. K., & Pohnert, G. (2010). Searching for signals in the noise: Metabolomics in chemical ecology. *Analytical and Bioanalytical Chemistry*, *396*(1), 193–197. <https://doi.org/10.1007/s00216-009-3162-5>
- Pujalte, M. J., Lucena, T., Ruvira, M. A., Arahal, D. R., & Macián, M. C. (2014). The Family Rhodobacteraceae. In E. Rosenberg, E. F. DeLong, S. Lory, E. Stackebrandt, & F. Thompson (Eds.), *The Prokaryotes: Alphaproteobacteria and Betaproteobacteria* (pp. 439–512). Springer. https://doi.org/10.1007/978-3-642-30197-1_377
- Putnam, D. F. (1971). *Composition and concentrative properties of human urine* (NASA-CR-1802). <https://ntrs.nasa.gov/citations/19710023044>
- Rasyid, E. (2021). *Prevalence of Dissolved Homarine in Puget Sound and North Pacific* [University of Washington]. <https://digital.lib.washington.edu:443/researchworks/handle/1773/47770>
- Relyea, R. A. (2001). Morphological and Behavioral Plasticity of Larval Anurans in Response to Different Predators. *Ecology*, *82*(2), 523–540. [https://doi.org/10.1890/0012-9658\(2001\)082\[0523:MABPOL\]2.0.CO;2](https://doi.org/10.1890/0012-9658(2001)082[0523:MABPOL]2.0.CO;2)
- Robinson, E. M., Lunt, J., Marshall, C. D., & Smee, D. L. (2014). Eastern oysters *Crassostrea virginica* deter crab predators by altering their morphology in response to crab cues. *Aquatic Biology*, *20*(2), 111–118. <https://doi.org/10.3354/ab00549>

- Roney, S. H., Cepeda, M. R., Belgrad, B. A., Moore, S. G., Smee, D. L., Kubanek, J., & Weissburg, M. (2023). Common fear molecules induce defensive responses in marine prey across trophic levels. *Oecologia*, Accepted.
- Sacks, J. S., Heal, K. R., Boysen, A. K., Carlson, L. T., & Ingalls, A. E. (2022). Quantification of dissolved metabolites in environmental samples through cation-exchange solid-phase extraction paired with liquid chromatography–mass spectrometry. *Limnology and Oceanography: Methods*, 20(11), 683–700. <https://doi.org/10.1002/lom3.10513>
- Scherer, A. E., Bird, C. E., McCutcheon, M. R., Hu, X., & Smee, D. L. (2018). Two-tiered defense strategy may compensate for predator avoidance costs of an ecosystem engineer. *Marine Biology*, 165(8), 131. <https://doi.org/10.1007/s00227-018-3391-2>
- Scherer, A. E., Garcia, M. M., & Smee, D. L. (2017). Predatory blue crabs induce stronger nonconsumptive effects in eastern oysters *Crassostrea virginica* than scavenging blue crabs. *PeerJ*, 5, e3042. <https://doi.org/10.7717/peerj.3042>
- Scherer, A. E., Lunt, J., Draper, A. M., & Smee, D. L. (2016). Phenotypic plasticity in oysters (*Crassostrea virginica*) mediated by chemical signals from predators and injured prey. *Invertebrate Biology*, 135(2), 97–107. <https://doi.org/10.1111/ivb.12120>
- Scherer, A. E., & Smee, D. L. (2017). Eastern Oysters *Crassostrea virginica* Produce Plastic Morphological Defenses in Response to Crab Predators Despite Resource Limitation. *The Biological Bulletin*, 233(2), 144–150. <https://doi.org/10.1086/695470>
- Schmidt, R., Ulanova, D., Wick, L. Y., Bode, H. B., & Garbeva, P. (2019). Microbe-driven chemical ecology: Past, present and future. *The ISME Journal*, 13(11), Article 11. <https://doi.org/10.1038/s41396-019-0469-x>
- Schmitz, O. J. (2008). Effects of Predator Hunting Mode on Grassland Ecosystem Function. *Science*, 319(5865), 952–954. <https://doi.org/10.1126/science.1152355>
- Selander, E., Kubanek, J., Hamberg, M., Andersson, M. X., Cervin, G., & Pavia, H. (2015). Predator lipids induce paralytic shellfish toxins in bloom-forming algae. *Proceedings of the National Academy of Sciences*, 112(20), 6395–6400. <https://doi.org/10.1073/pnas.1420154112>

- Shahid, I., Malik, K. A., & Mehnaz, S. (2018). A decade of understanding secondary metabolism in *Pseudomonas* spp. For sustainable agriculture and pharmaceutical applications. *Environmental Sustainability*, 1(1), 3–17. <https://doi.org/10.1007/s42398-018-0006-2>
- Sih, A., Englund, G., & Wooster, D. (1998). Emergent impacts of multiple predators on prey. *Trends in Ecology & Evolution*, 13, 350–355. [https://doi.org/10.1016/S0169-5347\(98\)01437-2](https://doi.org/10.1016/S0169-5347(98)01437-2)
- Siller, H., Rainey, F. A., Stackebrandt, E., & Winter, J. (1996). Isolation and characterization of a new gram-negative, acetone-degrading, nitrate-reducing bacterium from soil, *Paracoccus solventivorans* sp. Nov. *International Journal of Systematic Bacteriology*, 46(4), 1125–1130. <https://doi.org/10.1099/00207713-46-4-1125>
- Simon, M., Scheuner, C., Meier-Kolthoff, J. P., Brinkhoff, T., Wagner-Döbler, I., Ulbrich, M., Klenk, H.-P., Schomburg, D., Petersen, J., & Göker, M. (2017). Phylogenomics of Rhodobacteraceae reveals evolutionary adaptation to marine and non-marine habitats. *The ISME Journal*, 11(6), Article 6. <https://doi.org/10.1038/ismej.2016.198>
- Slattery, M., Hamann, M. T., McClintock, J. B., Perry, T. L., Puglisi, M. P., & Yoshida, W. Y. (1997). Ecological roles for water-borne metabolites from Antarctic soft corals. *Marine Ecology Progress Series*, 161, 133–144. <https://doi.org/10.3354/meps161133>
- Smee, D. L., & Weissburg, M. J. (2006). Hard Clams (*Mercenaria mercenaria*) Evaluate Predation Risk Using Chemical Signals from Predators and Injured Conspecifics. *Journal of Chemical Ecology*, 32(3), 605–619. <https://doi.org/10.1007/s10886-005-9021-8>
- Snell, T. W., & Persoone, G. (1989). Acute toxicity bioassays using rotifers. I. A test for brackish and marine environments with *Brachionus plicatilis*. *Aquatic Toxicology*, 14(1), 65–80. [https://doi.org/10.1016/0166-445X\(89\)90055-6](https://doi.org/10.1016/0166-445X(89)90055-6)
- Sogin, E. M., Anderson, P., Williams, P., Chen, C.-S., & Gates, R. D. (2014). Application of 1H-NMR metabolomic profiling for reef-building corals. *PloS One*, 9(10), e111274. <https://doi.org/10.1371/journal.pone.0111274>
- Sorochan Armstrong, M. D., de la Mata, A. P., & Harynuk, J. J. (2022). Review of Variable Selection Methods for Discriminant-Type Problems in Chemometrics. *Frontiers in*

- Spicer, R. A., Salek, R., & Steinbeck, C. (2017). A decade after the metabolomics standards initiative it's time for a revision. *Scientific Data*, 4(1), Article 1. <https://doi.org/10.1038/sdata.2017.138>
- Sullivan, T. P., & Crump, D. R. (1986). Feeding responses of snowshoe hares (*Lepus americanus*) to volatile constituents of red fox (*Vulpes vulpes*) urine. *Journal of Chemical Ecology*, 12(3), 729–739. <https://doi.org/10.1007/BF01012105>
- Sun, A., Davis, R., Starbuck, M., Ben-Amotz, A., Pate, R., & Pienkos, P. T. (2011). Comparative cost analysis of algal oil production for biofuels. *Energy*, 36(8), 5169–5179. <https://doi.org/10.1016/j.energy.2011.06.020>
- Sun, S., Dai, X., Sun, J., Bu, X., Weng, C., Li, H., & Zhu, H. (2016). A diketopiperazine factor from *Rheinheimera aquimaris* QSI02 exhibits anti-quorum sensing activity. *Scientific Reports*, 6, 39637. <https://doi.org/10.1038/srep39637>
- Tagatz, M. E. (1968). Biology of the blue crab, *Callinectes sapidus* Rathbun, in the St. Johns River, Florida. *Fishery Bull. Fish Wildl. Serv. U. S.*, 67(1), 17–33.
- Targett, N. M., Bishop, S. S., McConnell, O. J., & Yoder, J. A. (1983). Antifouling agents against the benthic marine diatom, *Navicula salinicola* Homarine from the gorgonians *Leptogorgia virgulata* and *L. setacea* and analogs. *Journal of Chemical Ecology*, 9(7), 817–829. <https://doi.org/10.1007/BF00987807>
- Tikunov, A. P., Johnson, C. B., Lee, H., Stoskopf, M. K., & Macdonald, J. M. (2010). Metabolomic Investigations of American Oysters Using ¹H-NMR Spectroscopy. *Marine Drugs*, 8(10), Article 10. <https://doi.org/10.3390/md8102578>
- Tollrian, R. (1993). Neckteeth formation in *Daphnia pulex* as an example of continuous phenotypic plasticity: Morphological effects of *Chaoborus* kairomone concentration and their quantification. *Journal of Plankton Research*, 15(11), 1309–1318. <https://doi.org/10.1093/plankt/15.11.1309>
- van den Berg, R. A., Hoefsloot, H. C., Westerhuis, J. A., Smilde, A. K., & van der Werf, M. J. (2006). Centering, scaling, and transformations: Improving the biological information content of metabolomics data. *BMC Genomics*, 7, 142. <https://doi.org/10.1186/1471-2164-7-142>

- Van Ginkel, S. W., Igou, T., Hu, Z., Narode, A., Cheruvu, S., Doi, S., Johnston, R., Snell, T., & Chen, Y. (2015). Taking advantage of rotifer sensitivity to rotenone to prevent pond crashes for algal-biofuel production. *Algal Research*, *10*, 100–103. <https://doi.org/10.1016/j.algal.2015.03.013>
- Wang, B., Tan, T., & Shao, Z. (2009). *Roseovarius pacificus* sp. Nov., isolated from deep-sea sediment. *International Journal of Systematic and Evolutionary Microbiology*, *59*(Pt 5), 1116–1121. <https://doi.org/10.1099/ijs.0.002477-0>
- Wang, D., Liu, H., Zheng, S., & Wang, G. (2014). *Paenirhodobacter enshiensis* gen. Nov., sp. Nov., a non-photosynthetic bacterium isolated from soil, and emended descriptions of the genera *Rhodobacter* and *Haematobacter*. *International Journal of Systematic and Evolutionary Microbiology*, *64*(Pt 2), 551–558. <https://doi.org/10.1099/ijs.0.050351-0>
- Wang, F., Liigand, J., Tian, S., Arndt, D., Greiner, R., & Wishart, D. S. (2021). CFM-ID 4.0: More Accurate ESI-MS/MS Spectral Prediction and Compound Identification. *Analytical Chemistry*, *93*(34), 11692–11700. <https://doi.org/10.1021/acs.analchem.1c01465>
- Webster, D. R., & Weissburg, M. J. (2009). The Hydrodynamics of Chemical Cues Among Aquatic Organisms. *Annual Review of Fluid Mechanics*, *41*(1), 73–90. <https://doi.org/10.1146/annurev.fluid.010908.165240>
- Weiss, L. C., Albada, B., Becker, S. M., Meckelmann, S. W., Klein, J., Meyer, M., Schmitz, O. J., Sommer, U., Leo, M., Zagermann, J., Metzler-Nolte, N., & Tollrian, R. (2018). Identification of Chaoborus kairomone chemicals that induce defences in *Daphnia*. *Nature Chemical Biology*, *14*(12), 1133–1139. <https://doi.org/10.1038/s41589-018-0164-7>
- Weissburg, M., Poulin, R. X., & Kubanek, J. (2016). You Are What you Eat: A Metabolomics Approach to Understanding Prey Responses to Diet-Dependent Chemical Cues Released by Predators. *Journal of Chemical Ecology*, *42*(10), 1037–1046. <https://doi.org/10.1007/s10886-016-0771-2>
- Weissburg, M., Smee, D. L., & Ferner, M. C. (2014). The sensory ecology of nonconsumptive predator effects. *The American Naturalist*, *184*(2), 141–157. <https://doi.org/10.1086/676644>

- Weller, M. G. (2012). A Unifying Review of Bioassay-Guided Fractionation, Effect-Directed Analysis and Related Techniques. *Sensors*, *12*(7), Article 7. <https://doi.org/10.3390/s120709181>
- Werner, E., & Gilliam, J. (2003). The Ontogenetic Niche and Species Interactions in Size-Structured Populations. *Annual Review of Ecology and Systematics*, *15*, 393–425. <https://doi.org/10.1146/annurev.es.15.110184.002141>
- Xi, B., Gu, H., Baniasadi, H., & Raftery, D. (2014). Statistical Analysis and Modeling of Mass Spectrometry-Based Metabolomics Data. *Methods in Molecular Biology (Clifton, N.J.)*, *1198*, 333–353. https://doi.org/10.1007/978-1-4939-1258-2_22
- Xie, F., Ma, H., Quan, S., Liu, D., Chen, G., Chao, Y., & Qian, S. (2014). *Pseudomonas kunmingensis* sp. Nov., an exopolysaccharide-producing bacterium isolated from a phosphate mine. *International Journal of Systematic and Evolutionary Microbiology*, *64*(Pt 2), 559–564. <https://doi.org/10.1099/ijms.0.055632-0>
- Xu, C., Wu, K., Van Ginkel, S. W., Igou, T., Lee, H. J., Bhargava, A., Johnston, R., Snell, T., & Chen, Y. (2015). The Use of the Schizonticidal Agent Quinine Sulfate to Prevent Pond Crashes for Algal-Biofuel Production. *International Journal of Molecular Sciences*, *16*(11), 27450–27456. <https://doi.org/10.3390/ijms161126035>
- Xu, L., Sun, C., Fang, C., Oren, A., & Xu, X.-W. (2020). Genomic-based taxonomic classification of the family Erythrobacteraceae. *International Journal of Systematic and Evolutionary Microbiology*, *70*(8), 4470–4495. <https://doi.org/10.1099/ijsem.0.004293>
- Yu, Y., Yan, S.-L., Li, H.-R., & Zhang, X.-H. (2011). *Roseicitreum antarcticum* gen. Nov., sp. Nov., an aerobic bacteriochlorophyll a-containing alphaproteobacterium isolated from Antarctic sandy intertidal sediment. *International Journal of Systematic and Evolutionary Microbiology*, *61*(Pt 9), 2173–2179. <https://doi.org/10.1099/ijms.0.024885-0>